Copper Recovery from Industrial Waste Water using Brown Coal

褐炭を用いた工業廃液からの銅回収の研究

A Dissertation Submitted to the
Department of Chemical and Environmental Engineering,
Graduate School of Engineering,
Gunma University

For the Degree of
Doctor of Engineering

博士学位論文

2015/9
平成 27 年 9 月期

Atsushi Yoshino
吉野　淳

Evaluation Committee

Professor Nobuyoshi Nakagawa, Chair
Faculty of Engineering, Gunma University

Professor Shinji Katsura, Vice-Chair
Faculty of Engineering, Gunma University

Professor Junichi Ozaki, Vice-Chair
Faculty of Engineering, Gunma University

Group Leader, Dr. Toshimasa Takanohashi, Vice-Chair
Advanced Fuel Group, Energy Technology Research Institute
National Institute of Advanced Industrial Science and Technology

Professor Takayuki Takarada, Vice-Chair
Faculty of Engineering, Gunma University

Abstract

The process of etching by copper chloride is widely used in printed circuit board manufacturing, but unfortunately, almost all of the copper waste solution is currently treated by neutralization, with the precipitated sludge being dumped into the ground without any attempt at copper recovery. In this regard, brown coal, which possesses an ion exchange ability because of its carboxy and hydroxyl groups has been studied for application to copper recovery from waste etching solutions using a low energy consumption method. The challenges for copper recovery are summarized in Chapter 2. In order to commercialize this copper recovery method, it is important to understand the effects of the copper loading conditions on copper loading, low temperature combustion and copper oxide particle formation. In this study, copper-loaded brown coal was combusted under low-temperature conditions, to take advantage of its catalytic abilities. These key factors, including the catalytic ability, were investigated in detail.

In Chapter 3, an ion exchange method by using Loy Yang brown coal for copper recovery from the waste etching solution of printed circuit board manufacturing was studied. Copper ions in the waste solution can be loaded onto Loy Yang brown coal to around 8.5wt% by adding ammonium hydroxide to adjust the pH to 9-11.5 while stirring the solution at room temperature. At this adjusted pH range, it is believed that ion exchange is the main mechanism for copper loading, with copper and ammonium complex ions such as tetraamminecopper(II) $[Cu(NH_3)_4]^{2+}$ being produced and exchanged with the protons of carboxy groups in brown coal.

In Chapter 4, the reaction kinetics and mechanisms of the low-temperature combustion of Cu-loaded brown coal were studied by TG analysis. It was found that Cu-loaded brown coal can be burnt at extremely low temperatures of 160–180°C, and that 0.5–1.0μm copper oxide particles are formed as the residue. Since the XRD spectra obtained of the sample at 165 °C indicates the presence of Cu_2O, this oxide is believed to play a role as a catalyst for gasification and/or oxidation. Through kinetic analysis using the TG data, it was revealed that the activation energy of initial combustion is affected by the Cu-loading amount. For example, with a Cu-loading of 8.6wt%, it is estimated that the activation energy is reduced to 56% that of raw coal. Thus, by loading with copper, initial volatile matter gasification and/or combustion appears to be accelerated. From the relationship between the ignition temperatures and activation energies analyzed using the Coats-Redfern method and Semenov theory, copper loaded on brown coal seems to also play a role in promoting heat transfer. The reaction path of Cu-ammonia complex to Cu metal was studied by Gaussian09, from which it was determined that deammoniation should occur first. It was also found that the $CO+CO_2$ emission of 8.6wt%-Cu-loaded brown coal is, at the early stage, four-times greater than that of raw brown coal.

In Chapter 5, the copper particle formation mechanism is studied and a modified percolation model proposed along with a coalesced particle formation model. These indicate

that at a point near complete combustion small particles of copper compounds coalesce together, and this point is likely to be the percolation threshold given that there is a good relation between the D_{50} of brown coal and the D_{50} of CuO particles. The effects of raw brown coal size and Cu-loading are also investigated, through which it is found that these effects can be explained by the coalesced particle formation model. It is revealed that the mode diameter of CuO is determined by the mode diameter of raw brown coal, and that this relation is also explained by the coalesced particle formation model.

In Chapter 6, applications for the recovered copper were studied and discussed. It was found that when NaOH is used as a pH adjusting agent, the copper deposition rate of a plating solution using the recovered copper is equivalent to the original plating solution. It is also found that when the washing process is improved, the impact energy and tensile strength of the sintered metal that is produced using the recovered copper becomes equivalent to the original metal. In addition, Cu-loaded brown coal can be used as a catalyst for oxidation-reduction.

It is concluded that copper can be recovered from waste etching solution with minimal energy consumption by exploiting the ion exchange ability of brown coal and the catalytic effect of copper-loaded brown coal. Copper plating solutions, metallurgical additives and catalysts for oxidation–reduction reactions such as gasification represent strong candidates for practical applications of the recovered copper.

Table of Contents

Chapter 1 Introduction

Worldwide consumption of resources and energy has been increasing every year due to global economic development, making it critical to promote recycling in order to create a more sustainable society for rapid economic development. **Fig.1.1** shows the worldwide consumption of copper, which has doubled in the 30 years from 1982 to 2012[1)].

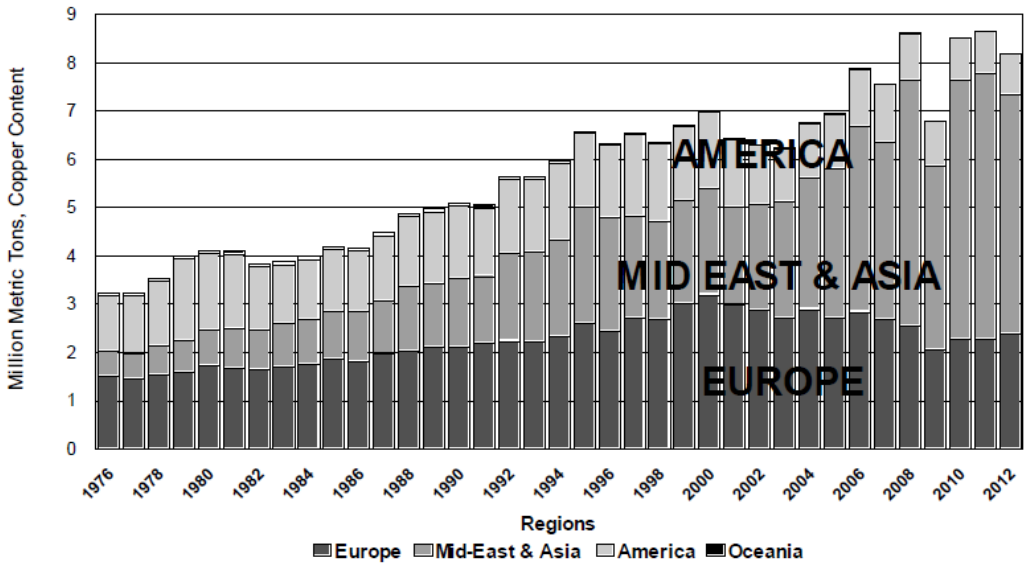

Fig.1.1 Worldwide consumption of copper from direct melt and refined scrap, by region, 1976-2012

Source: 2013 Technical Report by the Copper Development Association Inc.[1)]

The recycle ratio for copper scrap in recent years has been about 35%[1)], though the recovery of metals from appliances such as mobile phones in what are called urban mines has become a hot topic. Copper is used in appliances such as wiring, which is usually produced by lithography in the form of a printed circuit board, or PCB (**Fig.1.2**).

Fig.1.2 Printed circuit board (metal clad laminate)

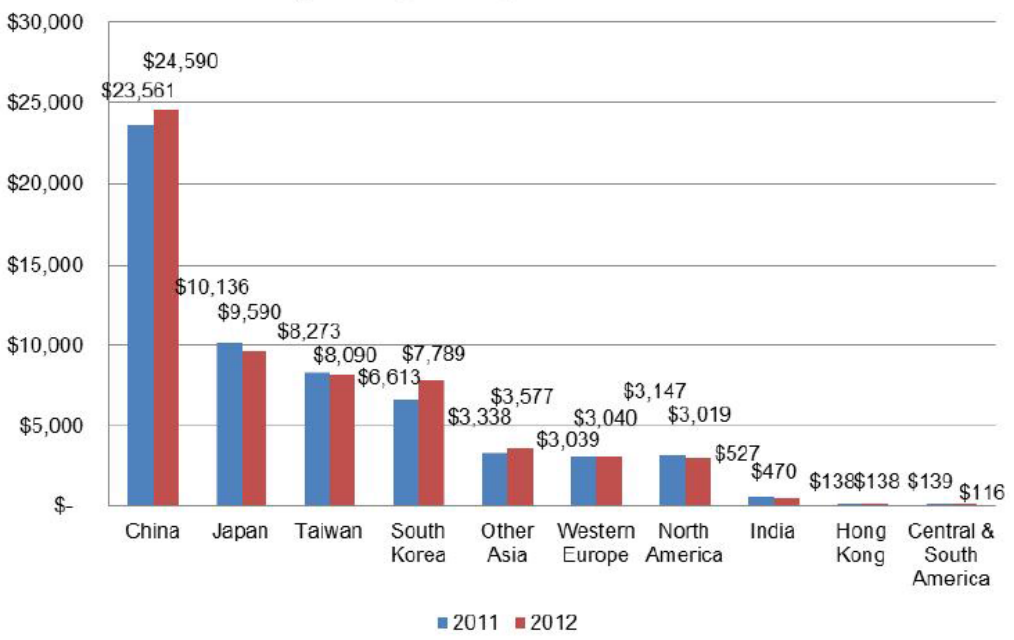

Fig.1.3 2011 and 2012 PCB production by major producing countries
Source: WECC Global PCB Production Report for 2012[2)]

Total worldwide production of PCBs in 2012 was 60.4 B$[2)], but as shown in **Fig.1.3**[2)], this production volume was growing in South Korea, China and other Asia countries in 2012.

In the lithography process used for PCB production, a dry film resist is laminated to a copper board, exposed and developed, and then the copper layer is etched to form a circuit. A schematic of this process is provided in **Fig.1.4**.

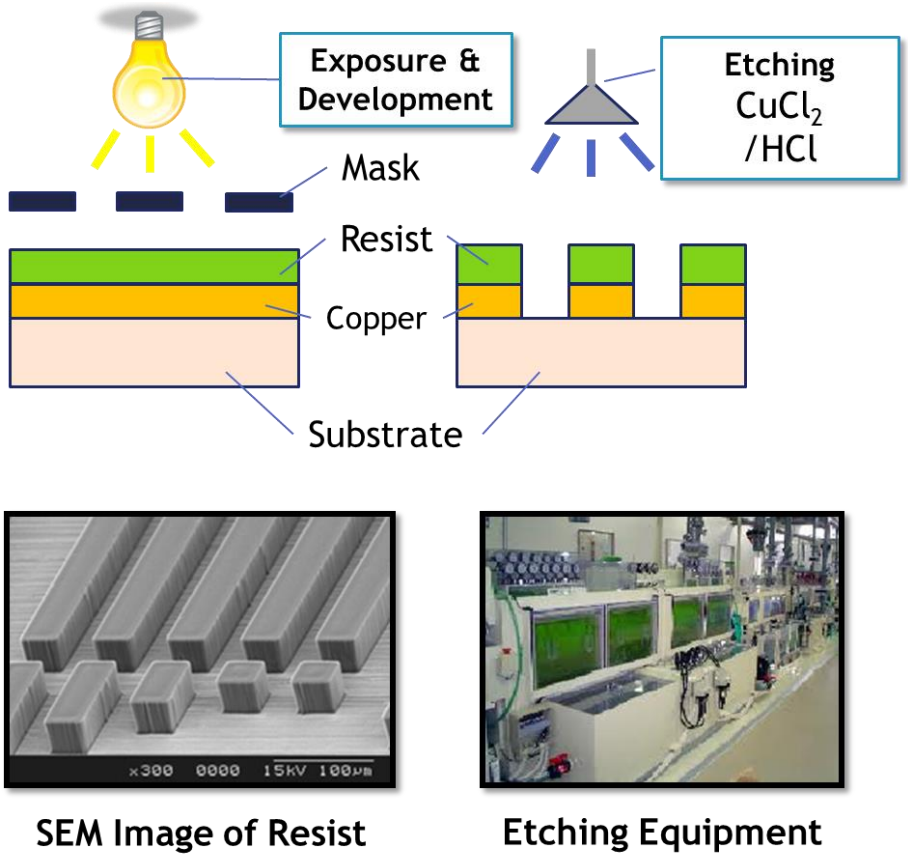

Fig.1.4 PCB lithography process

Turning the copper raw material into a PCB produces remnants during the cutting process and a dissolved copper solution during the etching process. The recycling of used PCBs and PCB remnants has been studied using several different approaches[3], but the focus of this thesis is on the recycling of the etching waste copper solution. This is expected to provide a technique that can be implemented within a PCB production site, eliminating the need to transport the waste solution to a waste treatment company.

Iron chloride and copper chloride are both widely used in the etching process; and in the case of iron chloride, separation of iron and copper is required. Although the possibility exists of separating them using a method such as ion exchange, copper recovery from copper chloride waste etching solution was selected as the research theme to provide the most simple and basic approach. Once this technology is established for copper chloride, it should be possible to expand it to also treat iron chloride waste etching solution.

1.1 Current State of Copper Recycling

The process of etching by copper chloride that is widely used in printed circuit board manufacturing is considered to consist of the following reactions.

$$Cu + CuCl_2 \rightarrow 2CuCl \quad \cdots \text{Eq. (1.1)}$$

$$CuCl + HCl \rightarrow CuCl_2^- + H^+ \quad \cdots \text{Eq. (1.2)}$$

Here, copper metal first reacts with $CuCl_2$, and the resulting CuCl solid product is then dissolved by HCl. When the concentration of copper ions becomes too high, the solution is replaced with a new etching solution. The waste etching solution therefore contains a high concentration of copper and chlorine ions.

Unfortunately, almost all copper waste solution is currently treated by neutralization, with the precipitated sludge being subsequently dumped into the ground without any attempt at copper recovery. In the neutralization and precipitation process, calcium hydroxide, iron sulfate, and/or iron chloride are typically used as a neutralizer and flocculating agents. Since this means that the precipitated sludge includes calcium and iron contaminants, the purification cost is too high to economically recycle copper[4]. Electrolysis can be used to recover copper from the waste solution[5]; however, this consumes a lot of energy and leaves residual chlorine ions in the deposited copper, thus making unsuitable for an on-site closed recycle system or other applications where residual chlorine ions could be detrimental. There is therefore a need to develop a simple, compact and low-cost process for copper recovery.

In this thesis, the ion exchange of copper from waste solutions by brown coal is studied. The premise behind this is that if only the copper ions are selectively adsorbed onto the brown coal, which is then washed by water to remove chlorine ions and combusted by applying a small input energy to recover pure copper oxide for a low process cost.

1.2 Utilization of Brown Coal

The total available amount of coal reserves in the world currently stands at around 890Btons[6], of which brown coal and sub-bituminous coal reserves make up about 54.8% (490Btons)[6]. Though these estimated amounts are quite huge, much of the brown coal is not available for thermal use because of its high water content and its low calorific value. The reforming and gasification of low-grade coals is currently the subject of investigation by researchers around the world, but there is still a significant cost issue associated with this. Nevertheless, a number of integrated coal gasification combined cycle (IGCC) demonstration plants have been built and operated, but this technology is still being established[7].

Brown coal has an ion exchange ability because of its carboxy and hydroxyl groups, as shown in the structural unit model presented in **Fig.1.5**[8] and the schematic model of ion exchange in **Fig.1.6**[9),10]. This ion exchange capability suggests that other uses for brown coal warrant further study.

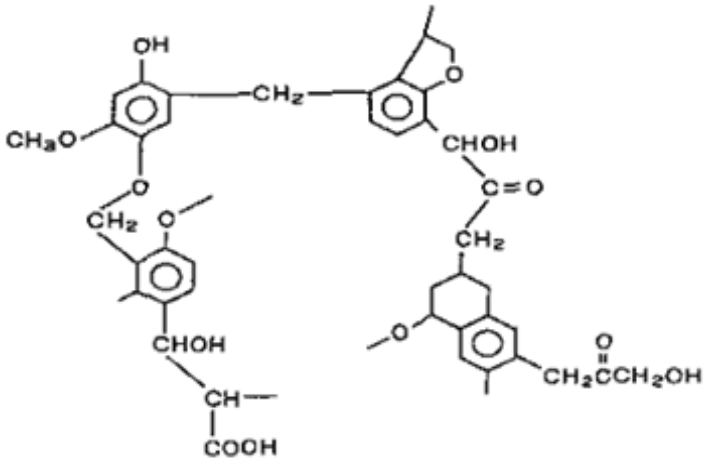

Fig.1.5 Structural unit model of brown coal[8]

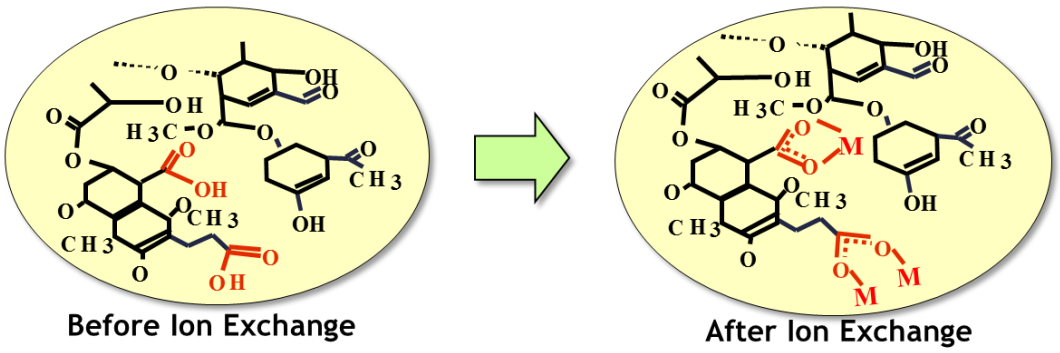

Fig.1.6 Schematic model of ion exchange by brown coal[9),10]

Table 1.1 Classification of the maceral of huminite, Source: Sykorova et al.[11)]

Maceral group	Maceral subgroup	Maceral
Huminite	Telohuminite	Textinite
		Ulminite
	Detrohuminite	Attrinite
		Densinite
	Gelohuminite	Corpohuminite
		Gelinite

The structural constituent of brown coal was identified as huminite by Sza´decky-Kardoss in 1949. **Table 1.1** shows the classification of huminite, with attrinite of the detrohuminite subgroup typically making up around 90% of the groundmass of soft brown coal.[11)] The Loy Yang brown coal used in this study is classified as a soft brown coal.

The catalytic behavior of metal-loaded brown coal has been studied by many researchers, with an investigation by Tomita et al. into the low-temperature gasification of brown coals catalyzed by nickel concluding that around 85% of Yallourn brown coal reacts within 30 min in a steam environment at 500°C.[12)] Walker Jr. et al. also investigated the catalytic gasification of brown coal char, stating that Ca, K and Na loaded low-rank coals providing excellent catalysts for char gasification in O_2, CO_2 and H_2O environments.[13)] Tomita et al. studied the pyrolysis and steam gasification of nickel-loaded Yallourn brown coal, finding that around 80 wt% conversion was achieved at 600℃ and the gas yield was twelve-times that of the uncatalyzed reaction.[14)] Miura et al. investigated the gasification rates of chars from lower rank coals, through which they found that the gasification rate is controlled mainly by the catalytic effect of coal minerals such as Ca, K, Na.[15)] Nishiyama et al. investigated the reactivity of catalysts such as Na, Ca, Ni and Fe, which revealed that the composition of CO and CO_2 was in equilibrium with the steam partial pressure, indicating the presence of a water gas shift reaction downstream of the reaction bed.[16)] Domazetis et al. investigated the decarboxylation of brown coal containing iron hydroxyl complexes, from which they then proposed two reaction models for CO_2 and CO formation from carboxyl groups with iron hydroxyl complexes using computational chemistry[17).] Pyrolysis and gasification studies of brown coal from Victoria, Australia were reviewed by Li C.Z., who stated that finely dispersed alkali and alkaline earth metallic species in brown coal affects gasification reactivity, and summarized the effects of many kinds of catalyst conditions.[18)] The catalytic activity of brown coal containing metals is obvious from these studies, but although gasification reactions have been investigated at temperatures between 300 and 1000°C, only decarboxylation has been studied at temperatures less than 300°C.

Nickel-loaded Loy Yang brown coal was studied by Takarada et al. as an outstanding gasification catalyst[19)-27)], through which it became evident that nickel was loaded by ion

exchange. Furthermore, the Ni-loaded brown coal functioned as a gasification catalyst, and fine particles of nickel oxide were produced by burning at low temperatures of around 200°C. A schematic of this process is presented in **Fig.1.7**. Using this ability of brown coal, it is considered that copper ions from waste etching solution could be recovered by the same ion exchange method as nickel.

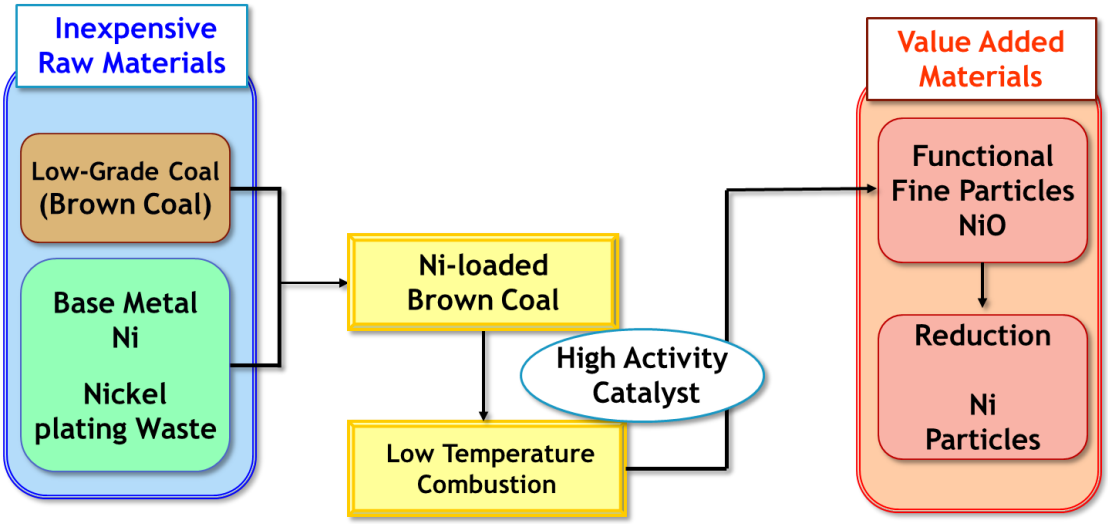

Fig.1.7 Conversion to value-added materials from inexpensive raw materials

1.3 Utilization of Recovered Copper

Fine copper oxide particles recovered from the combustion of Cu-loaded brown coal could have the following possible uses.

1) Copper Compound Solution

1-1) Remaking Etching Solution

Divalent copper chloride is reproduced by re-ion exchange of Cu-loaded brown coal with hydrochloric acid. Since combustion is no longer required, the brown coal could be reused as ion exchange media, offering most inexpensive process option. It is necessary though to pay attention to the presence of impurities such as residual chlorine ions and ammonium ions as pH adjusting agents and ash components originally included in the brown coal.

1-2) Plating Solution

Copper sulfate produced by leaching Cu-loaded brown coal with sulfuric acid can be used to produce a copper plating solution. Combustion of the Cu-loaded brown coal is not required, nor is copper chloride produced. It is, however, still necessary to pay attention to any impurities present.

2) Copper Compound Particles

2-1) Powder Metallurgy Material

Copper metal is often added into powder metallurgy materials to improve their strength, high temperature lubricity, thermal conductivity or protection performance.

Since such processes are typically carried out in a reducing atmosphere, recovered copper oxide particles can be directly added to metal powders without first requiring reduction. However, any residual chlorine ions are detrimental to such use.

2-2) Copper Catalyst

Fine copper particles could be used as a catalyst for:

a) Oxidation-reduction, or

b) Hydrogen generation in a fuel cell

Here, a high added value is obtained, but particle size control is important. Copper-loaded brown coal can also play the role of a catalyst, but the brown coal is combustible.

1.4 Combustion Models and Mechanisms

1.4.1 Gas-Solid Reaction Models

Many researchers have investigated gas-solid reactions, with several reaction models having been proposed. This includes the unreacted shrinking core model presented by Kunii and Levenspiel, as well as several reaction models of the reaction zone such as the volume reaction model, grain model and random pore model listed in **Fig.1.8**.[28)-32)]

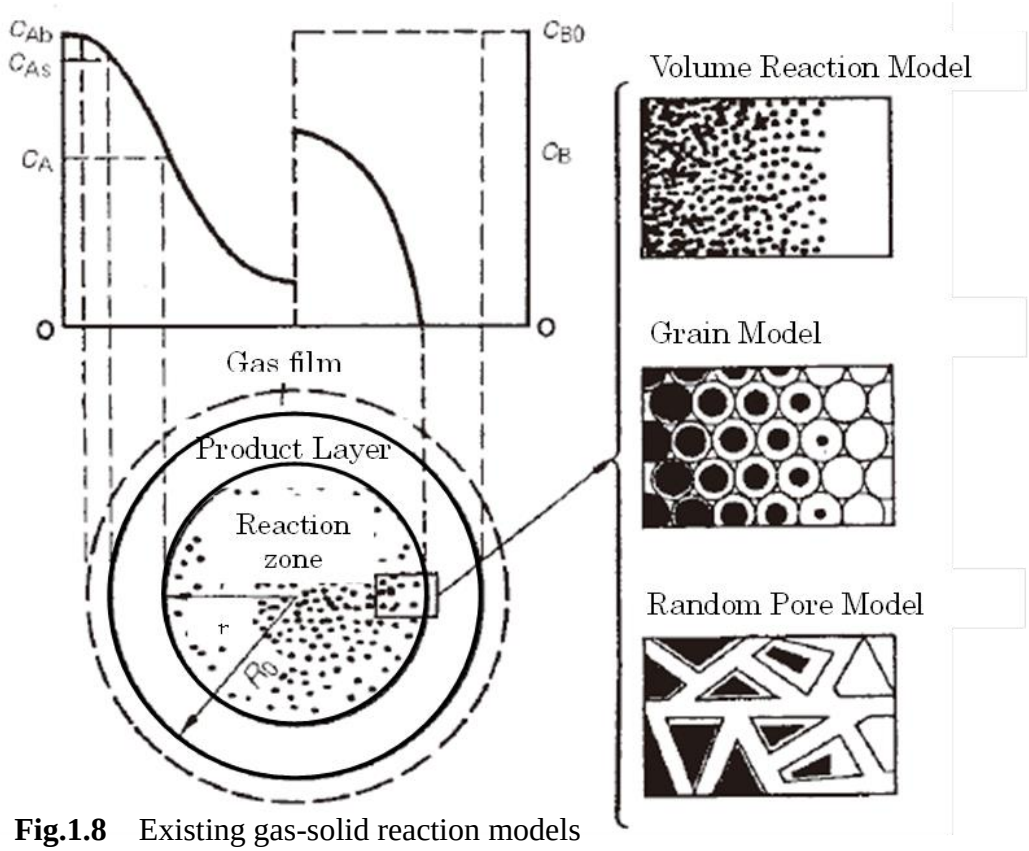

Fig.1.8 Existing gas-solid reaction models

Source: Kagaku Kougaku Binran 6th Edition, p951[28)]

The unreacted shrinking core model exhibits some discrepancies when compared with actual brown coal combustion phenomena. This is caused by the fact that the model considers the particle size to remain stable during reaction, whereas SEM observation has shown that it in fact changes during combustion. Since brown coal contains pores, residual ash is

simultaneously produced inside the core of the coal particles. Thus, in the case of catalytic reaction by an ion-exchanged metal, the main reaction zone may in fact occur on the walls of the pores inside the coal particles.

1.4.2 Catalytic reaction mechanisms

There are two kinds of surface reaction exhibited by a metal loaded catalyst, both of which are illustrated in **Fig.1.9**. [33)]

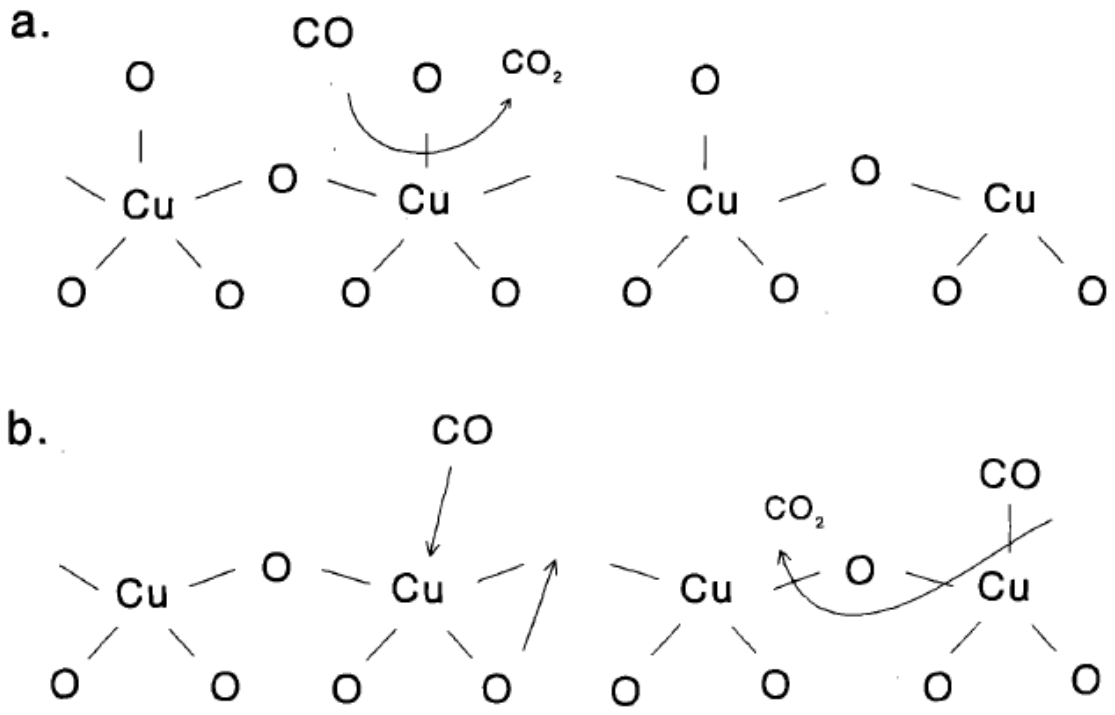

Fig.1.9 Catalytic reaction mechanisms: (a) Eley-Rideal mechanism, (b) Langmuir-Hinshelwood mechanism and lattice oxygen diffusion. Source: Dekker et al. [33)]

In the Eley-Rideal mechanism (Fig.1.9a), oxygen is adsorbed on the copper surface where it reacts with gaseous CO, with the resulting CO_2 being then desorbed from the copper surface. With the Langmuir-Hinshelwood mechanism (Fig.1.9b), on the other hand, CO is adsorbed on the copper surface and reacts with oxygen present there, with the CO_2 formed being then desorbed from the copper catalyst. In the case of copper oxide, lattice oxygen can provide the reactant oxygen, and so the diffusion of this lattice oxygen to the reaction surface is a possible reaction rate controlling step.

1.5 Purpose of This Research

In order to commercialize the copper recovery method proposed here, critical control factors of copper particle size, chemical structure, purity, process cost and ease of scale-up need to be clarified. Since the copper loading of brown coal and combustion temperature of Cu-loaded brown coal are key factors in determining the process cost, the copper loading

conditions and reaction kinetics of low temperature combustion were studied by TG analysis. With the subsequent discovery that Cu-loaded brown coal combusts at a lower temperature than nickel-loaded brown coal, the mechanism of this low-temperature combustion was studied further for its potential catalyst application. The CuO particle formation mechanisms were also studied, as the particle size is strongly related to performance when used for powder metallurgy. The ultimate purpose of this research, however, is to recover and produce valuable copper materials from industrial waste water using the intrinsic properties of inexpensive brown coal.

1.6 Configuration of this Thesis

Chapter 2 summarizes the challenges faced in copper recycling, identifying the key factors of process cost and various technical issues. The research procedure was planned so as to investigate these key points.

The ion exchange capability of brown coal is studied in Chapter 3, where it is found that in order to minimize the process cost of this recovery process, it is necessary to ensure a greater copper loading per unit mass of brown coal mass, reduce the amount of pH adjusting agent, use less wash water, reuse the brown coal, reduce the process time and maximize the copper yield. As part of this, the effects of pH, stirring time, repetition and dilution on copper loading were investigated. The chemical structure of Cu-loaded brown coal was also analyzed and is discussed.

In Chapter 4, the low-temperature combustion of Cu -loaded brown coal is studied and the copper compounds produced by combustion are characterized. Kinetic studies made to quantify the advantage of using Cu -loaded brown coal and investigate the mechanisms by which it functions are also reported. Estimated reaction mechanisms are proposed and discussed using references and simulation. The decarboxylation and deammoniation reactions are studied to quantify their effect on the rate of weight loss, and the catalytic effect was investigated and discussed using computational chemistry.

The formation of copper particles by the combustion of Cu-loaded brown coal is studied in Chapter 5, where a modified percolation model and coalesced particle formation model are proposed and discussed. The effects of raw brown coal size and copper loading on the CuO particle size were investigated to verify these models.

Chapter 6 provides a summary of the potential applications for the recovered copper, with its use in creating copper plating solutions or as a metallurgical material being investigated. As the catalytic effect of the copper could also find use in oxidation-reduction or hydrogen generation, the optimal conditions for this are also discussed in this chapter.

The conclusions drawn from this research and the prospects for future work are summarized in Chapter 7.

In Appendix-1, the simulation code for the Langmuir-Hinshelwood（LH）model is listed, while Appendix-2 present the code for the 2D-modified percolation model. Both simulations were coded using visual basic for excel.

1.7 References

1) Copper Development Association Inc., *2013 Technical Report*, www.copper.org
2) WECC, *WECC Global PCB Production Report For 2012*, August (2013)
3) Horiuchi, T., Shimizu, H., Shibata, K., *Hitachi Chemical Technical Report*, 36, 33-36(2001)
4) Matsumoto, M., Nakayasu, K., Yamakawa, H., *Fujitu.*52, 3, 218-224(2001)
5) Iosaki, M., Z117, *SCEJ 39th Autumn Meeting at Sapporo* (2007)
6) World Energy Council, *World Energy Resources 2013 Summary Report*
7) http://www.tepco.co.jp/fukushima_hq/reconstruction/igcc-j.html
8) Wender, I., *Catal. Rev. – Sci. Eng.*, 14, 1, 97–129 (1976)
9) Murakami, M.; Fuda, K.; Sugai, M., *J. of MMIJ*, 125, 38-42 (2009)
10) Lafferty, C.J., Hobday, M., *Fuel*, 69, 1, 78-83(1990)
11) Sykorova, I., Pickel, W., Christanis, K., Wolf, M., Taylor, G.H., Flores, D., *Int. J. Coal Geol.*, 62, 85-106 (2005)
12) Tomita, A., Ohtsuka, Y., Tamai, Y., *Fuel*, 62, 2, 150–154 (1983)
13) Walker Jr., P.L., Matsumoto, S., Hanzawa, T., Muira, T., Ismail, I.M.K., *Fuel*, 62, 2, 140–149 (1983),
14) Tomita, A., Watanabe, Y., Takarada, T., Ohtsuka, Y., Tamai, Y., *Fuel*, 64, 6, 795–800 (1985)
15) Miura, K., Hashimoto, K., Silveston, P., *Fuel*, 68, 11, 1461–1475 (1989)
16) Nishiyama, Y.; Terada, K., *Kagaku Kougaku Ronbunsyu*, 20(1), 793 (1994)
17) Domazetis, G., Raoarun, M., James, B.D., *Energy Fuels*, 20, 1997-2007 (2006)
18) Li, C.Z., *Fuel*, 86, 1664–1683 (2007)
19) Le, D., Xiao, X., Morishita, K., Li, L., Takarada, T., *J. Chem. Eng. Jpn.*, 43, 443-450 (2010)
20) Li, L., Morishita, K., Mogi, H., Yamasaki, K., Takarada, T., *Fuel Process. Technol.*, 91, 889-894 (2010)
21) Meesuk, S., Cao, J., Sato, K., Ogawa, Y., Takarada, T., *Energy Fuels*, 25, 4113-4121 (2011)
22) Meesuk, S., Cao, J., Sato, K., Ogawa, Y., Takarada, T., *Energy Fuels*, 25, 5438-5443 (2011)
23) Meesuk, S., Cao, J., Sat, o K., Ogawa, Y., Takarada, T., *J. Anal. Appl. Pyrolysis*, 94, 238-245 (2012)
24) Cao, J. P., Li, L. Y., Morishita, K., Xiao, X. B., Zhao, X. Y., Wei, X. Y., Takarada, T., *Fuel*, 104, 1-6 (2013)
25) Xiao, X., Meng, X., Le, D. D., Takarada, T., *Bioresour. Technol*., 102, 1975-1981 (2011)
26) Cao, J. P., Xiao, X. B., Zhang, S. Y., Zhao, X. Y., Sato, K., Ogawa Y., Wei, X. Y., Takarada, T., *Bioresour. Technol*., 102, 2009-2015 (2011)
27) Le, D. D., Xiao, X., Morishita, K., Xianbin, X., Takarada, T., *J. Chem. Eng. Jpn.*, 57, 4251

(2009)
28) The society of chemical engineering Japan, *Kagaku Kougaku Binran 6th Edition*, p951, Maruzen publishing co., ltd. (1999)
29) Ishida, M., Wen, C.Y., *AIChE Journal*, 14, 2, 311-317 (1968)
30) Bahatia, S.K., Perlmutter, D.D., *AIChE Journal*, 26, 3, 379-385 (1980)
31) Homma, S., Ogata, S., Koga, J., Matsumoto, S., *Chem. Eng. Sci.*, 60, 4971-4980 (2005)
32) Amrei, H.D., Jamshidi, E., Ebrahim, H.A., *Cornel University Library*, Sept.(2014)
33) Dekker, F.H.M., Klopper, G., Bliek, A., Kapteijin, F., Moulijin, J.A., *Chem. Eng. Sci.*, 49, 24A, 4375-4390(1994)

Chapter 2 Challenges of Copper Recycling

2.1 Introduction

The recycling of copper from industrial waste solutions has been studied by a number of researchers around the world[1-5]; however, as neutralization is impaired by calcium and iron contaminants, the purification cost is usually too high to economically recycle copper. Moreover, electrolysis consumes a lot of energy and leaves residual chlorine ions in the deposited copper, making it unsuitable as an on-site recycling system. In this work, an ion exchange method based on using brown coal is studied as an alternative approach. The key factors influencing the process cost and the technical issues of ion exchange using brown coal are discussed in this chapter, based on which a research procedure is developed and outlined.

2.2 Key Process Cost Factors

The copper recovery processes proposed in this work is illustrated in **Fig.2.1** and **Fig.2.2**. Fig.2.1 shows the wet process, in which the products are all copper solutions. As this eliminates the need for drying or combustion of the coal, the energy cost is minimized. The recovered copper chloride can be used as an etching solution, while the copper sulfate can be used as a copper plating solution. Brown coal is used in the copper loading process as an ion-exchange agent, and since the trapped copper is re-exchanged or leached using acid, this brown coal could conceivably be reused. Material cost other than the waste etching solution therefore consists simply of the pH adjusting agent, brown coal (re-usable) and acid. The other major cost is that associated with treating the water used to remove the pH adjusting agent and chlorine ions, which is mostly influenced by the copper loading per unit of brown coal mass. This, in turn, is determined by the batch size of the operation, the make-up cost for damaged brown coal, and the waste water volume. Other factors include the amount of pH adjusting agent, chlorine ions and metallic impurities present in the initial brown coal that can be allowed to remain, which will vary depending on the intended application.

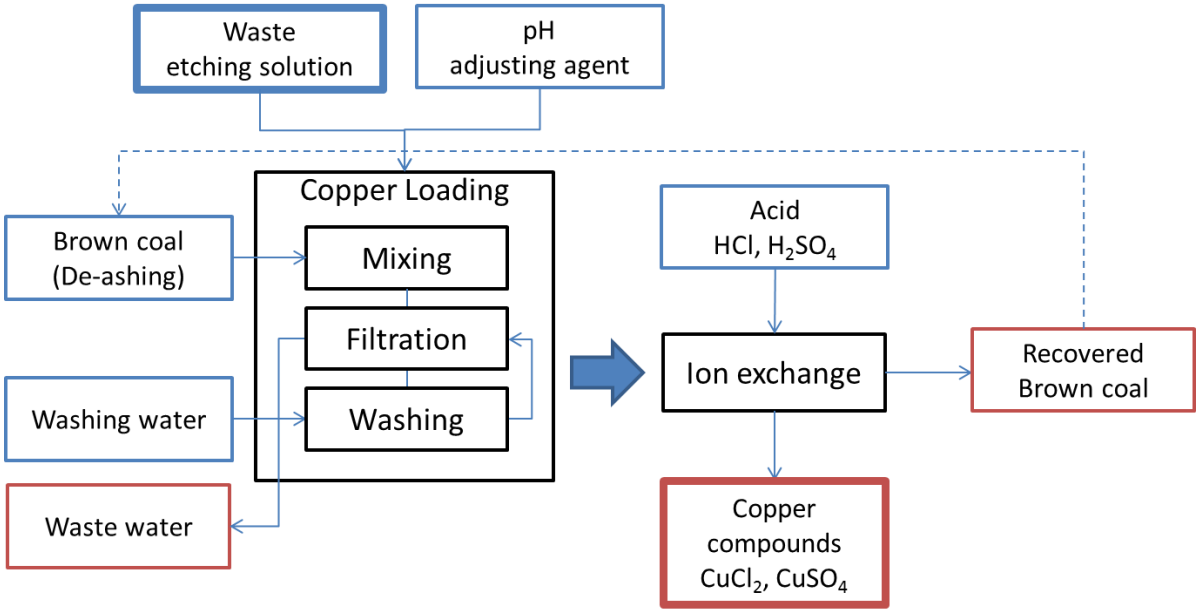

Fig.2.1 Schematic diagram for the recovery of copper from waste copper solutions

Fig.2.2 shows the process for producing copper oxide particles. Here, once the brown coal is loaded with copper, it is dried and combusted to produce copper oxide particles. The key factors influencing the process cost in this case are the copper loading and energy required. Low-temperature combustion of the Cu-loaded brown coal is obviously beneficial to reducing the energy consumption method. Also important are the allowable amounts of residual pH adjusting agent, chlorine ions and metallic impurities initially present in the brown coal or in previous process, which are determined by the intended application. Furthermore, as the temperature at which dioxin is typically produced (300–400°C) is reduced to 200°C with copper chloride[6], a lower temperature is desirable when residual chloride is present.

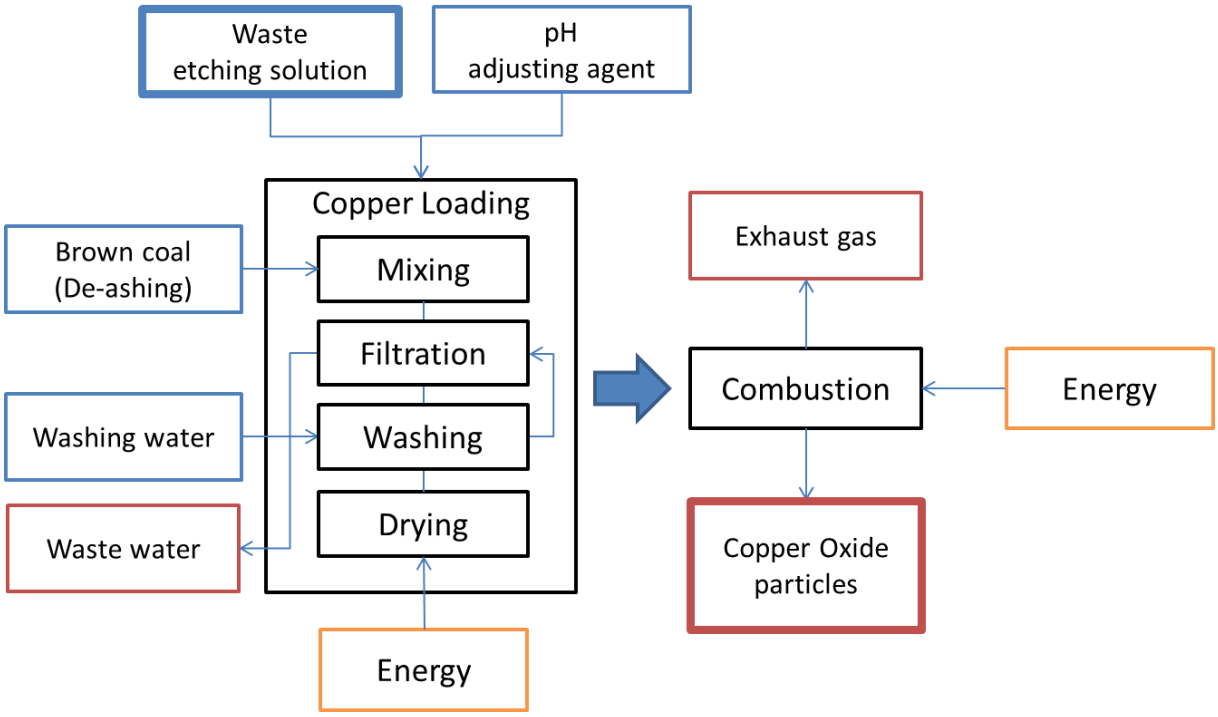

Fig.2.2 Schematic diagram for the recovery of copper as copper oxide particles

2.3 Technical Issues to be Studied

There are three key points of focus to this study:

1) To investigate the optimal conditions for maximum Cu-loading

   Because Cu-loading is one of the key factors influencing the process cost.

2) To study why Cu-loaded brown coal combusts at a lower temperature

   It is important to understand the mechanism behind the low-temperature combustion of Cu-loaded brown coal, as this affects the potential for scale up and the catalytic properties.

3) To elucidate the mechanism by which copper oxide particles form

   It is also important to achieve a desired particle size in this process, as this affects the metallurgical and catalytic properties.

A schematic of the research procedure is presented in **Fig.2.3** with each of the key points being studied and discussed in Chapter 3, 4 and 5.

Process cost was estimated in this study, but was omitted in this thesis on account of the fact that it depends on the process scale, material, labor, waste treatment and energy cost; all of which are in flux. The energy consumption of electrolysis is about 4-8kWh/kg-Cu[3)-4)], and is there is no heating in the case of the wet process, the total energy consumption is relatively small. In the case of CuO particle recovery, the heat of combustion of brown coal is around 62-63kWh/kg-Cu, and the heat of drying is around 2kWh/kg-Cu. Thus, with a continuous process, the heat of reaction is much greater than that required for drying and the heat loss. Consequently, the energy consumption is also quite small.

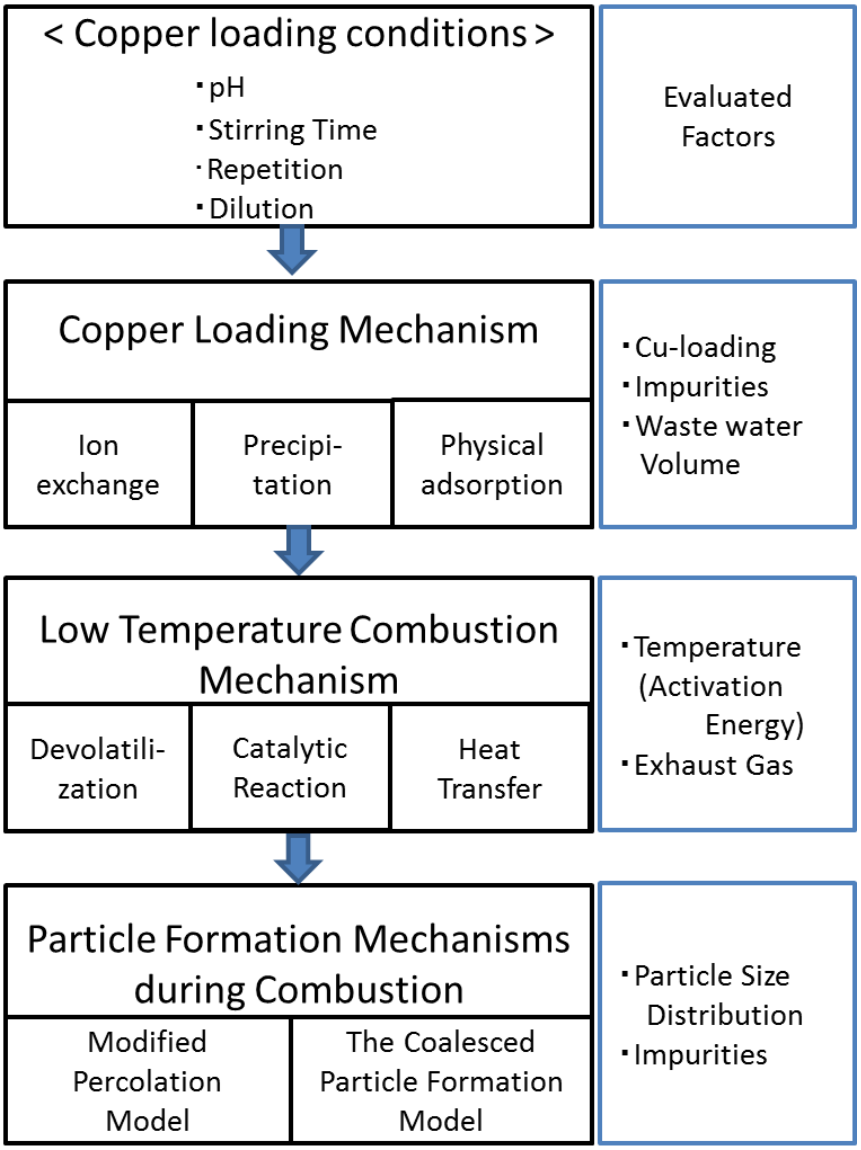

Fig.2.3 Schematic of the research procedure used for this thesis

2.4 Conclusion

The main challenges to recycling copper through ion exchange with brown coal have been outlined, with the key factors identified being the maximum copper loading, as well as the mechanisms behind low temperature combustion and copper oxide particle formation. These three key points were investigated via the research procedure of this thesis. Since Cu-loaded brown coal combusts under low-temperature conditions, it is believed to take advantage of the natural catalytic effect of metal-loaded brown coal. All these factors, including the catalytic ability, are investigated and discussed in Chapter 3, 4 and 5.

2.5 References

1) Matsumoto, M., Nakayasu, K., Yamakawa, H., *Fujitu*.52, 3, 218-224 (2001)
2) Hyvarinen, O., Hamalainen, M., *Hydrometallurgy*, 77, 61-65 (2005)
3) Huang, Z., Xie, F., Ma Y., *J. Hazard. Mater.*, 185, 155-161 (2011)

4) Gayar, D.A., El-Shazly, A.H., El-Taweel, Y.A., Sedahmed, G.H., *Chem. Eng. J.*, 162, 877-882 (2010)
5) Iosaki, M., *SCEJ 39th Autumn Meeting*, Sapporo (2007)
6) Takaoka, M., *Housyakou*, 20, 3 (2007)

Chapter 3 Ion Exchange using Brown Coal

3.1 Introduction

Copper ions in the waste etching solution are captured by brown coal through an ion exchange process, and so to apply this to the commercial recovery of copper from waste etching solution it is essential to quantify the copper ion exchange ability of brown coal and the effects of the operating conditions on loading, as well as clarify the mechanism of copper loading. It is these factors that determine the cost of the copper recovery process.

The pH of the solution, the mixing time and repetition, and the dilution effect on the loading were studied in detail. This found that the pH of the solution, and the repetition and dilution effect, are related to the amount of ammonia and waste water present in the ion exchange process, and that these influence the material cost and waste treatment cost of the process. Mixing time is related to the reactor size, and therefore also to the direct labor cost and energy consumption of the process.

Loading mechanisms were discussed by analyzing the loading structure using XPS. This indicated that it is possible to confirm the reasonableness of the process and estimate its scale-up effects by understanding the mechanisms involved.

3.2 Experimental

3.2.1 Materials

The medium used for recovering copper ions from the waste solution was brown coal sourced from Loy Yang in Australia, which was sifted to a size of 200–325 mesh. **Table 3.1** and **Table 3.2** show the proximate and ultimate analysis results for this coal. De-ashed coal was prepared by stirring at 60°C for 1 hr in 5 M HCl twice, then once in 12 M HF. This was followed by stirring in acid, dewatering by suction filtration, washing with deionized water, and finally drying for 6 hrs in an oven at 107°C under a N_2 atmosphere. The ash content of the resulting de-ashed brown coal was 0.017 wt%.

A copper chloride waste etching solution from the manufacturing of printed circuit boards (hereafter referred to as ETS (Cl)) was provided by Hitachi Chemical (**Table 3.3**).

Table 3.1 Proximate analysis of Loy Yang brown coal [wt%]

Moisture	Fixed Carbon (diff.)	Volatile Matter	Ash
18.17	27.33	53.84	0.66

Table 3.2 Ultimate analysis of Loy Yang brown coal [wt%]

C	H	N	S	O (diff.)
65.92	4.75	0.74	0.11	28.48

Table 3.3 Main components of ETS(Cl) [wt%]

Cu	Cl	pH
12	13	< 1

3.2.2 Copper Loading Method

The copper loading method is summarized in **Fig. 3.1**. Here, once the pH of the ETS (Cl) was adjusted by adding ammonium hydroxide, 1 g of dried Loy Yang coal was added to 0.2 g of the solution and stirred for 24 hrs at room temperature. This was then dewatered by suction filtration, washed with deionized water, and dried in an oven at 107°C for 6 hrs under a N_2 atmosphere. The dried Cu-loaded brown coal was then milled and sifted to a size of 200–325 mesh.

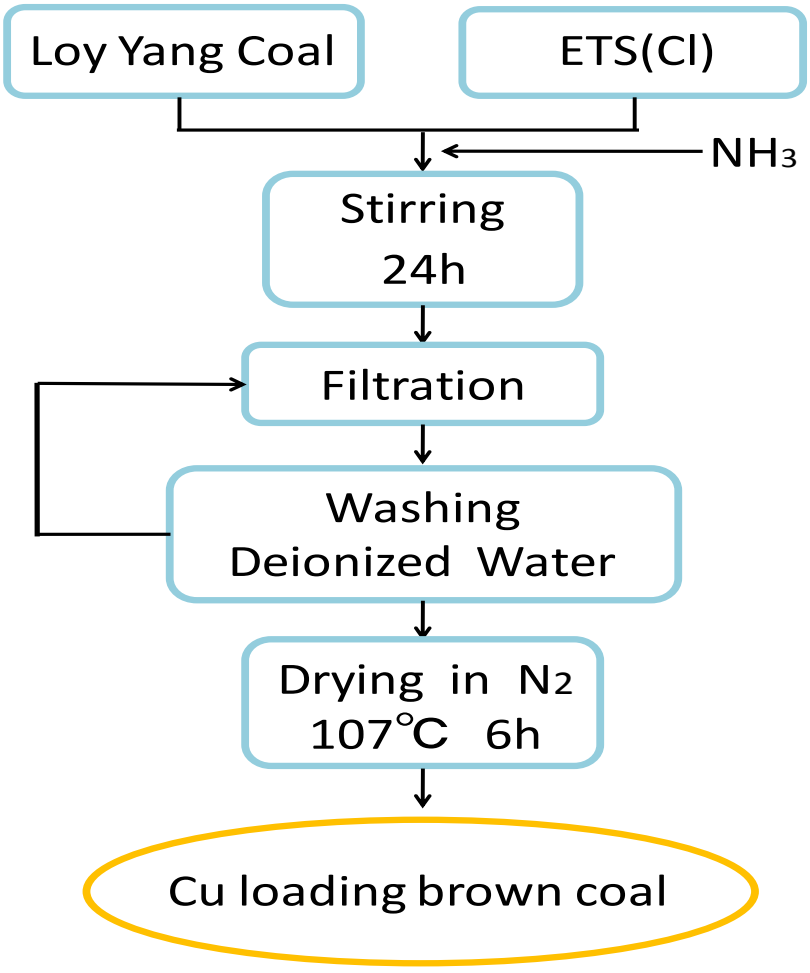

Fig. 3.1 Copper loading method

3.2.3 Evaluation Methods

Copper loading of the brown coal was measured using by a Shimadzu AA-6400F atomic absorption spectrophotometer. For this, the copper loaded onto the brown coal was extracted 3

times using 1 M nitric acid, and then diluted with deionized water to a concentration suitable for AA measurement. The structure of the loaded copper was analyzed by XPS (Rigaku Smart Lab). The absorption spectrum of the solution was measured by a Shimadzu UV-1800 across a wavelength range of 300–800nm with step size of 2nm.

3.3 Results and Discussion

3.3.1 Mechanism of Copper Loading on Brown Coal from ETS(Cl)

3.3.1.1 Effect of pH on Copper Loading

Given that the pH of the waste etching solution is adjusted by adding ammonium hydroxide as part of the ion exchange process, its effect on copper loading was studied. The results obtained are summarized in **Fig. 3.2**, in which it can be seen that around 8.5wt% copper can be loaded on Loy Yang brown coal by ion exchange when the pH is between 9 and 11.5.

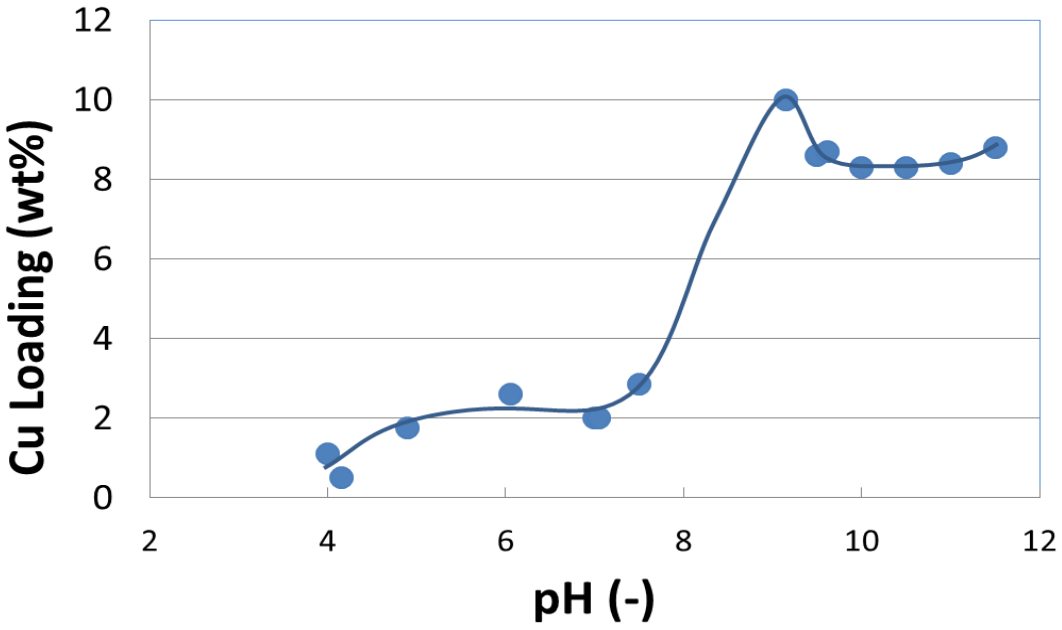

Fig. 3.2 Effect of pH on copper loading

When the pH is lower than 8, the Cu-loading is reduced to around 2.5wt% or less. Since $Cu(OH)_2$ particle deposition and/or physical absorption could be the mechanism for Cu-loading in this low-pH range, the Cu-loading by ion exchange is estimated to be 76% (=6/8.5) or more of the total based on the loading amounts pH values lower and higher than 8 in Fig.3.2.

Since the chemical structure and particle size of the copper compounds formed could potentially affect the catalytic activity of Cu-loaded brown coal, various Cu-loadings were prepared under different pH conditions. The reaction kinetics of low temperature combustion of Cu-loaded brown coal, as determined by TG analysis, are presented in Chapter 4.

The ion exchange mechanism is believed to be one in which the carboxy groups of brown coal exchange protons and complex cations such as $[Cu(NH_3)_4]^{2+}$, as is shown below[1)]:

$$2COOH + [Cu(NH_3)_4]^{2+} \Leftrightarrow COO\text{-}[Cu(NH_3)_4]\text{-}COO + 2H^+ \quad \cdots \text{Eq. (3.1)}$$

This means that with a low pH condition and high concentration of protons, the equilibrium reaction can't go any further to the right. When pH range is between 2.5 to 8.8, however, copper ions react with hydroxyl ions to precipitate $Cu(OH)_2$ particles. When the pH is increased above 8.8 these $Cu(OH)_2$ particles dissolve, resulting in copper and ammonium complex ions such as tetraamminecopper(II) $[Cu(NH_3)_4]^{2+}$ being produced. Consequently, a pH greater than 9 is suitable for the ion exchange of copper by brown coal.

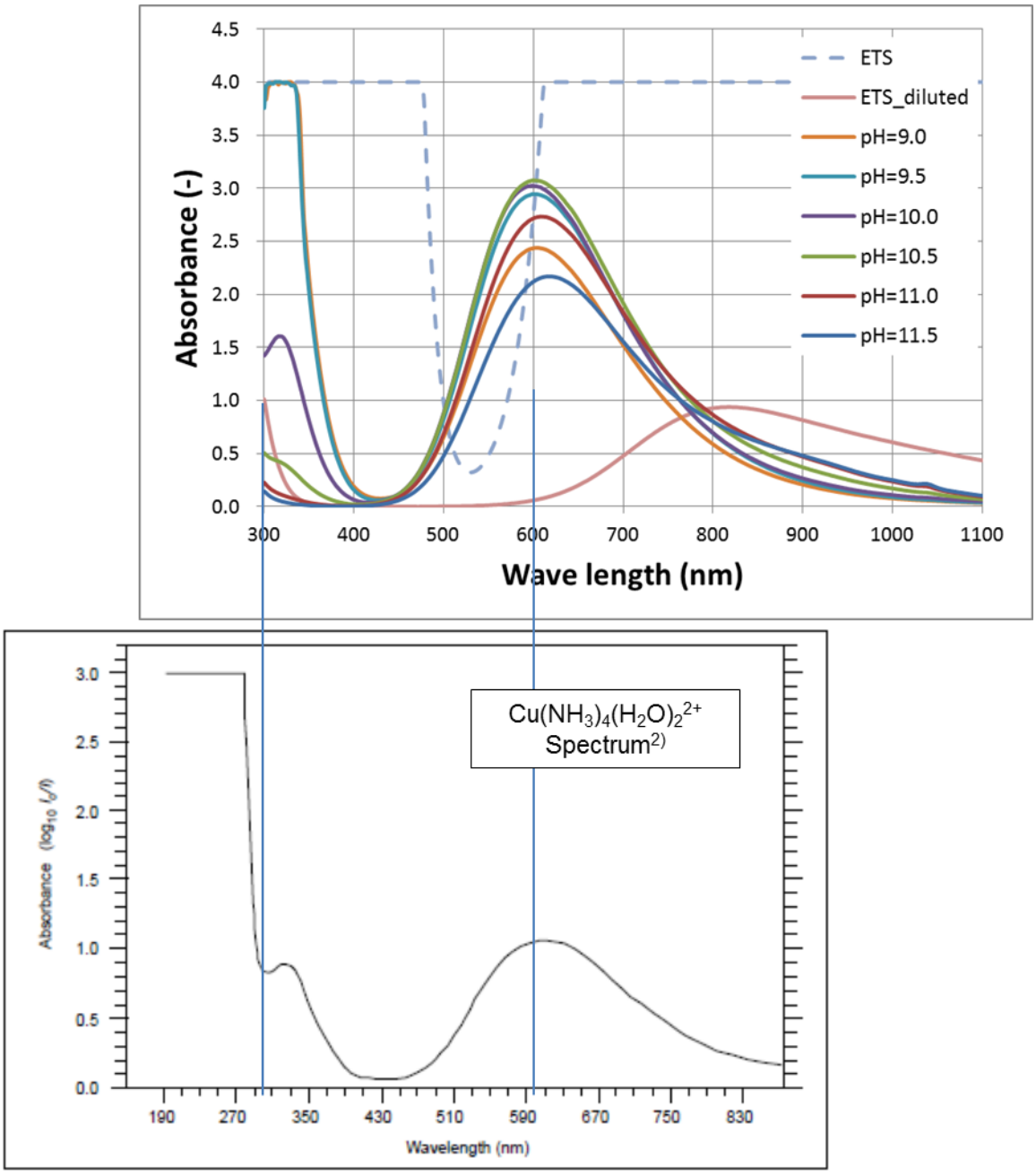

Fig. 3.3 Absorption spectrum of ETS(Cl) and pH adjusted (NH_4OH) waste etching solutions

Source of bottom graph: 'Modern chemical techniques: ultraviolet/visible spectroscopy', 99 (2015)[2)]

The absorption spectrum of the ETS(Cl) and pH-adjusted waste etching solutions are shown in **Fig.3.3**. Note that the maximum absorption wavelength of the ETS when diluted by deionized water is at around 800nm, while the maximum absorption wavelength of the pH-adjusted solution is shifted to 600nm. The bottom graph shows the absorption spectrum data for $Cu(NH_3)_4(H_2O)^{2+}$, which has been sourced from the Royal Society of Chemistry[2)]. Since the maximum absorption wavelength of the reference is also 600nm, this indicates that copper and ammonium complex ions such as tetraamminecopper(II) $[Cu(NH_3)_4]^{2+}$ are produced when the pH of ETS is adjusted by ammonium hydroxide.

Multiple mechanisms have been suggested as being capable of loading copper onto brown coal, namely ion exchange, $Cu(OH)_2$ particle deposition and physical absorption[3)-6)]. The Cu-loaded brown coal in this study was measured by XPS analysis to better understand the Cu-loading mechanism, the results of which are shown in **Fig. 3.4**. Note that after loading the COOH and NH_3 binding energies are shifted, and that a Cu(II)-N bond can now be detected, suggesting that copper and ammonium complex ions can be exchanged with protons of the carboxy group of brown coal. Moreover, in the Cu(2p) spectra, Cu (II)-N, $Cu(OH)_2$ and Cu_2O are all readily identified by wave form separation. Ion exchange is therefore not the only mechanism for copper loading, with $Cu(OH)_2$ particle deposition and physical absorption being very real possibilities.

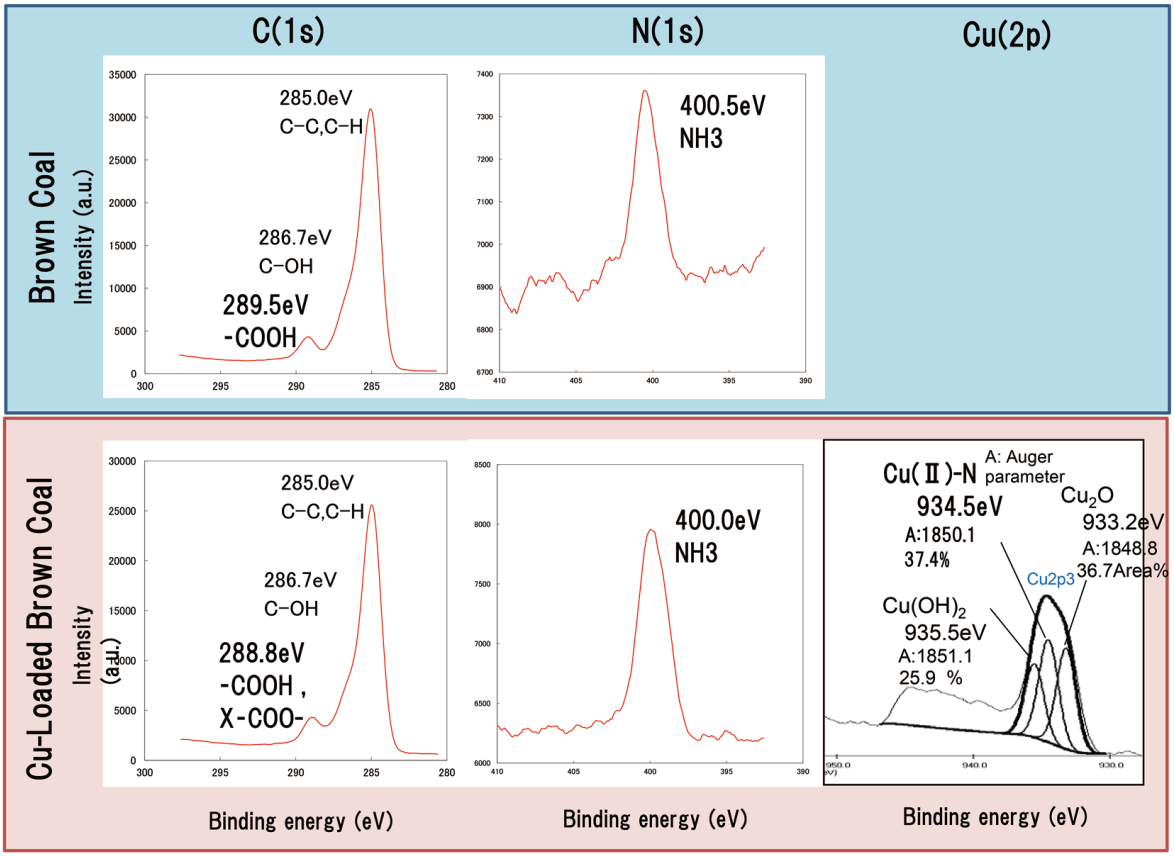

Fig. 3.4 XPS spectra of brown coal and copper-loaded brown coal

3.3.1.2 Effect of Stirring Time on Copper Loading

The dependency of copper loading on time was evaluated up till 1440 min, though **Fig. 3.5** shows that only 5 min stirring is sufficient for the exchange of copper ions and a copper loading of around 10.5 wt%. Increasing the time beyond 5 min results in a slight drop in copper loading; however, this can be attributed to the increase in solution temperature generated by the exothermic neutralization reaction when adding ammonium hydroxide, which shifts the endothermic equilibrium reaction Eq. (3.1) to the right.

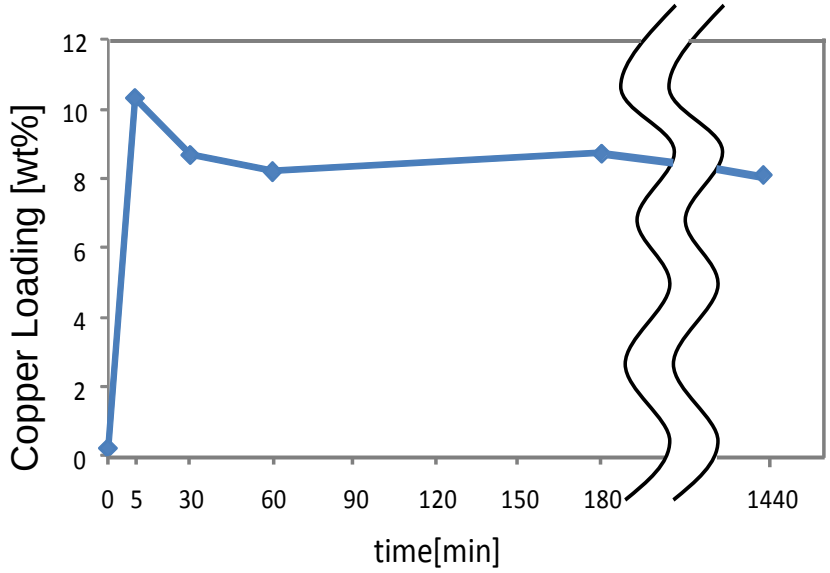

Fig. 3.5 Effect of stirring time on copper loading

3.3.1.3 Effect of Repetition on Copper Loading

Table 3.4 shows the results of repeated loading cycles on the total copper loading, wherein fresh brown coal was added to the filtrate after the first and second cycle. By the third loading, copper still remained in the filtrate despite the presence of more than enough brown coal. One reason for this might be the pH being lower than 8.8 during the loading process, as the copper ions can react with hydroxyl ions under these conditions (see Section 3.3.1.1). Consequently, a re-adjustment of the pH would be needed for repeated loading. The copper concentration is another factor limiting the copper loading, and so a diluted ETS (Cl) solution was tested to see whether copper recovery is still possible at low copper concentrations.

Table 3.4 Effect of repetition on copper loading

Item			1st time loading	2nd time loading	3rd time loading
Before Loading	Cu content of ETS(Cl) [g]		1.028	0.590	0.183
	pH		9.60	9.54	8.95
	Brown coal added [g]		5.05	5.04	5.07
After Loading	Cu-loading on Brown coal	[g]	0.438	0.407	0.152
		[wt%]	8.68	8.08	3.00
	Cu content of Filtrate [g]		0.590	0.183	0.031
	pH		9.54	8.95	7.54

3.3.1.4 Copper Loading from Dilute ETS (Cl) Solution

Low copper concentration solutions (1 and 10 ppm) were prepared by diluting the original ETS (Cl) solution with deionized water. These gave a filtrate copper concentration after ion exchange of 0.002 and 0.003 ppm, respectively, thereby demonstrating that copper recovery by brown coal from low concentration copper solutions is indeed possible.

3.3.2 State of the Copper Ion Exchanged

Multiple mechanisms are considered in this chapter: ion exchange, $Cu(OH)_2$ particle deposition and physical absorption.

Ion exchange (pH 9–11.5) : COO-[$Cu(NH_3)_4$]-COO and similar complexes
Particle deposition (pH2.5-8.8) : $Cu(OH)_2$
Physical absorption : $CuCl_2$ and other copper compounds

The residual chloride in the CuO particles recovered was around 0.06–0.1wt%, even after multiple washings of the Cu-loaded brown coal, which is an undesirable level for using the recovered copper as a powder metallurgy material. There is therefore clearly a need to further optimize the process to reduce the washing cost and/or the amount of chloride residue.

The particle size of the CuO produced from $Cu(OH)_2$ particles is compared that obtained via a complex ion in Chapter 5. These results show that the initial state of the copper is not a significant factor in determining the CuO particle size. However, as the amount of copper loaded per unit weight of brown coal is higher when the pH is more than 9, the material cost of the process can be reduced by keeping the pH at 9.

3.4 Conclusion

An ion exchange method that uses Loy Yang brown coal for the recovery of copper from waste etching solutions of printed circuit board manufacturing was studied in this chapter, from which it was found that:

1. Copper ions in the waste solution can be loaded onto Loy Yang brown coal at room temperature to a concentration of around 8.5 wt% by adding ammonium hydroxide to adjust the pH to 9–11.5 while stirring. At this pH range, copper and ammonium complex ions such as tetraamminecopper(II) $[Cu(NH_3)_4]^{2+}$ are considered to be produced and exchanged with protons from the carboxy groups in brown coal, causing the copper to become highly dispersed in the brown coal when adsorbed.

2. The maximum copper loading achieved differs significantly with pH, decreasing from 8.5wt% at a pH of more than 9 to around 2.5wt% when the pH is reduced below 9. At a pH of 9–11.5, it is believed that ion exchange is the main mechanism for copper loading, accounting for around 76% (=6/8.5) or more.

3. Ion exchange is not the only mechanism of copper loading, with $Cu(OH)_2$ particle deposition and physical absorption being other possibilities.

4. The rate of copper loading is so rapid at room temperature that only 5 min is needed to achieve a maximum, at least on a laboratory scale.

5. Adjusting the pH is important to ensuring the effectiveness of loading and ion exchange, making it possible to recover copper even from low concentration solutions.

All this combined illustrates the effectiveness of the ion exchange method in terms of providing a fast, low energy process that works at room temperature.

3.5 References

1) Murakami, M., Fuda, K., Sugai, M., *J. of MMIJ*, 125, 38-42 (2009)
2) http://www.rsc.org/learn-chemistry, *'Modern chemical techniques: ultraviolet/visible spectroscopy'*, 99 (2015)
3) Takarada, T., *Funsai*, No.53,50-56 (2010)
4) Goyal, M., Rattan, V.K., Aggarwal, D., Bansal, R.C., *Colloids Surf.*, A190,229-238 (2001)
5) Panayotova, M.I., *Waste Manage.*, 21,671-676(2001)
6) Milicevic, S., Boljanac, T., Martinovic, S., Vlahovic, M., *Fuel Process. Technol.*, 95,1-7 (2012)

Chapter 4 Low Temperature Combustion of Copper-Loaded Brown Coal

4.1 Introduction

Copper oxide particles can be recovered by simply combusting Cu-loaded brown coal, and previous studies have found that Ni-loaded brown coal combusts at a low temperature of around 200°C. The combustion behavior of Cu-loaded brown coal was therefore evaluated through TG analysis and compared with the behavior of Ni-loaded brown coal.

If combustion can be achieved at low temperature and in a short period of time, this will offer the benefit of a low energy consumption. Furthermore, as dioxin is typically produced from copper chloride at 300–400°C, a lower temperature is desirable in instances in which there is some residual chloride.

Here, the reaction kinetics and mechanism are discussed using Coats-Redfern method[1)] to determine the activation energy, with Semenov's theory[2)] of spontaneous combustion being used as a model for computer simulation to estimate the reaction mechanisms. An understanding of the kinetics and reaction mechanisms is considered essential to the design and scale-up of a cost effective process.

4.2 Experimental

4.2.1 Formation of Fine Copper Oxide Particles

Dried Cu-loaded brown coal (1 g) was placed in a square tray, and then heated in an electric muffle from RT to 500°C over a period of 45 min (ramp1), then from 500 to 815°C over 60 min (ramp2), as per JIS M8812. Small samples representing various temperature conditions were also prepared for thermo-gravimetric (TG) analysis.

4.2.2 Evaluation methods

Weight loss during combustion was measured using the TG apparatus shown in **Fig.4.1**, in which the sample volume, gas flow rate, heating ramp rate and maximum temperature were all varied depending on the experimental purpose. Typical conditions used are listed in Fig.4.1. A perforated cell was used to prevent the reaction being controlled by oxygen diffusion. Sample volume was considered important because the thickness of the powder layer directly influences the difference in temperature and gas composition between the inside and outside of the layer. Morphological studies of the residual ash were performed by XRD (MAC M03XHF22 and RINT RAPID), with the particle shape being observed by FE-SEM (JEOL JSM-6700F).

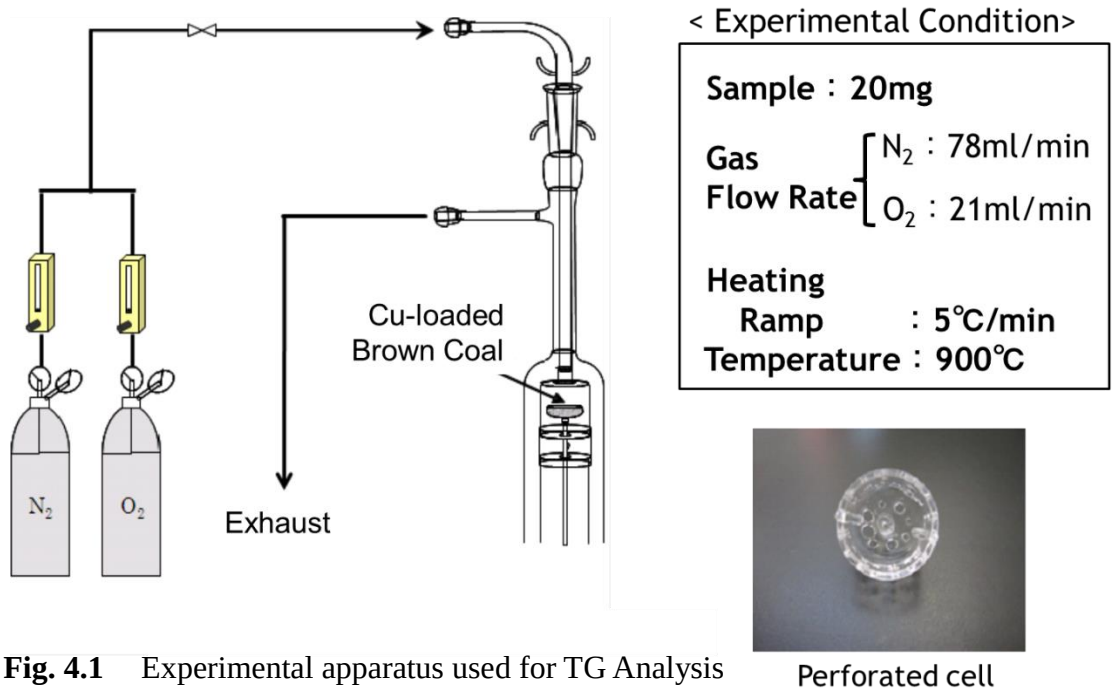

Fig. 4.1 Experimental apparatus used for TG Analysis

4.3 Results and Discussion

4.3.1 Combustion Phenomena of Cu-loaded Brown Coal

4.3.1.1 Analysis of Burnt Cu-loaded Brown Coal Residue

Dried Cu-loaded brown coal with a copper loading of 8.56wt% was burnt at 815°C under the conditions outlined in the JIS M8812 method. **Fig. 4.2** shows a SEM image and **Fig. 4.3** the XRD spectra of the burnt Cu-loaded brown coal residue. This data reveals that the size of the particles is around 0.5–1.0μm, and that they have a chemical formula of CuO. The total CuO content of the residue is 91.8wt%, but when de-ashed brown coal is used for copper loading, this increases to 98.8wt%.

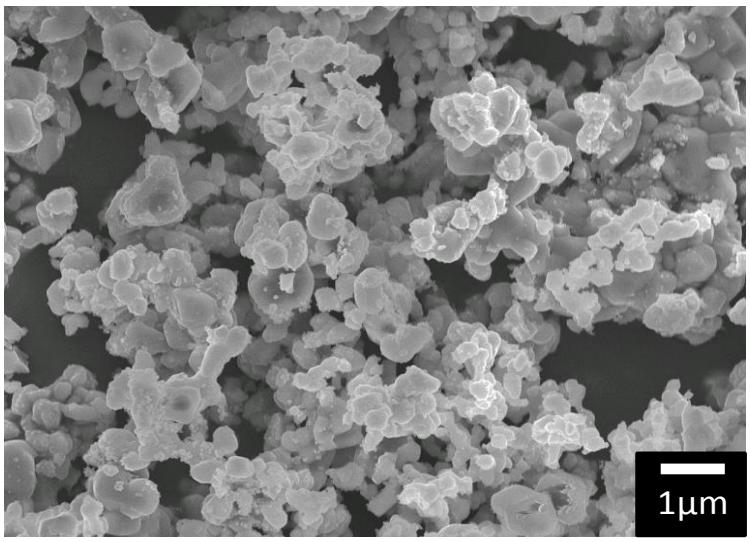

Fig. 4.2 SEM image of ash produced by burning Cu-loaded Loy Yang brown coal at 815°C (Cu-loading 8.56wt%)

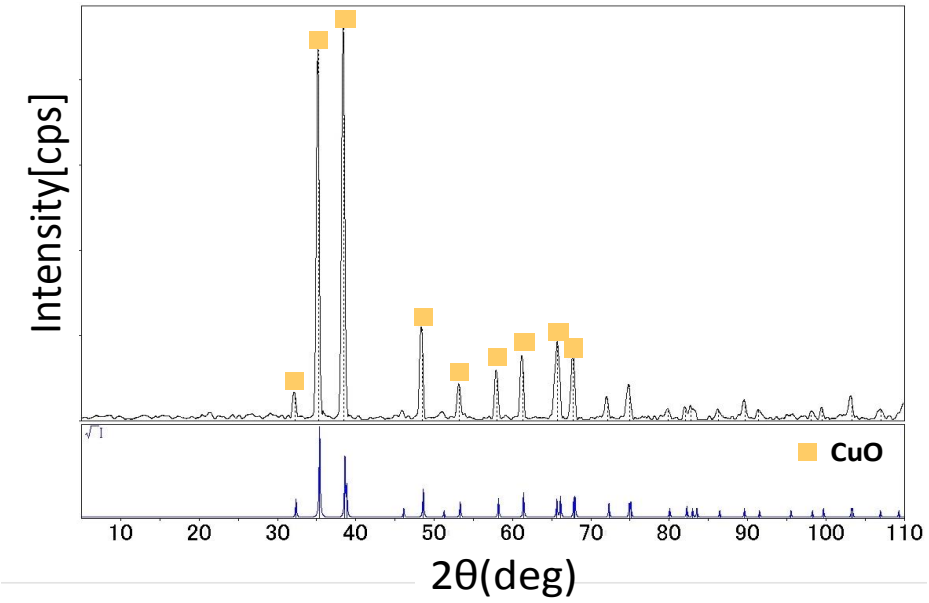

Fig. 4.3 XRD spectra of ash produced by burning Cu-loaded Loy Yang brown coal at 815°C (Cu-loading 8.56wt%)

4.3.1.2 Weight Loss Curve of Cu-loaded Brown Coal

The weight loss curves obtained by TG analysis for Cu-loaded brown coal that are presented in **Fig. 4.4** reveal a copper loading of 8.56wt% when de-ashed, which compares well with the 8.8wt% Ni content of the Ni-loaded brown coal. The weight of the Cu-loaded brown coal gradually decreases in the early stages of combustion due to moisture evaporation, with a more rapid decrease observed at 160–180°C that finishes within 3–5 min. The dotted line shows the weight loss curve of the Ni-loaded brown coal for comparison, which only starts to rapidly lose weight at 200–210°C. As volatile matter is normally only released from coal and burnt at 400–600°C, it would seem that both copper and nickel play a catalytic role in gasification and/or oxidation.

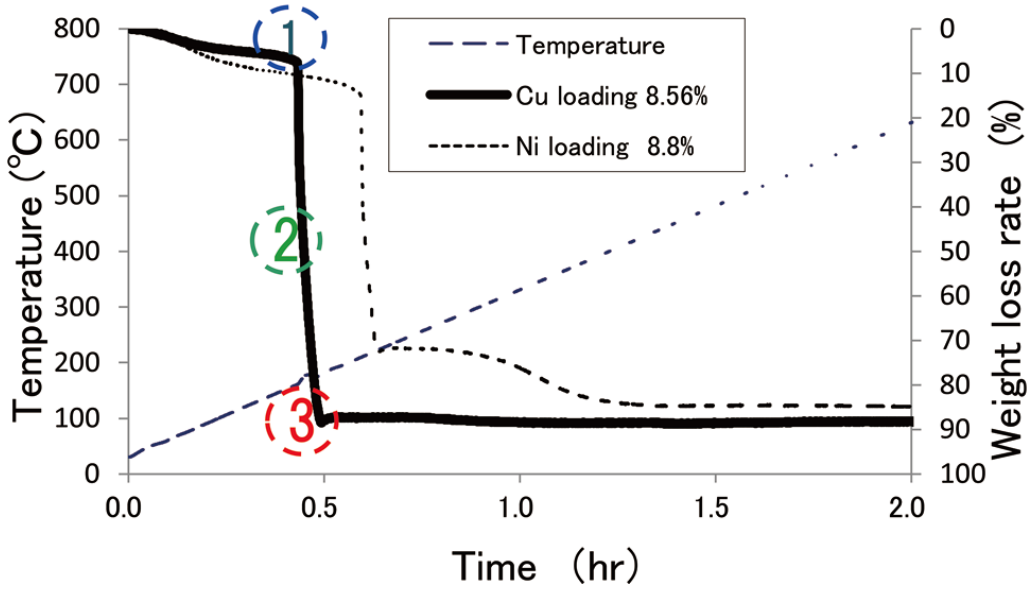

Fig. 4.4 Weight loss curves of Cu-loaded brown coal (Cu-loading 8.56wt%, de-ashed) and Ni-loaded brown coal (Ni-loading 8.8wt%, de-ashed)

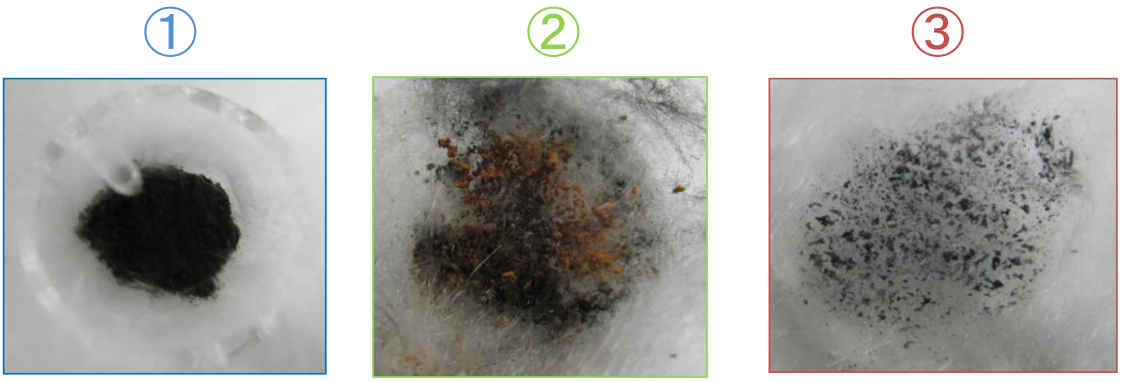

Fig. 4.5 Photos of de-ashed, Cu-loaded Loy Yang brown coal (Cu-loading:8.56wt%) during burning in a simulated air atmosphere ①before heating, ② at 165°C and ③ at 180°C

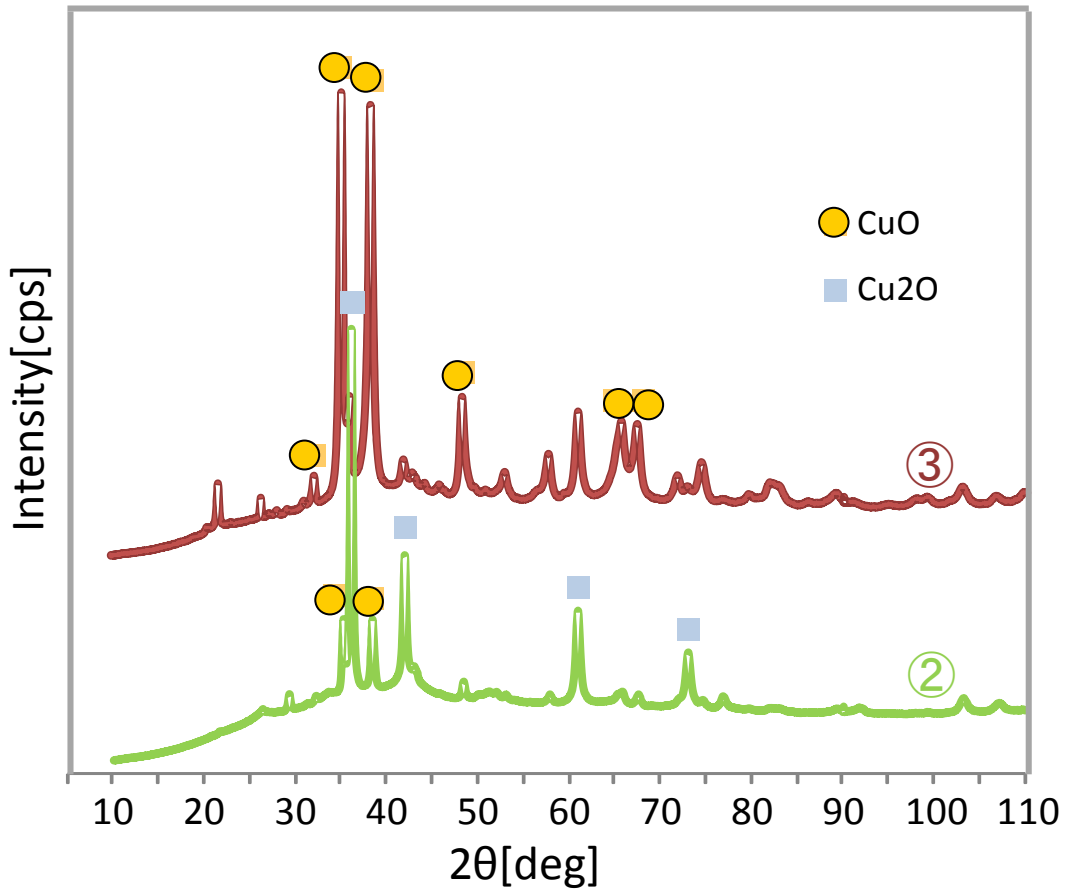

Fig. 4.6 XRD spectra of de-ashed, Cu-loaded Loy Yang brown coal during combustion at ② 165°C and ③ 180°C in simulated air

It was found that Cu-loaded brown coal can be burnt at an extremely low temperature of 160–180°C, which is even lower than the temperature of Ni-loaded brown coal combustion. As shown in Fig. 4.4, samples were taken: ① before heating, and during burning at ② 165°C and ③ 180°C. Photographs and XRD spectra for these samples are presented in **Fig. 4.5** and **Fig. 4.6**, respectively. Note that sample ② has a reddish-brown color, whereas sample ③ appears black. Similarly, the XRD spectra of sample ② is consistent with Cu_2O, while sample ③ matches with CuO. It is obvious from this that Cu_2O plays an important role as a catalyst for the gasification and/or oxidation of brown coal[3-9], and so further TG analysis was

undertaken to understand the formation mechanism of the Cu_2O particles. This entailed using a temperature ramp rate of 10°C/min, and stopping heating when the weight decrease reached intervals of 25, 50, 75 and 100%. **Fig. 4.7** shows the results of the subsequent XRD analysis, from which we see that only Cu was detected at 25% weight loss. At 50% loss both Cu and Cu_2O were detected, while at 75% loss Cu_2O, CuO and small peaks of Cu were observed. Finally at 100% loss, only CuO was detected. These results show that Cu captured by the carboxy group of brown coal is reduced and crystallized during the initial stage of combustion, when volatile matter is released, and that the Cu particles are then oxidized to Cu_2O and finally CuO. The overall combustion process can therefore be described as:

$$COO\text{-}[Cu(NH_3)_4]\text{-}OOC \rightarrow Cu \rightarrow Cu_2O \rightarrow CuO \qquad \cdots \text{Eq. (4.1)}$$

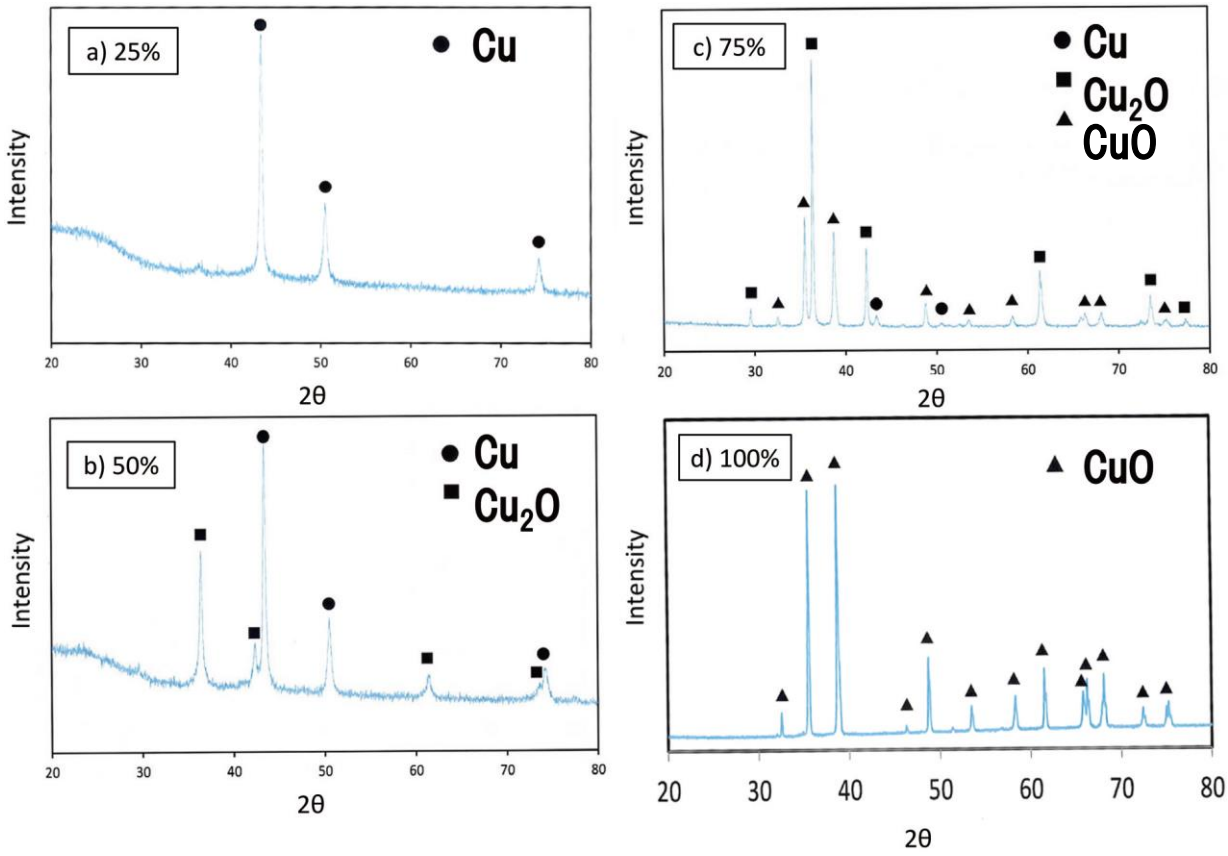

Fig.4.7 XRD spectra of Cu-loaded Loy Yang Brown Coal after a) 25%, b) 50%, c) 75% and d) 100% thermal weight loss at a ramp of 10°C/min

The SEM image of the residue of sample ③ at 180°C that is shown in **Fig. 4.8** reveals a particle size of around 0.5–1.0μm and a cubic shape suggestive of a cubic Cu and/or Cu_2O crystal structure. In contrast, the particles at 815°C in Fig. 4.2 all have rounded angles, which means that these particles were partially fused and sintered at this temperature. The particle formation and shape are discussed in more detail in Chapter 5.

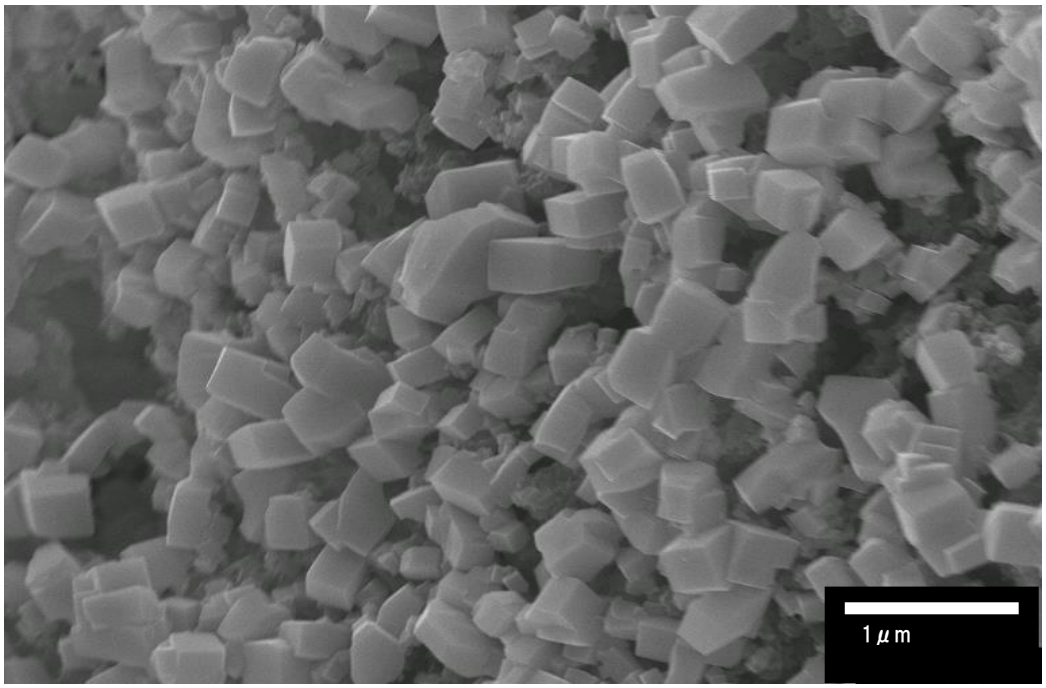

Fig. 4.8 SEM image of Cu-loaded brown coal particles heated to 180°C

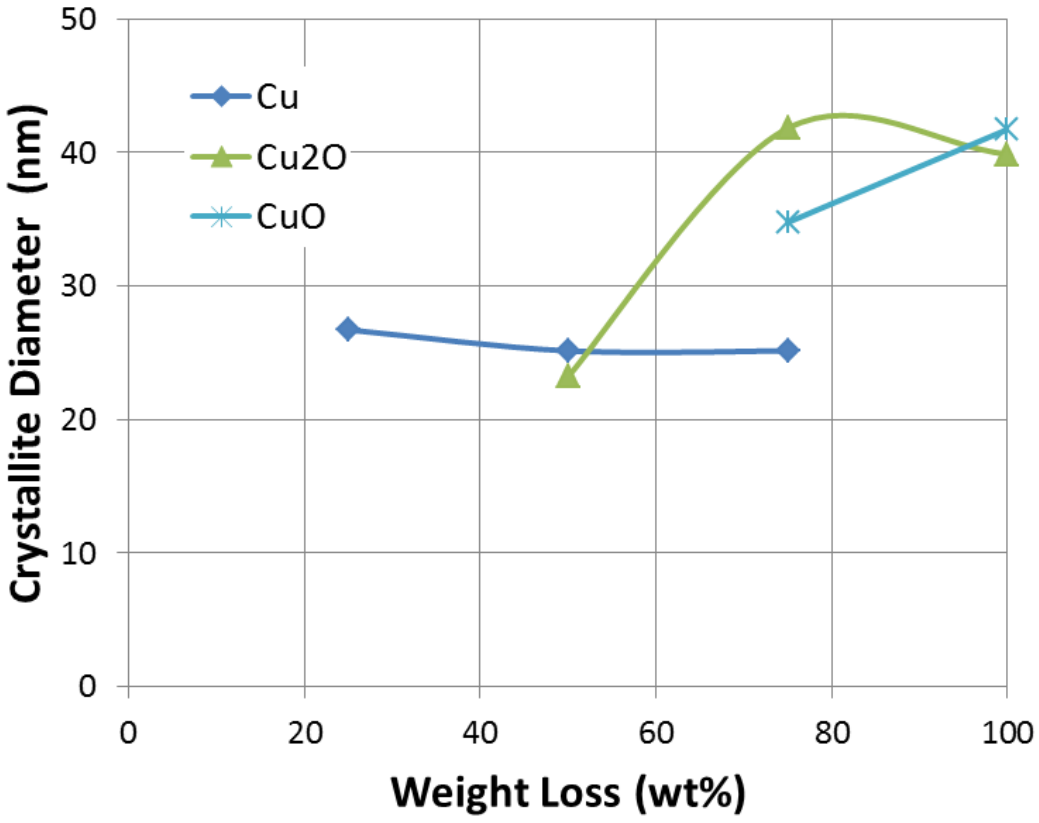

Fig.4.9 Crystallite diameter at different weight loss intervals of Cu-loaded brown coal heated at a rate of 10°C/min

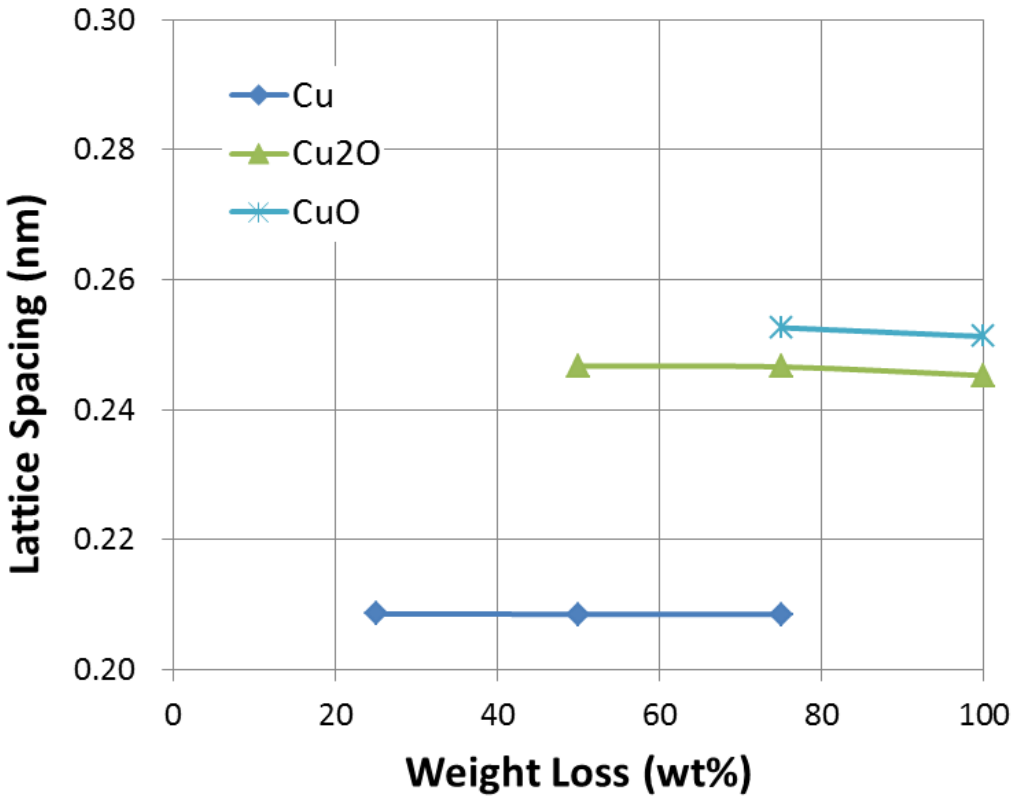

Fig.4.10 Lattice spacing of Cu-loaded brown coal at different weight loss intervals when heated at a rate of 10°C/min

Fig.4.9 shows the relation between crystallite diameter and weight loss (i.e., the conversion), in which we see that the crystallite diameter of Cu is stable from 25 to 75% conversion. Any further increase in the conversion, however, results in growth of the Cu_2O and CuO crystallite diameters. This further confirms that the crystal initially formed is Cu, and that this changes to Cu_2O and grows before finally changing to a CuO crystal. Since the residual particle size is around 0.5–1.0μm, and the crystallite diameter is 25–42nm, the particles clearly grow as polycrystalline particles.

The relation between lattice spacing and weight loss is plotted in **Fig.4.10**. Since the crystal structures of Cu, Cu_2O and CuO are different (face-centered cubic, cubic and monoclinic, respectively), the differences in distance seen in the plot are consistent with phase transitions from Cu to Cu_2O and from Cu_2O to CuO.

4.3.2 Reaction Kinetics of Low Temperature Combustion

The weight loss curves obtained by TG analysis for 100mg samples of brown coal and a temperature ramp of 10°C/min shown in **Fig.4.11** show the effect of increasing the copper loading of the coal.

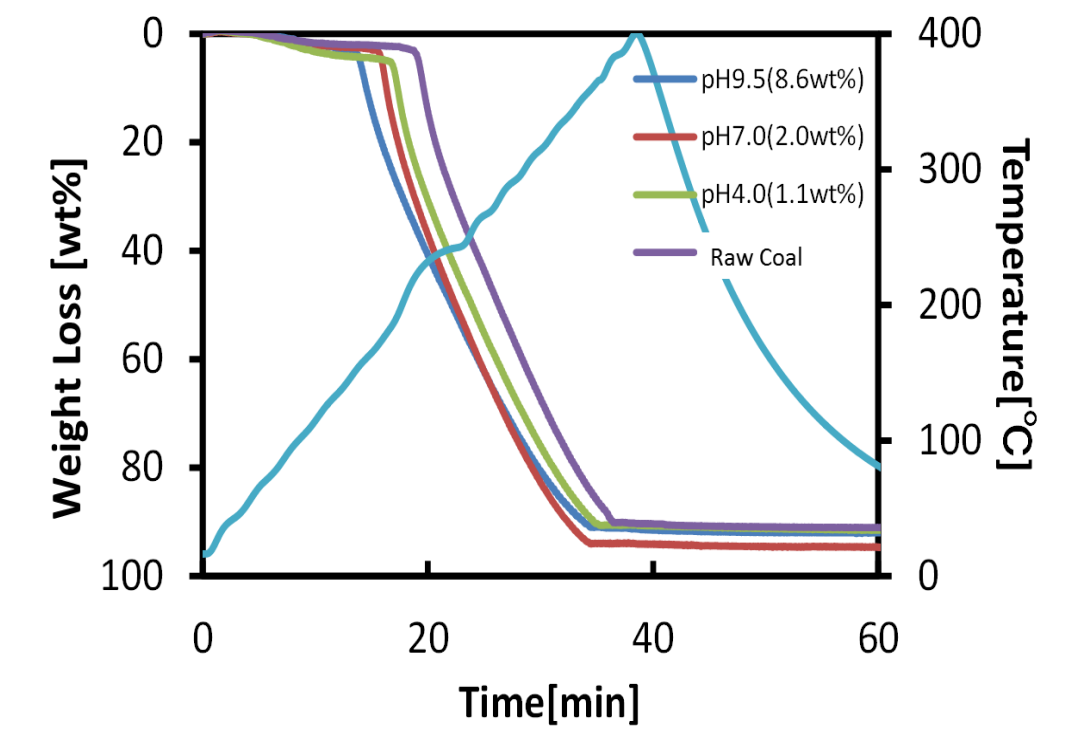

Fig. 4.11 Weight loss curves of Cu-loaded brown coal

(Cu-loading 8.6, 2.0, 1.1 wt%, de-ashed) and Raw brown coal (de-ashed)

The data from the weight loss curves is summarized by an Arrhenius plot in **Fig.4.12**, for which the reaction rate was assumed to be a 1st order reaction:

$dX/dt = kPo_2(1-X)$ ･･･Eq. (4.2)

where,

X: Conversion of combustible matter by weight (-)

k: Reaction coefficient (1/(Pa･hr))

Po_2: Partial pressure of oxygen (Pa)

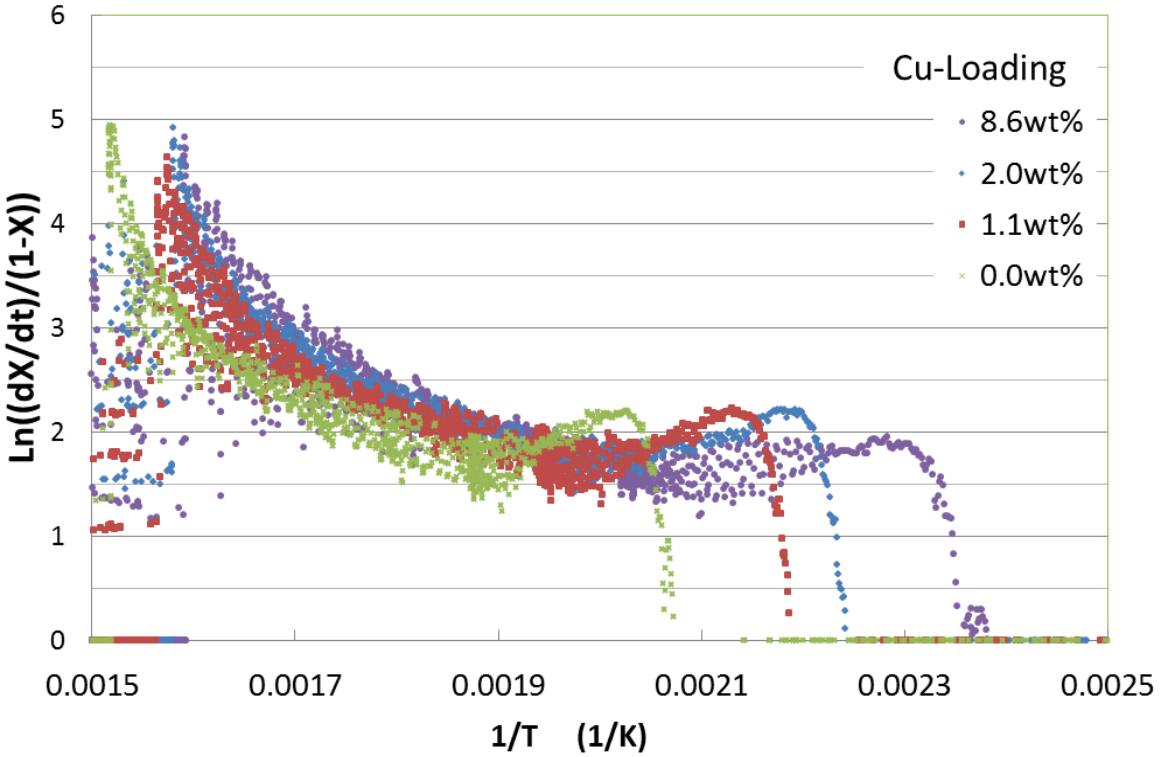

Fig.4.12 Arrhenius plots of different Cu-loadings (0, 1.1, 2.0 and 8.6wt%), where: $dX/dt=kPo_2(1-X)$

There is a notable differences between the various Cu-loadings in Fig.4.12 in terms of the point at which the weight starts to decrease. Near the point of complete burn out, the reaction rates start to increase, with a significant difference in the point at which this occurs between Cu-loaded and raw brown coal. This rate difference could be caused by the catalytic effect of Cu-loading, as the difference between the various Cu-loading amounts is not so significant, though the slope is slightly affected. Interestingly, although copper is loaded by ion exchange, at a pH of 9.5 (Cu-loading 8.6wt%), but by $Cu(OH)_2$ particle deposition and physical absorption at a pH of less than 7.0, there is little change in the rate of loading. Instead, the rate increase is more likely the result of the particle temperature exceeding ambient through the accumulation of reaction heat. In order to consider the effect of a non-uniform temperature on the kinetic analysis, the Coats-Redfern method[1)] was used to analyze the TG data. For this, the temperature ramp rate was defined as:

$T = T_0+\beta t$ ・・・Eq. (4.3)

Eq. (4.2) gives,

$dX/dT = (Po_2/\beta)(1-X)A\exp(-E/RT)$ ・・・Eq. (4.4)

On integration, Eq.(4.4) becomes:

$\ln(-\ln(1-X)/T^2) = \ln C-E/RT$ ・・・Eq. (4.5a)

$C=(P_{O2}AR/\beta E)(1-2RT_{av}/E)$ ・・・Eq. (4.5b)

where,

T_0: Initial temperature of TG analysis (K)

T_{av}: Average temperature of TG analysis (K)

β: Temperature ramp rate (K/hr)

A: Frequency factor (-)

E: Activation Energy at ignition (J/mol)

R: Gas constant (J/molK)

Plots of Eq. (4.5a) for the TG data are presented in **Fig.4.13.** In the case of an 8.6wt% Cu-loading, the activation energies can be estimated as 50kJ/mol for the initial combustion of the volatile matter, and 25kJ/mol for the 2nd char combustion region. In the case of raw brown coal without Cu-loading, these energies are 90kJ/mol and 38kJ/mol respectively. This estimation shows that activation energy of the initial reaction is reduced to 56% that of raw coal by an 8.6% Cu-loading.

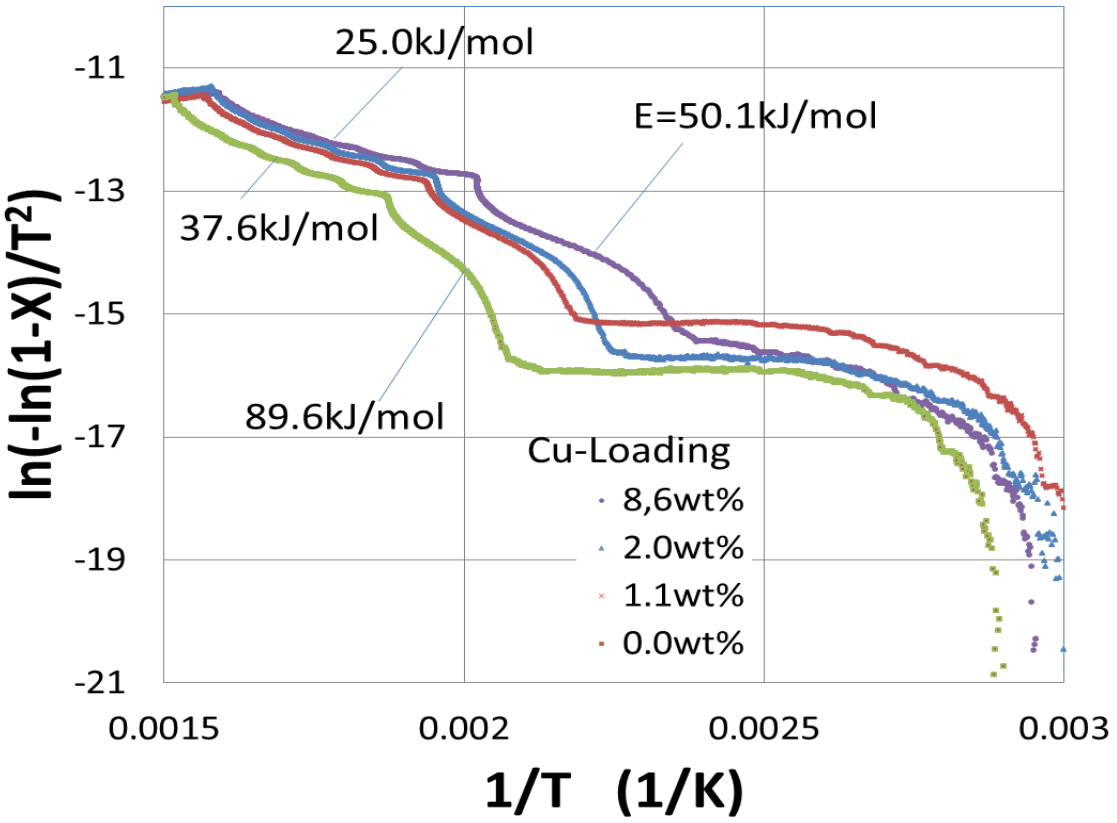

Fig. 4.13 Coats-Redfern estimate of activation energy for each set of Cu-loaded brown coal TG analysis data

In the 2nd char combustion region the curves are almost linear, and so the Coats-Redfern method would seem well suited to analyzing such data. However, in the initial volatile matter combustion region the curves are s-shaped, which is indicative of more complex phenomena; i.e. the gasification and combustion of volatile matter must have occurred.

4.3.3 Reaction Mechanisms of Cu-loaded Brown Coal Combustion

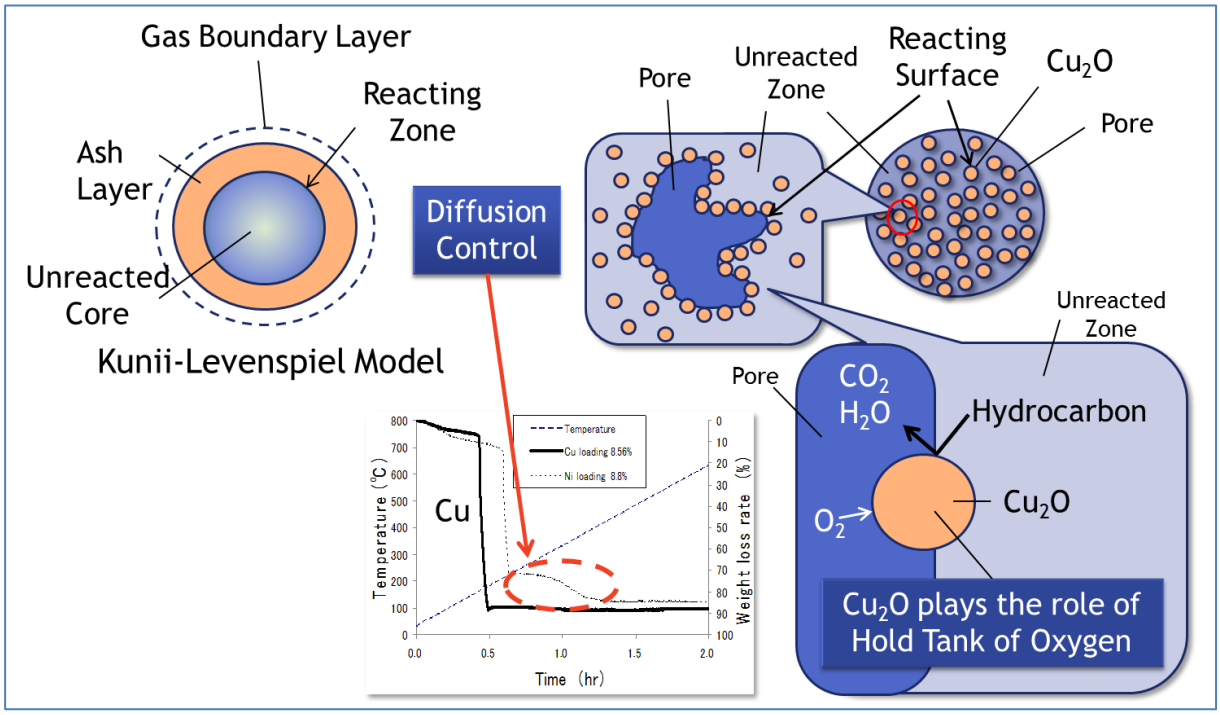

Fig. 4.14 Proposed reaction mechanism for the low temperature combustion of Cu-loaded brown coal

Fig.4.14 shows the reaction mechanism that is believed to occur when Cu-loaded brown coal is combusted at low temperature. The model on the left-hand side shows the unreacted core (Kunii-Levenspiel) model that was used to explain diffusion control by the reacted ash layer. In Fig.4.4, we saw that the weight decrease curve of Ni-loaded brown coal has a step at about 70% weight loss that is absent from the curve of Cu-loaded coal. This means that oxygen supply is promoted by Cu-loading, which is explained by the pore model on the right-hand side of Fig.4.14. Here, Cu ions are highly dispersed in the brown coal by the ion exchange process, but change to Cu metal during the initial stage of combustion. They are then changed to Cu_2O during the initial release and combustion of volatiles, as per Eq.(4.1). These Cu_2O particles are likely to concentrate at the interface between the gas phase and unreacted solid, where they could then play a role as a catalyst by acting as a carrier or holding site for oxygen[3-9].

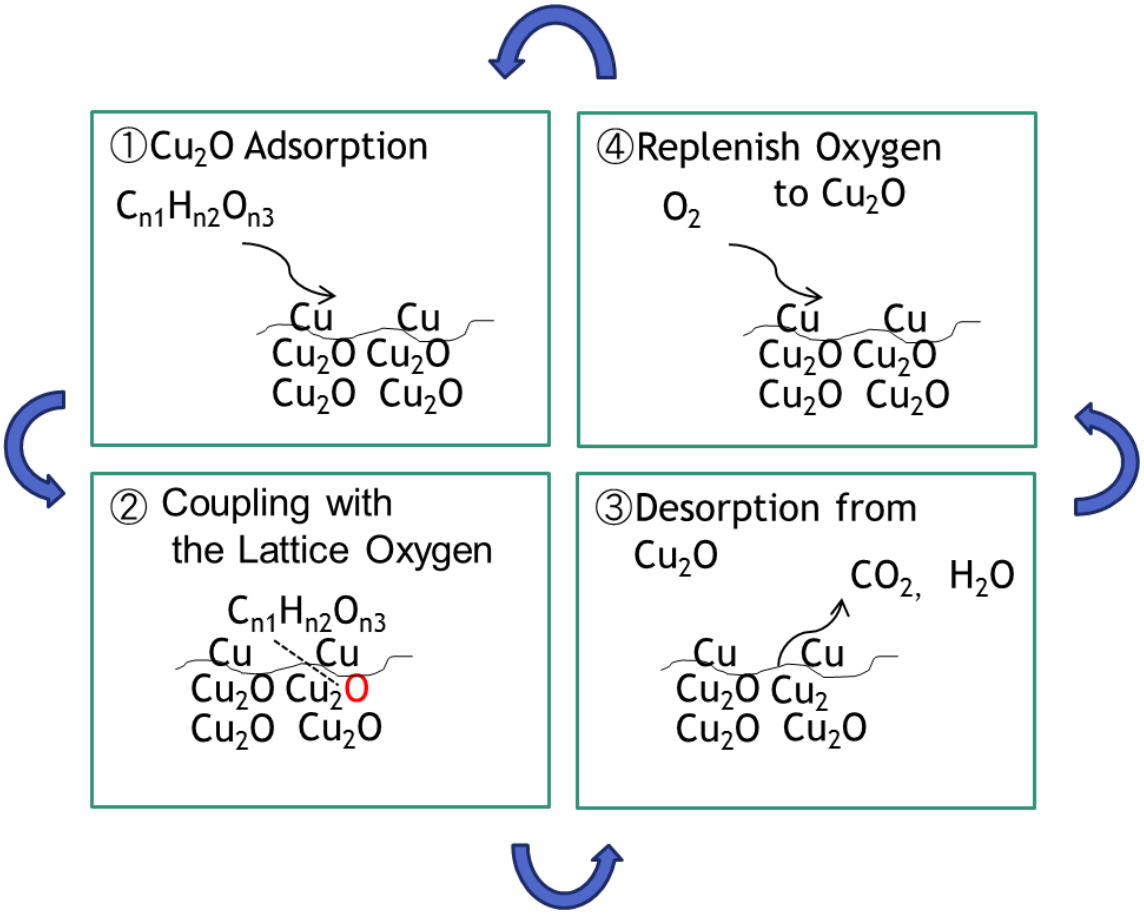

Fig. 4.15 Catalytic role of Cu_2O in the proposed reaction mechanism

Fig.4.15 shows the mechanism believed to be behind the catalytic reaction of the Cu-loaded brown coal. This is a Langmuir-Hinshelwood type model, which is estimated to consist of the following loop: ① hydrocarbons are adsorbed on Cu_2O, ② they react with the lattice oxygen of Cu_2O, ③ they desorb to the gas phase, ④ oxygen is replenished from the gas phase back to ①. Dekker et al studied the process of CO oxidation on Cu_2O, and determined that this reaction is similarly represented by a Langmuir-Hinshelwood (LH) model when the surface of Cu_2O is not fully oxidized. The activation energies they obtained experimentally (E=46±6kJ/mol for the LH process and 24±8kJ/mol for the diffusion control of lattice oxygen)[3] are very close to the results presented here in Fig.4.13 at a Cu-loading = 8.6wt%. White et al[4] also studied CO oxidation on Cu_2O, and calculated the adsorption energy of CO on O and Cu atoms. They concluded that although CO adsorption on O has a barrier energy, this is not the case with CO adsorption on Cu. Kasai et al.[5] calculated that the local density of states (LDOS) for the d-orbital of Cu-terminated Cu_2O are shifted to the Fermi level region in a similar manner to Rh. These studies would therefore seem to support the notion that Cu_2O that is not fully oxidized (i.e. Cu/Cu_2O) could play a role in promoting adsorption and the redox reaction.

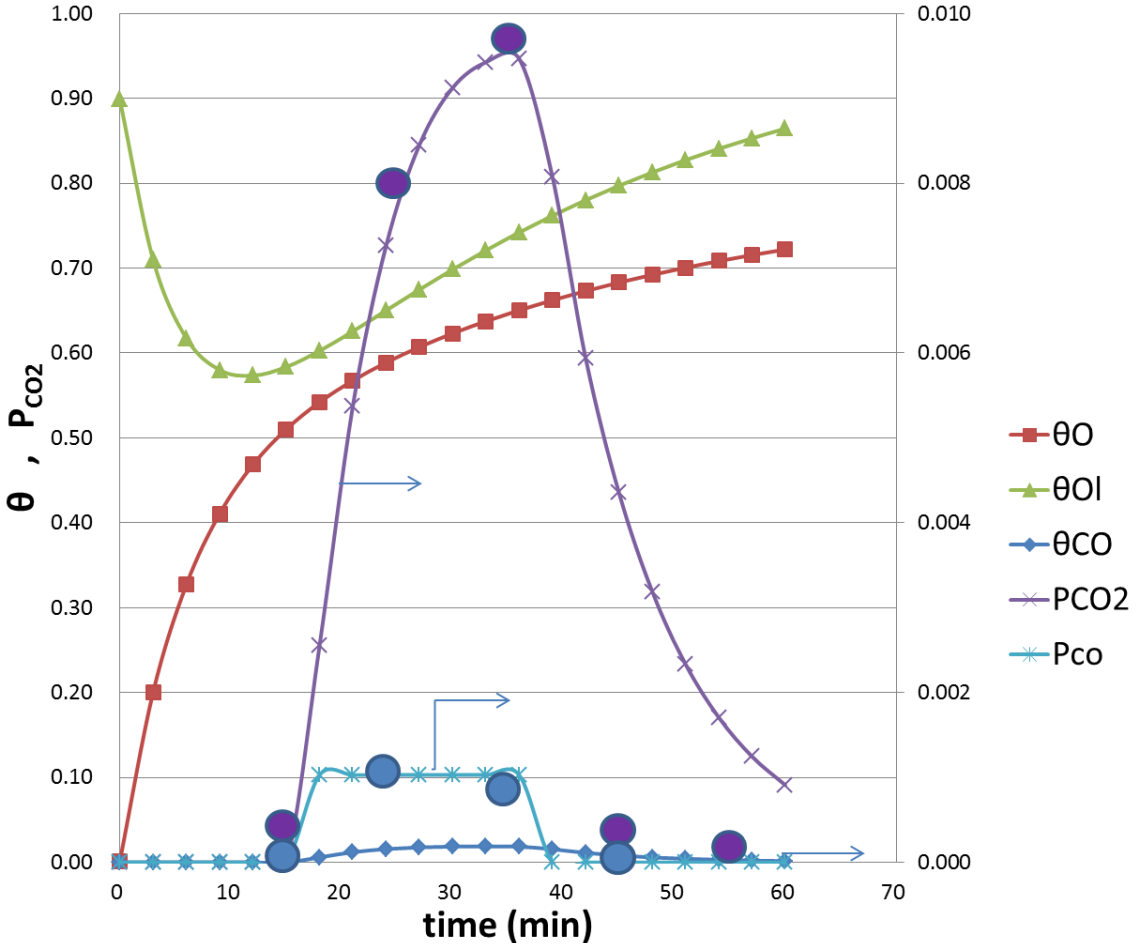

Fig. 4.16 Simulated results for the combustion of Cu-loaded brown coal (LH model). Large circles show experimental results for Pco_2 and Pco

Fig.4.16 provides an example of the simulation results for the combustion of Cu-loaded brown coal using the LH model to calculate the reaction. Experimental results for the gas partial pressure of CO_2 and CO are fitted by this simulation, from which the abundance ratio of lattice oxygen (θ_{OL}) and ratio of adsorbed CO and O atoms on adsorption sites ($\theta_{CO,}$ θ_O) are calculated. These calculated results suggest that although lattice oxygen is initially consumed, it is eventually replenished to the extent that the abundance ratio of lattice oxygen θ_{OL} fully recovers.

4.3.4 Estimation of Ignition Temperature

The Semenov theory[2)] of spontaneous combustion was used to confirm the estimated activation energies:

$C_p w \partial T/\partial t = Q_r - Q_c$ ・・・Eq.(4.6)

$Q_r = \Delta H \cdot dX/dt$ ・・・Eq.(4.6a)

$Q_c = U \cdot S(T - T_a)$ ・・・Eq.(4.6b)

where T = T_f, that is in the ignition point, and $\partial T/\partial t = 0$. Equation (4.6) then gives:

$$dQ_r/dT = dQ_c/dT \quad \cdots \text{Eq.(4.7)}$$

From Equation (4.6a), (4.6b) and (4.7):

$$E = R \cdot T_f^2 / (T_f - T_a) \quad \cdots \text{Eq.(4.8)}$$

where,

C_p: Specific heat (J/kg·K)

w: Sample mass (kg)

T, T_f, T_a: Temperature of coal, ignition and ambient (K)

Q_r, Q_c: Heat generation rate and heat transfer rate (J/hr)

ΔH: Heat of reaction (J/kg)

U: Heat transfer coefficient (J/m^{2}hrK)

S: Heat transfer area (m^2)

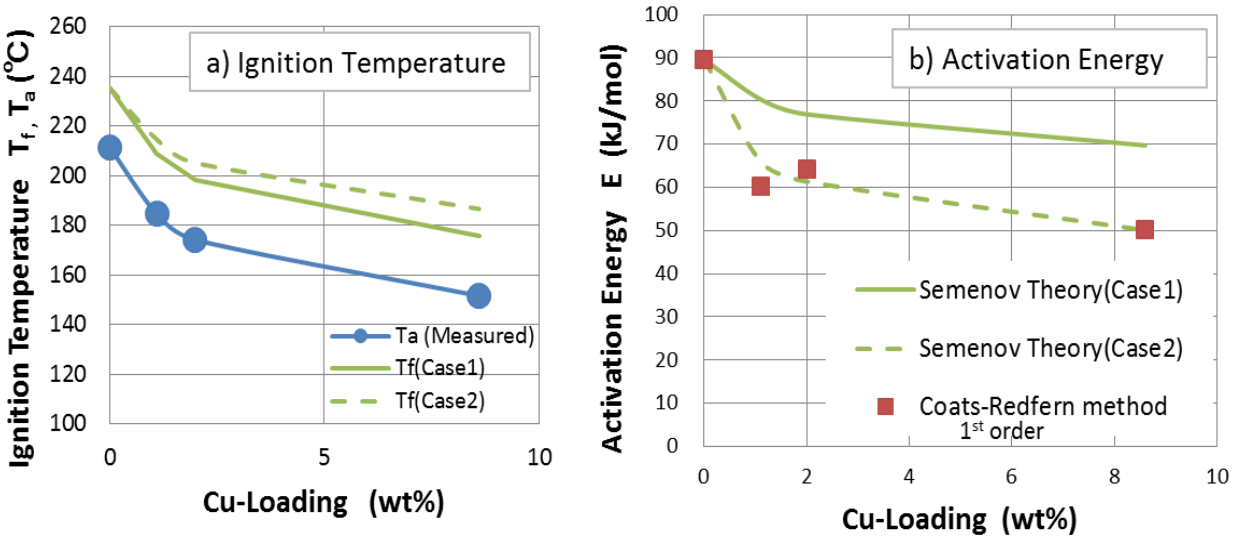

Fig. 4.17 Effect of Cu-loading on ignition temperature and estimated activation energy

The temperature at which the rapid weight decrease starts in Fig.4.12 is used to represent the ignition temperature, T_a, of **Fig.4.17(a)**. The value of T_f is assumed in two ways. In case1, the T_f of Eq.(4.8) is obtained by fitting the activation energy of the raw coal, with the same temperature difference of $(T_f - T_a) = 24$K being then used to obtain the remaining Cu-loading data. In case2, each individual value of T_f in Eq.(4.8) is adjusted to fit the activation energy obtained by the Coats-Redfern method. These T_f values and activation energies for the initial combustion region are plotted in Fig.4.17(a) and (b). Note that in case1 (Fig.4.17(b)) the activation energies obtained experimentally by the Coats-Redfern method become different to those estimated by Semenov theory. As in case2, in order to adjust these activation energies, the coal temperature needs to slightly increase with the amount of Cu-loading (i.e., $(T_f - T_a)$ = 24→35K with 0→8.6wt% Cu)

Given that the specific heat of brown coal (1000–1500 J/kg·K) is much greater than that of

copper (385J/kg･K), it stands to reason that the specific heat of Cu-loaded brown coal would decrease with increasing Cu loading. This, in turn, would increase the temperature difference ($T_f - T_a$) in Eq. (4.6). In other words, the estimated temperature difference ($T_f - T_a$) of 24→35K explains the lower activation energy and ignition temperature of the 8.6wt% Cu-loaded brown coal predicted by Semenov theory. Copper would therefore seem to play a role in promoting heat transfer, in addition to acting as a catalyst.

4.3.5 Decarboxylation and Deammoniation Reaction

In the reaction scheme summarized in **Fig.4.18**, Cu-ammonia complexes such as tetraamminecopper(II) $[Cu(NH_3)_4]^{2+}$ change first to Cu metal, then to Cu_2O and finally CuO. Two reaction paths are considered for this. In path 1, a decarboxylation reaction occurs first, while in path 2 it is a deammoniation reaction that occurs first. Computational chemistry was used to determine each reaction path[10].

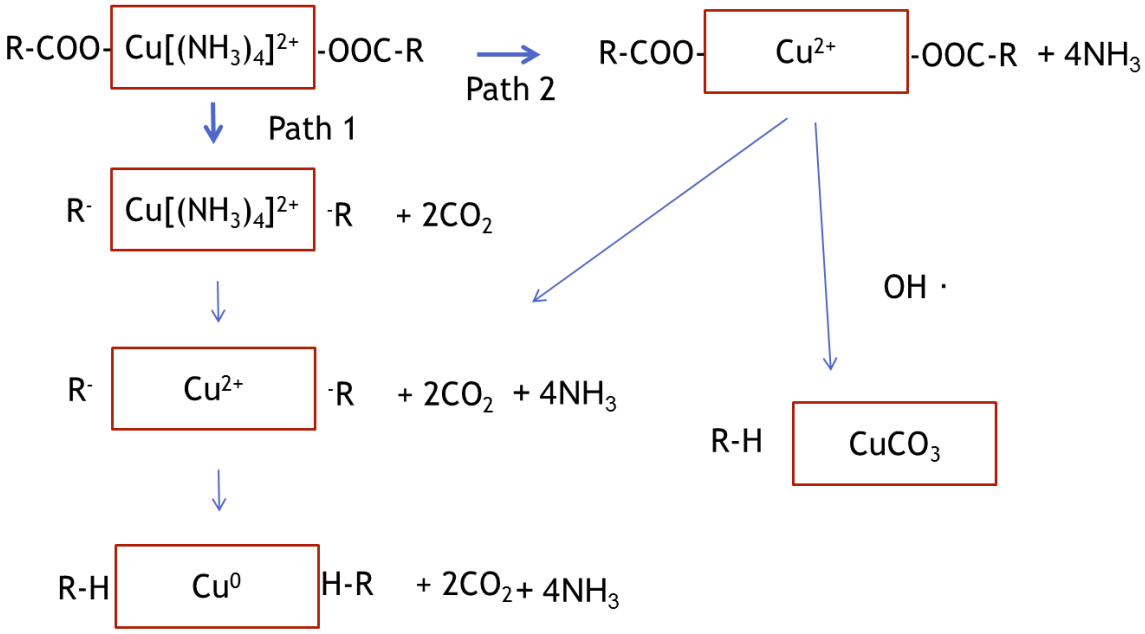

Fig. 4.18 Reaction scheme for Cu

Table 4.1 shows the heat results calculated for each reaction using Gaussian09, from which it is apparent that the heat of reaction for deammoniation (3,042kJ/mol) is smaller than that of decarboxylation (4,534kJ/mol). In other words, deammoniation should occur first. The total heat of reaction is exothermic with either path.

Table 4.1 Heat of reaction for two different paths, as calculated using Gaussian09

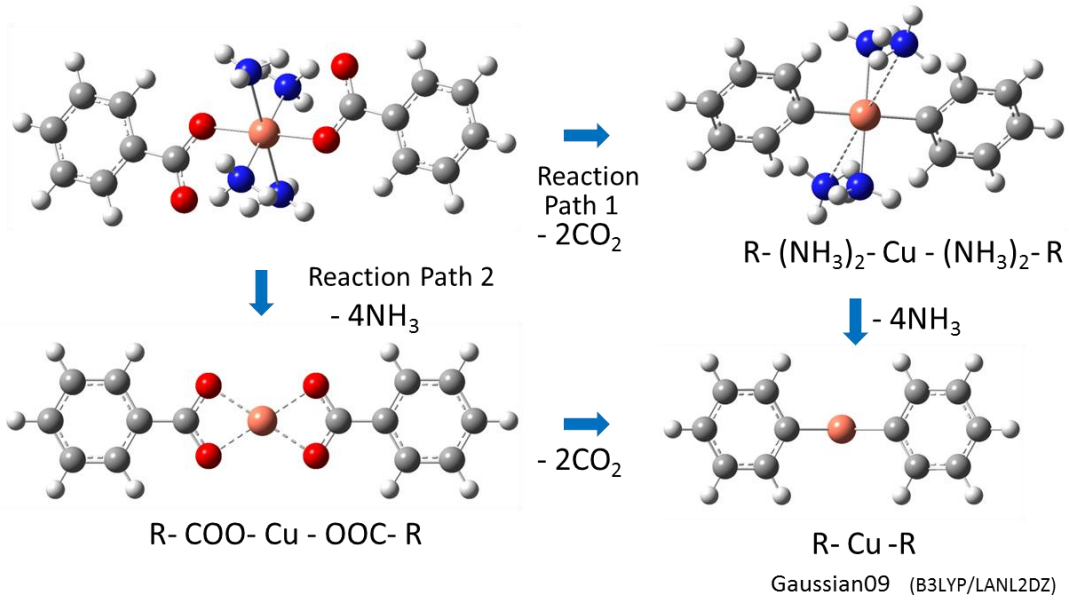

1	Cu(NH3)4(OCOPh)2 → Cu(NH3)4(Ph2) + 2CO2 Cu(NH3)4(Ph)2 → Cu(Ph)2 + 4NH3 Cu(Ph)2 + 2H3O+ → Cu + 2C6H6 + 2H2O	4534kJ/mol 2007kJ/mol -16970kJ/mol	Endotherm Endotherm **Exotherm**
	Total	**-10429kJ/mol**	**Exotherm**
2	Cu(NH3)4(OCOPh)2 → Cu(OCOPh2) + 4NH3 Cu(OCOPh2) → Cu(Ph)2 + 2CO2 Cu(Ph)2 + 2H3O+ → Cu + 2C6H6 + 2H2O	3042kJ/mol 3500kJ/mol -16970kJ/mol	Endotherm Endotherm **Exotherm**
	Total	**-10428kJ/mol**	**Exotherm**

Deammoniation and decarboxylation occur with the initial weight decrease during combustion[11-12], and so these reactions were quantitatively analyzed by TG and exhaust gas GC. **Fig.4.19** shows the initial weight decrease with several Cu-loading conditions in either an air or Ar environment. The graph on the right is a magnified view of the one on the left. Initial weight loss is greatest with 6.5wt% Cu, which confirms that weight loss is predominantly due to combustion, though a higher Cu-loading produces a greater weight loss in both air and Ar environments.

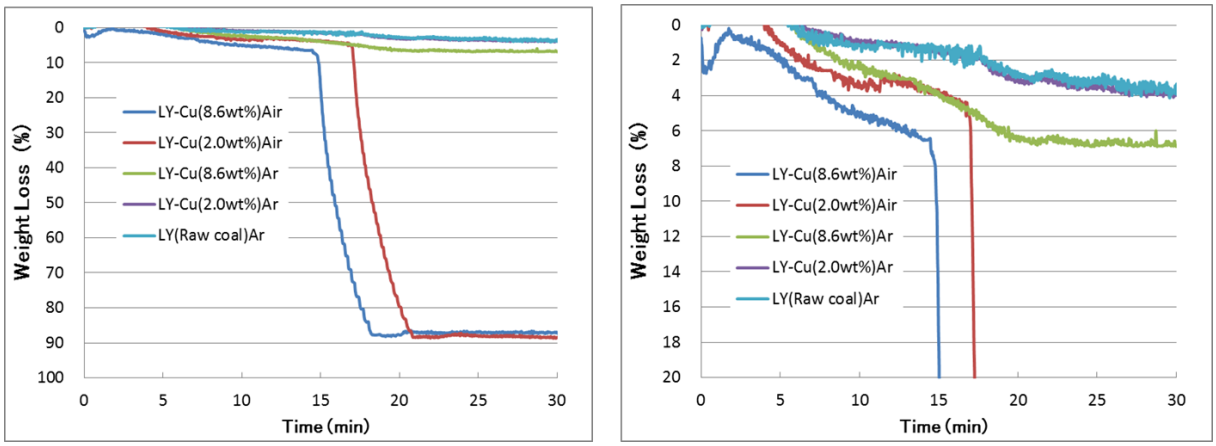

Fig. 4.19 TG weight loss curves in Air and Ar gas

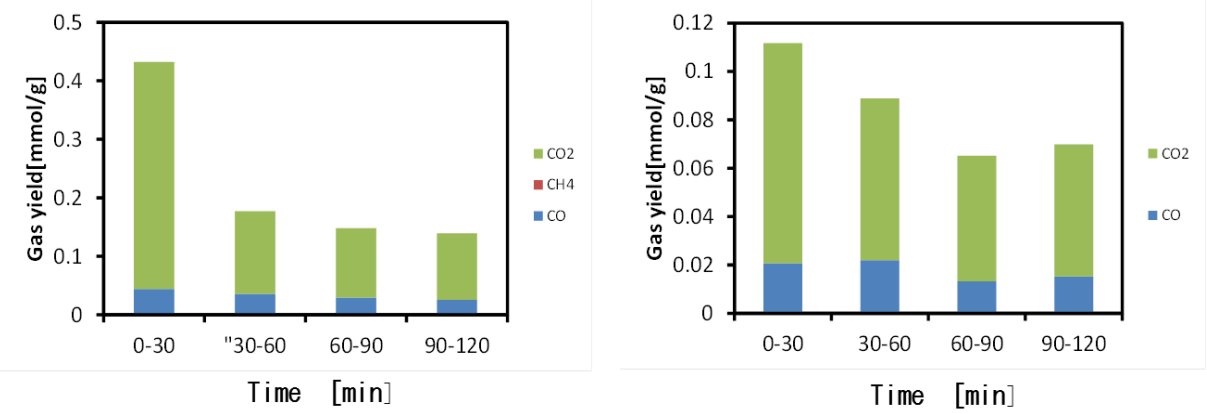

(a) 200℃, LY-Cu:8.6wt%　　(b) 200℃, LY Raw coal

Fig. 4.20 Product gas composition during pyrolysis

The composition of the gas produced during pyrolysis was measured and is summarized in **Fig 4.20**. In the first 0–30min the major gases were found to be CO_2 and CO, with the gas yield of the 8.6wt% Cu-loaded brown coal being around four-times greater than that of raw coal. The heat of reaction was therefore calculated to investigate the reason for this advantage of Cu-loading.

Table 4.2 Effect of copper loading on the heat of reaction, as calculated using Gaussian09

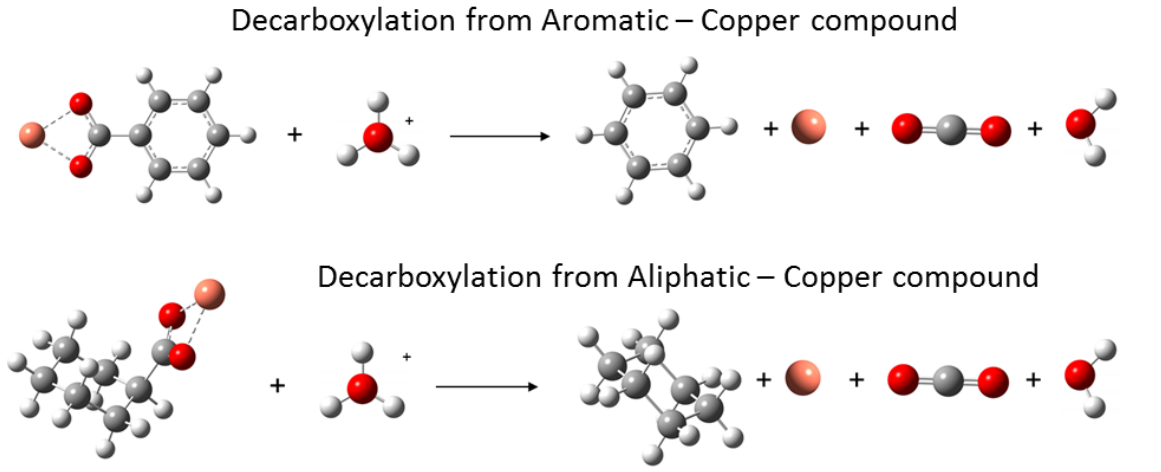

	E (Hartree)	⊿E (Hartree)	⊿E (kcal/mol)	⊿E (kJ/mol)
Cu-carboxy_benzoate	−616.3			
benzoic_acid	−420.7			
H3O+	−76.70			
benzene	−232.2	−0.003986	−2.5	**−10**
Cu	−196.1			
CO2	−188.5			
H2O	−76.41	−0.2528	−158.6	**−664**

	E (Hartree)	⊿E (Hartree)	⊿E (kcal/mol)	⊿E (kJ/mol)
Cu-carboxy_cyclohexate	−619.9			
cyclohexyl-carboxylic_acd	−424.4			
H3O+	−76.70			
cyclohexane	−235.8	0.003965	24.9	**104**
Cu	−196.1			
CO2	−188.5			
H2O	−76.41	−0.2605	−163.5	**−684**

Table 4.2 shows the effects of copper loading on the heat of reaction for two separate cases, each calculated using Gaussian09. The first of these was decarboxylation from an aromatic-Cu compound, while the other was decarboxylation from an aliphatic-Cu compound. The blue-hatched data represents the heat of reaction for a non-loaded reference, with the Cu-loaded data indicated in orange. A positive value indicates an endothermic reaction and a negative value an exothermic reaction. It is evident from this data that in either case the heat of reaction increases with Cu-loading, indicating that this promotes the decarboxylation reaction.

4.4 Conclusion

As the low-temperature combustion of Cu-loaded brown coal is a key factor influencing process cost, the reaction kinetics and mechanisms were studied. From the TG analysis results obtained, the following conclusions have been reached:

1. Copper-loaded brown coal can burn at an extremely low temperature of 160–180°C, forming 0.5–1.0μm copper oxide particles as a residue. The presence of Cu_2O at 165°C indicates that this phase provides a catalyst for gasification and/or oxidation, which helps make possible the low-energy recovery of copper using brown coal.

2. The activation energy of initial combustion is affected by the amount of Cu-loading, being reduced to 56% that of raw coal when the Cu-loading is 8.6wt%. This is considered to be the result of an increase in the initial rate of volatile matter gasification and/or combustion, as copper is considered to be mainly in an ion exchanged state on carboxy groups of brown coal (e.g. as COO-$[Cu(NH_3)_4]$-OOC) that is reduced to Cu metal in the early stages of burning (X=around 25wt%).

3. A Cu_2O-concentrated pore model of combustion and Langmuir-Hinshelwood model for the surface of Cu_2O are proposed for the reaction mechanism. This indicates that the activation energy of Cu-loaded brown coal is close to that of Cu-terminated Cu_2O, which is likely an important factor in its catalytic ability.

4. The relationship between the ignition temperature and activation energy, as determined using the Coats-Redfern method and Semenov theory, suggests that in addition to acting as a catalyst the copper loaded on brown coal also promotes heat transfer.

5. The reaction path from Cu-ammonia complex to Cu metal it considered to begin with deammoniation, with a 8.6wt% Cu loading increasing the $CO+CO_2$ emission during this early stage by four-times that of raw brown coal. The catalytic ability provided by subsequent decarboxylation is explained by the higher heat of reaction with Cu-loading. It

has also been confirmed that weight loss is primarily due to combustion.

4.5 References

1) Coats, A.V., Redfern, J. P., *Thermochim. Acta*, 340/341: 53-68 (1999)
2) Semenov, N.N. *Some Problems in Chemical Kinetics and Reaction*, 2, Princeton Univ. Press., NJ (1959)
3) Dekker, F.H.M., Klopper, G., Bliek, A., Kapteijin, F., Moulijin, J.A., *Chem. Eng. Sci.*, 49, 24A, 4375-4390 (1994)
4) White, B., Yin, M., Hall, A., Le, D., Stolbov, S., Rahman, T., Turro, N., O'Brien, S., *Nano Lett.*, 6, 9, 2095-2098 (2006)
5) Kasai, H., Padama, A.A.B., Nishihata, Y., Tanaka, H., Mitachi, C., *J. Jpn. Petrol. Inst.*, 56, (6), 357-365(2013)
6) Schedel-Niedrig, T., Neisius, T., Bottger, I., Kitzelmann, E., Weinberg, G., Demuth, D., Schlogl, R., *Phys. Chem. Chem. Phys.*, 2,2407-2417 (2000)
7) Soon, A., Todorova, M., Delley, B., Stampfl, C., *Physical Review*, B 73, 165424 (2006)
8) Illan-Gomez, M.J., Raymundo-Pinero, E., Garcia-Garcia, A., Linares-Solano, A., Salinas-Martinez de Lecea, C., *Appl. Catal. B*, 20, 267-275 (1999)
9) Lopez-Suarez, F.E., Bueno-Lopez, A., Illan-Gomez, M.J., *Appl. Catal. B*, 12, 84, 3-4 (2008)
10) Murakami, Y., Oguchi, T., Hashimoto, K., *J. Combust. Soc. Jpn.*, 53, 165,165-171 (2011)
11) Gooβen, L.J., Thiel, W.R., Rodriguez, N., Linder, C., Melzer, B., *Adv. Synth. Catal.*, 349, 2241-2246 (2007)
12) Karabulut, S., Yurum, Y., *Energy Sources*, 25, 10 (2003)

Chapter 5 Copper Particle Formation by Combustion of Copper-Loaded Brown Coal

5.1 Introduction

The combustion of Cu-loaded brown coal allows fine copper oxide particles to be recovered, for which several applications were considered. This includes their use as a powder metallurgy material or as a copper catalyst for redox reactions (e.g., CO oxidation for biomass combustion, NO reduction for exhaust gas treatment, water gas shift reaction for fuel cells, etc.). Note that in all of these applications the particle size is important to ensuring maximum performance, and so a thorough understanding of the particle formation mechanism and factors influencing the particle size is essential to reducing the costs associated with secondary milling and classifying.

5.2Experimental

5.2.1 Fine Copper Oxide Particle Formation

Small samples (100 mg) for particle formation were analyzed using the TG apparatus shown in Fig.4.1 by heating at a ramp rate of 10°C/min from room temperature to 200°C and holding for 30min at this temperature. This was conducted under an atmosphere of 21% O_2 and 79% Ar, which was introduced at a flow rate of 100ml/min.

5.2.2 Evaluation Methods

A 0.5–1.0mg sample was ultrasonically dispersed in methanol for 10min, filtered, and then coated with gold for observation of the particle shape by FE-SEM (JEOL JSM-6700F) under an accelerating voltage of 10kV. The particle size distribution was analyzed by Image processing software ImageJ; http://imagej.nih.gov/ij/. The area of the particles was also measured, from which a representative particle diameter was calculated as (major axis + minor axis)/2. A total of 300–1,200 particles were measured to determine the particle size.

5.3 Results and Discussion

5.3.1 Modified Percolation Model for Particle Growth

When conversion is less than 100%, the crystals are small and cubic in shape, as shown in Fig.4.8. However, when the conversion is almost at 100%, the corners of the particles become rounded and some seem to fuse together, despite the relatively low temperature of 200°C. In the SEM images of CuO particles after combustion in **Fig.5.1**, the cubic crystal shape of Cu_2O can be readily distinguished from the monoclinic form of CuO. This suggests that a crystal phase transition occurs during the last stages of combustion; and since the melting points of Cu_2O and CuO are 1235 and 1201°C, respectively, this may well be related to the fused structure seen.

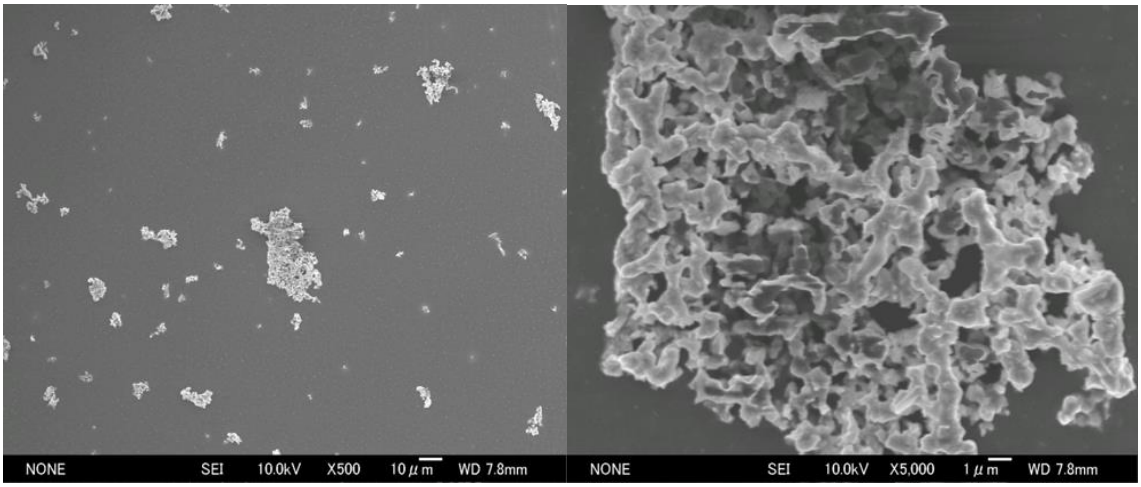

Fig. 5.1 SEM images of CuO particles formed during combustion of Cu-loaded brown coal (Cu-loading 9.0 wt%) at 200°C

Percolation theory can be used to explain particle growth by the coalescence of particles[1-3], as it allows the calculation of percolation, thermal conductivity and electrical conductivity. In the typical 2D lattice model shown in **Fig.5.2**, an increase in the occupied ratio of lattice cells causes p to increase to the percolation threshold (p_c) of 0.593[1], with the occupied cells connecting together to form one big cluster.

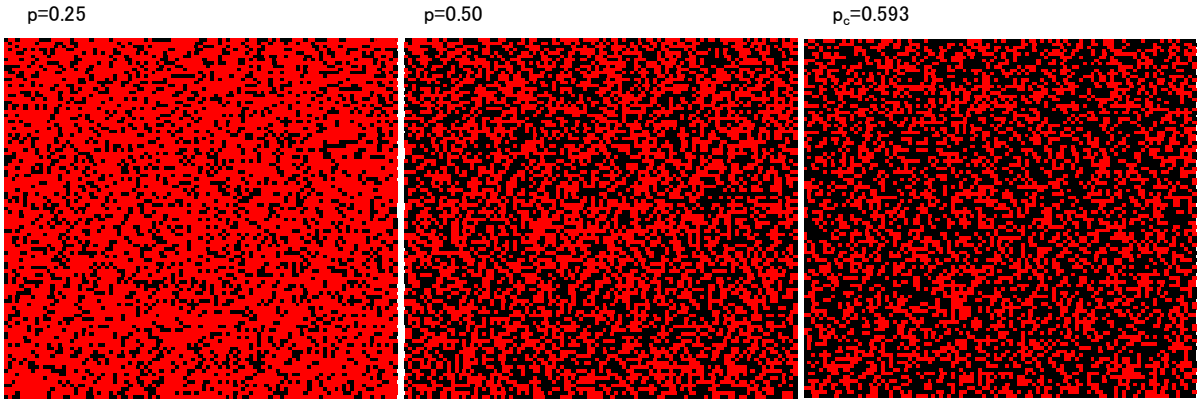

Fig. 5.2 2D lattice percolation model

In a conventional percolation model, the occupied ratio in the fixed lattice cells increases with the number of black cells. Thus, when the number of black cells is constant, the total lattice number is reduced by a decreasing number of red cells, meaning that the occupied ratio must increase.

A modified percolation model is proposed in this study. Starting with the big red circle shown in **Fig.5.3**, the red cells represent unburned carbon, while the black cells indicate a Cu compound of some form. The initial occupied ratio (p_0) is set to 0.0143 so as to correspond to a copper loading of 8.5wt%. During combustion, red unburned carbon is removed by increasing the conversion (x), which causes the red circle to shrink. In this modified model one cell is chosen at random, and if this happens to be red, then it is removed and the model is shrunk in a random direction. If, on the other hand, the chosen cell is black, then nothing happens. In effect, this represents a kind of Monte Carlo simulation for char combustion. In

Fig.5.3, a conversion of x=0.991 results in p becoming p_c, as the black cells are now connected as one cluster. It is therefore confirmed that this modified shrinking percolation model produces the exact same threshold value as a 2D lattice cell.

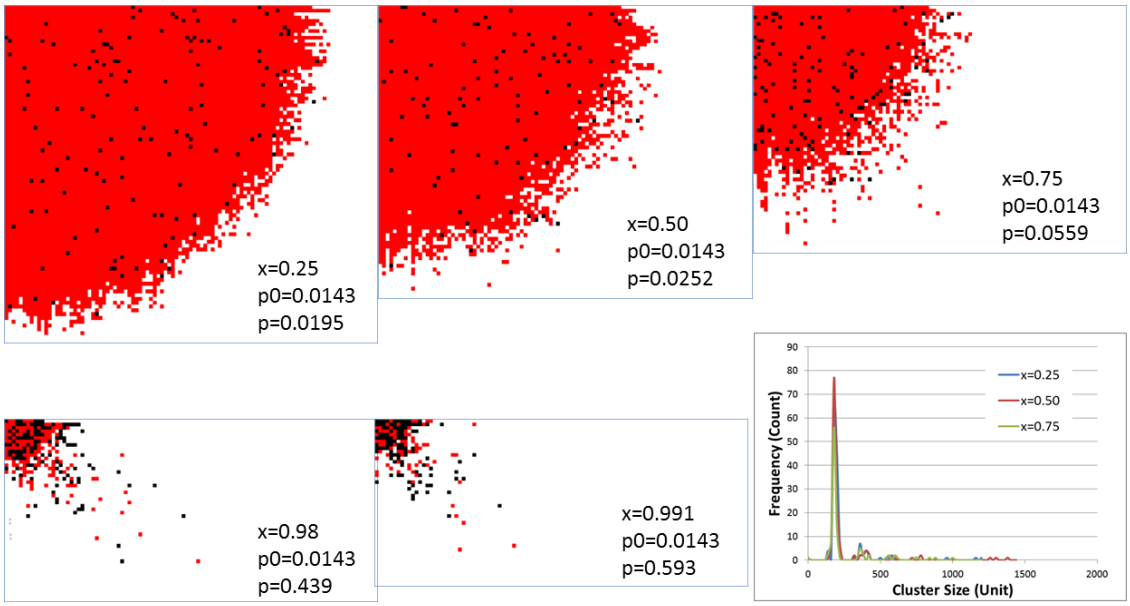

Fig. 5.3 2D Percolation model for copper particle formation (p_0=0.0143)

It is apparent that the percolation threshold corresponds to x=0.991, or in other words, is very close to complete combustion. At this point, a single connected cluster could be formed from a Cu-loaded brown coal particle. The graph on the right-hand side of Fig.5.3 shows the cluster size distribution calculated by this simulation and counted using imageJ when x=0.25, 0.50 and 0.75. We see from this that the cluster size distribution does not change much until the percolation threshold is reached.

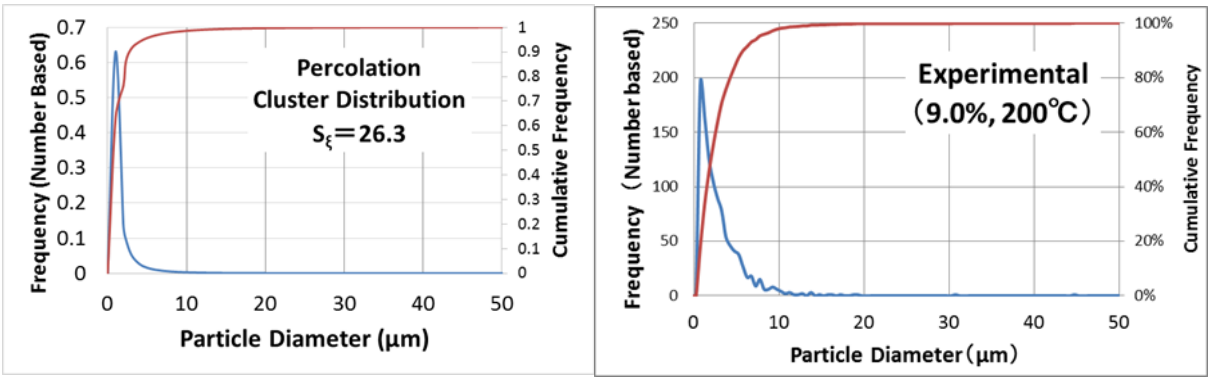

a) Number based distribution

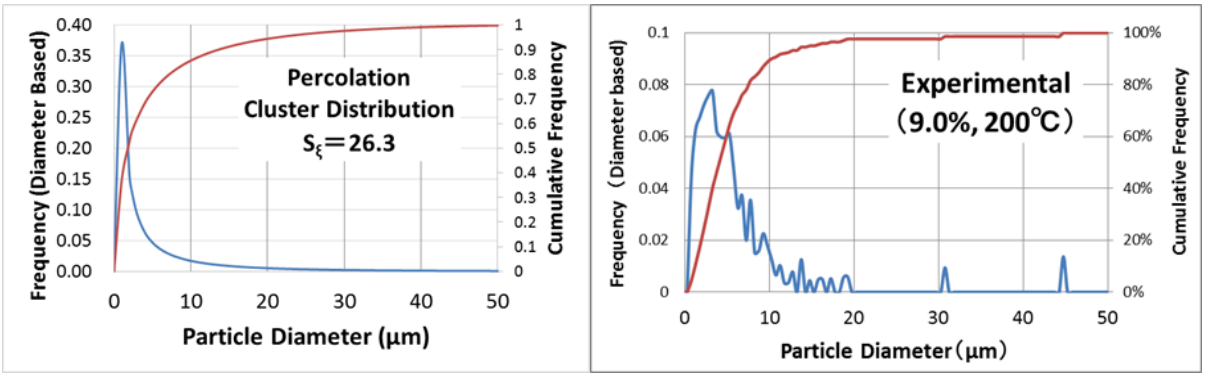

b) Diameter based distribution

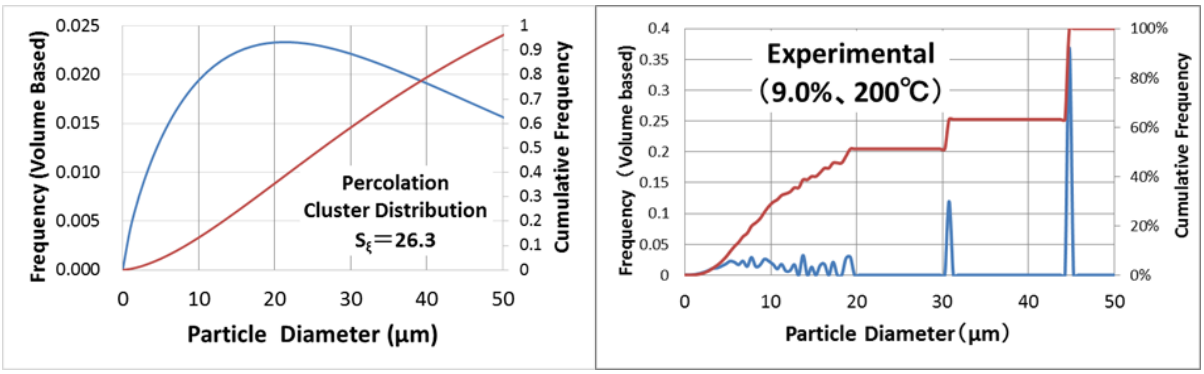

c) Volume based distribution

Fig. 5.4 Comparison between percolation cluster distributions (s_ξ=26.3) and experimental data (Cu-loading=9.0wt%, Heating=10°C/min, 200°C)

Fig 5.4 presents a comparison between percolation cluster distributions (s_ξ=26.3) for 3D cubic cells and experimental results. **Eq.(5.1)** was used to determine the percolation cluster size distribution function, $n_s(s)$, of the 3D cubic cells[1)] at $p < p_c$.

$$n_s(s) = s^{-(2.189)} \cdot \exp(-s/s_\xi) \quad \text{… Eq.(5.1)}$$

where s_ξ is the representative cluster size (26.3 in this instance).

The three graphs on the left-hand side of Fig.5.4 show the cluster size distribution calculated by Eq.(5.1), while the three graphs on the right show experimental results obtained by SEM and counted by ImageJ software. The number, diameter and volume based

distributions on the left and right side seem to be quite similar, meaning that cluster formation can be explained by the percolation model. The volume based experimental results do show some intermittent distribution, but this is considered to be the result of an insufficient number of sample particles, particularly at the larger end of the size range.

5.3.2 Coalesced Particle Formation Model

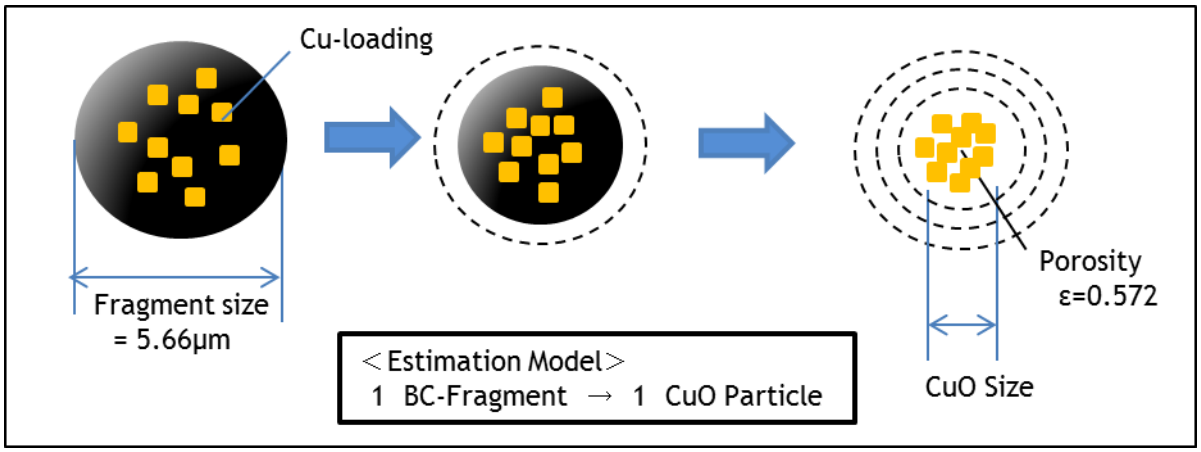

Fig. 5.5 CuO Coalesced Particle Formation Model by combustion of Cu-loaded Brown Coal

The coalesced particle formation model devised is illustrated in **Fig 5.5**. In this, a single brown coal fragment containing a copper compound is burnt and shrinks with increasing conversion. When the conversion is close to 1, the volume occupied by the copper compound becomes the percolation threshold (p_c=0.312) of a 3D cube, and the small copper oxide clusters then become one large chunk.

SEM images taken of copper compound particles removed during combustion and dispersed in methanol are shown in **Fig.5.6** and **Fig5.7**. The large particles in Fig.5.6 that were obtained at 50% weight loss appear to be unburned particles, though some do seem to have a coalesced particle structure (e.g. the one in the right-most picture). In contrast, particles of a copper compound can be seen in Fig.5.7 inside the large particles removed at 75% weight loss. There are also holes and craters around 3–5μm present in the large particles, which are believed to be created by the passage of volatile matter. In the right-most picture of Fig.5.7, copper compound particles can also be seen at the walls of the holes and craters, with small particles of around 0.1μm in size also present in the unburned area that are considered to grow with increasing combustion. The crystallite diameter of around 25–42nm at 75% weight loss indicates that these particles grow as a polycrystalline structure. It should also be noted that the primary particle size of the coalesced large particles is around 0.5–0.7μm, suggesting that polycrystalline growth could be regulated by some as yet unidentified mechanism.

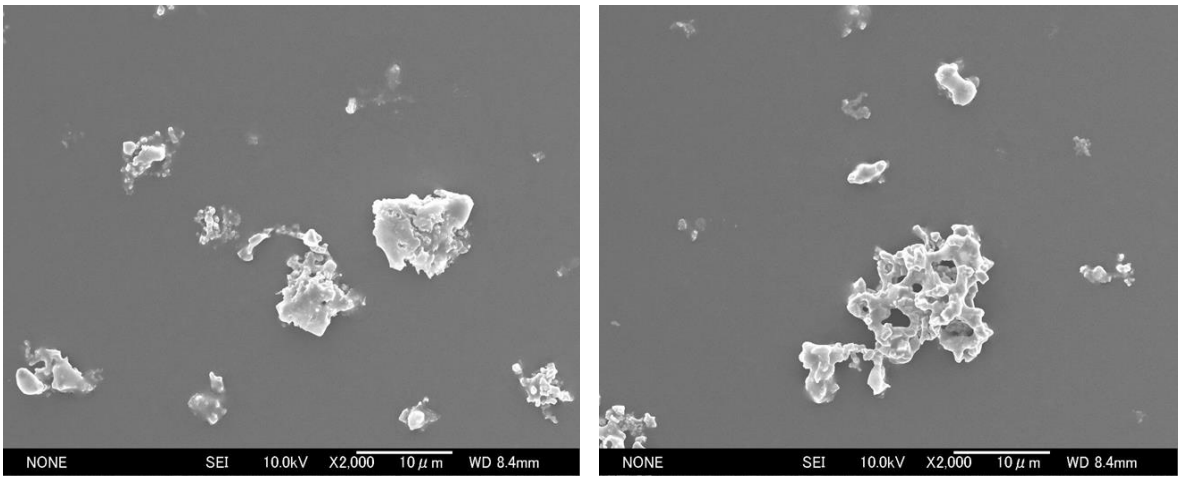

Fig. 5.6 SEM images of copper compound particles at 50% weight loss.
Cu-loading 9.0wt%, 5°C/min, 180°C

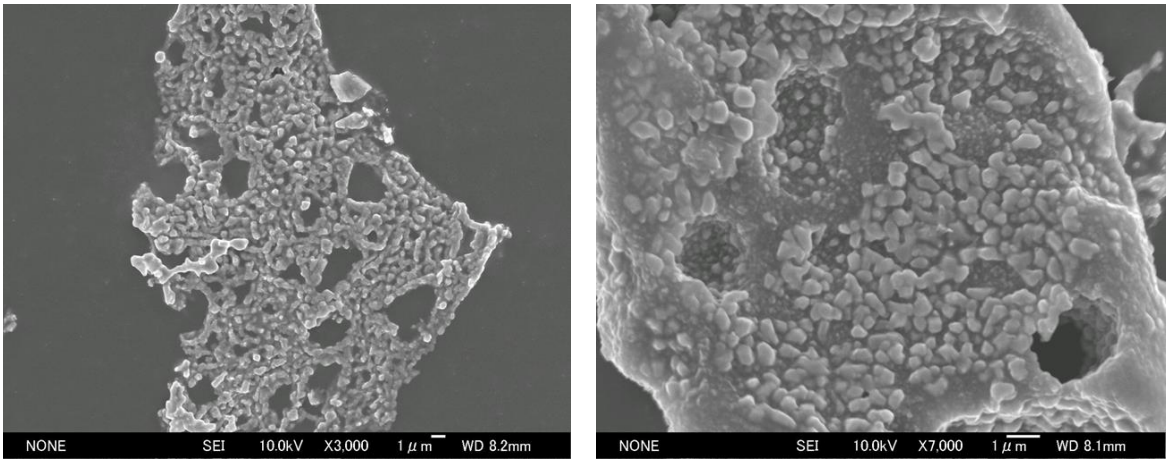

Fig. 5.7 SEM images of copper compound particles at 75% weight loss.
Cu-loading 9.0wt%, 5°C/min, 180°C

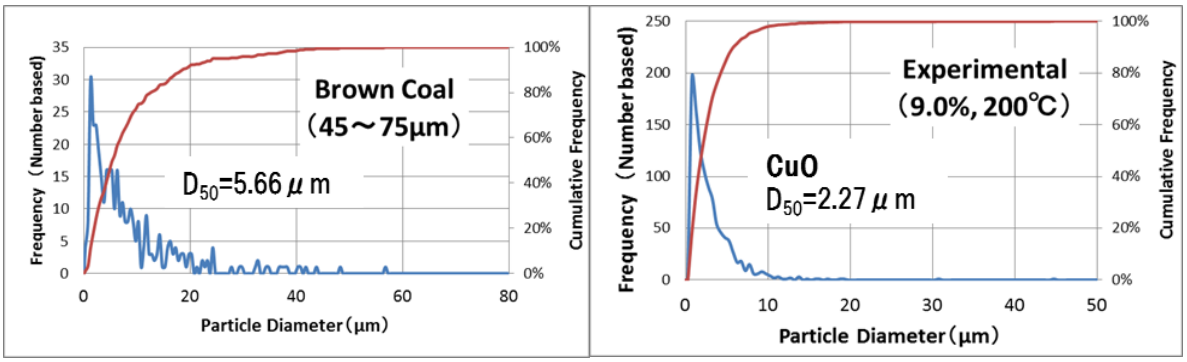

a) Number based distribution

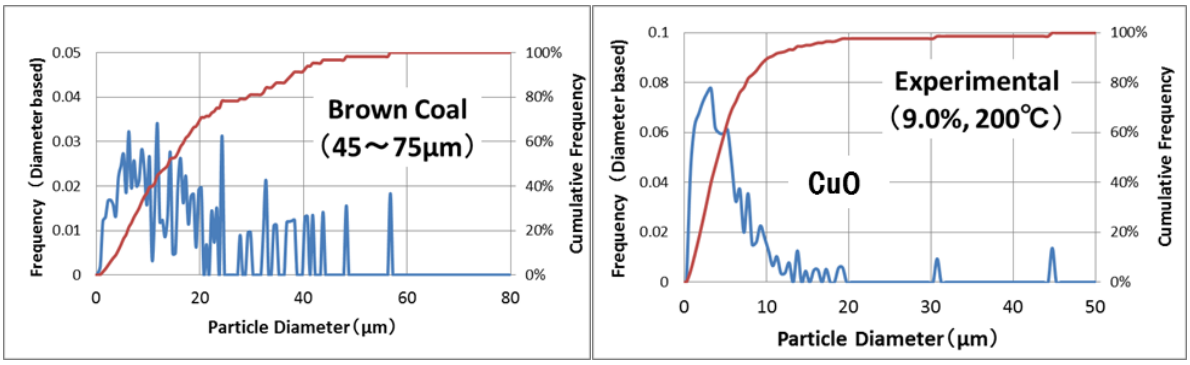

b) Diameter based distribution

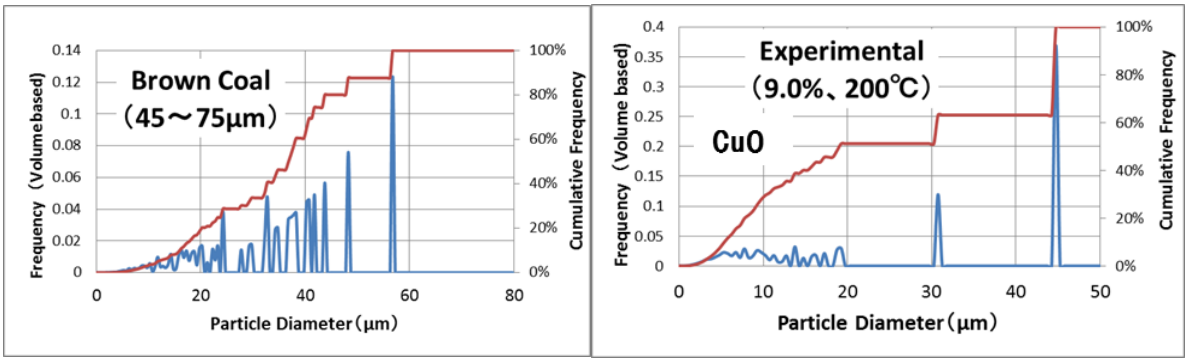

c) Volume based distribution

Fig. 5.8 Particle distributions of raw brown coal and CuO
(Cu-loading= 9.0wt%, Heating=10°C/min, 200°C)

Fig.5.8 shows the particle size distributions of Cu-loaded brown coal and the CuO particles formed when it is combusted. The D_{50} of the brown coal is 5.66μm, while that of the CuO is 2.27μm in the number based results.

If the coalesced particle formation model shown in Fig.5.5 represents the phenomenon well, then there should be a simple relationship between the particle size of brown coal and that of CuO. In **Table 5.1** and **Fig.5.9**, the volume occupied by CuO particles at the percolation threshold can be calculated from the Cu-loading on one brown coal particle. The calculated CuO size is then adjusted by the porosity of the coalesced CuO particle to fit the experimental CuO size. The calculation method used for this is as follows:

One molecule unit volume of CuO, v_{CuO} is,

$v_{CuO} = Mw_{CuO}/(\rho_{CuO} \cdot N_a)$: CuO-volume/pcl (m^3/pcl-c_uo) …Eq.(5.2)

where, Mw_{CuO} : molecular weight of CuO (g/mol)

N_a : Avogadro's constant (1/mol)

ρ_{CuO} : density of CuO (g/m^3)

The volume and mass of one brown coal particle, v_{bc} and w_{bc} are,

$v_{bc} = (\pi/6)D_{bc}^3$: brown coal volume/particle (m^3/pcl-bc) …Eq.(5.3)

where, D_{bc} : particle diameter of brown coal (m); sphere equivalent

$w_{bc} = v_{bc} \cdot \rho_{bc}$: brown coal mass/particle (g/pcl-bc) …Eq.(5.4)

where, ρ_{bc} : density of brown coal (g/m^3)

The copper loading on a single brown coal particle, Wc_u is,

$Wc_u = w_{bc} \cdot y/(1-y)$: Cu-loading on a brown coal particle (g/pcl-bc) …Eq.(5.5)

where, y : Cu-loading (－); weight ratio

One unit molecule mass of copper, w_{cu} is,

$w_{cu} = Mw_{Cu}/N_a$: Cu mass/Cu particle (g/pcl) …Eq.(5.6)

where, Mw_{Cu} : molecular weight of Cu (g/mol)

The number of molecular units of copper loaded on a brown coal particle, N_{cu} is,

$N_{cu} = Wc_u / w_{cu}$: Cu particle/brown coal (pcl-cu/pcl-bc) …Eq.(5.7)

Since one CuO molecule is changed for every copper molecule, the total volume of CuO included in a brown coal particle, V_{cuo} is,

$V_{cuo} = v_{CuO} \cdot N_{cu}$: CuO volume/brown coal (m^3/pcl-bc) …Eq.(5.8)

The volume of unburned brown coal at the percolation threshold, v_{bcx} is,

$v_{bcx} = V_{cuo} \cdot (1-p_c)/p_c$: volume of unburned brown coal (m^3/pcl-bc) …Eq.(5.8)

Where, p_c : percolation threshold, 0.312 for 3D Cubic

The conversion of brown coal at the percolation threshold, x is,

$x = 1-(v_{bcx} / v_{bc})$: conversion of brown coal (－) …Eq.(5.9)

As it is considered in this model that CuO particles coalesce into one large CuO particle with a porosity of ε., the CuO particle size, Dc_uo is estimated as,

$Dc_u o = (6\, V_{cuo}/(1-\varepsilon)\pi)^{(1/3)}$: CuO particle size (m); sphere equivalent …Eq.(5.10)

Where, ε : porosity of a CuO particle (－)

When the D_{50} of brown coal=5.66μm and the D_{50} of CuO=2.27μm, as in Fig.5.8, the porosity ε of CuO becomes 0.572. The linear nature of this relation is evident in Fig.5.9, where the porosity remains constant regardless of the size of the brown coal.

When the percolation model is used the small cluster size remains stable until near the percolation threshold, at which point coalesced particles are produced. Consequently, if only small sized CuO particles are needed, it may be necessary to quench combustion prior to it reaching the percolation threshold. This may, however, leave unburned carbon in the particles, which may or may not be acceptable depending on the intended application.

Table 5.1 CuO particle size calculated by coalesced particle formation model

Cu	Mwcu	g/mol	63.546	63.546	63.546	63.546
	ρ cu	g/m^3	8.94E+06	8.94E+06	8.94E+06	8.94E+06
	Na	pcl-cu/mol	6.02E+23	6.02E+23	6.02E+23	6.02E+23
	wcu	g/pcl-cu	1.06E-22	1.06E-22	1.06E-22	1.06E-22
	vcu	m3/pcl-cu	1.18E-29	1.18E-29	1.18E-29	1.18E-29
Cubic	dcu	m	2.28E-10	2.28E-10	2.28E-10	2.28E-10
CuO	Mwcuo	g/mol	79.545	79.545	79.545	79.545
	ρ cuo	g/m^3	6.31E+06	6.31E+06	6.31E+06	6.31E+06
	Na	pcl-cu/mol	6.02E+23	6.02E+23	6.02E+23	6.02E+23
	wcuo	g/pcl-cu	1.32E-22	1.32E-22	1.32E-22	1.32E-22
	vcuo	m^3/pcl-cu	2.09E-29	2.09E-29	2.09E-29	2.09E-29
	vcuo/vcu	-	1.77E+00	1.77E+00	1.77E+00	1.77E+00
3D-Cubic	pc		3.12E-01	3.12E-01	3.12E-01	3.12E-01
Brown Coal	ρ bc	g/m^3	1.40E+06	1.40E+06	1.40E+06	1.40E+06
Particle Diameter	Dbc	m	5.00E-05	5.66E-06	2.50E-06	5.00E-07
			50.0	5.66	2.5	0.5
Sphere	Vbc	m^3/Pcl-bc	6.54E-14	9.50E-17	8.18E-18	6.54E-20
	wbc	g/Pcl-bc	9.16E-08	1.33E-10	1.15E-11	9.16E-14
	vbc	m^3/Pcl-bc	6.54E-14	9.50E-17	8.18E-18	6.54E-20
Cu-loading	y	-	0.09	0.09	0.09	0.09
Loading Amount	wcu･Ncu	g/Pcl-bc	9.062E-09	1.316E-11	1.13E-12	9.06E-15
Loading atoms	Ncu	pcl-cu/Pcl-bc	8.59E+13	1.25E+11	1.07E+10	8.59E+07
Loading Volume	vcuo･Ncu	m^3/Pcl-bc	1.80E-15	2.61E-18	2.25E-19	1.80E-21
	x	-	0.939	0.939	0.939	0.939
	vbcx		3.97E-15	5.77E-18	4.96E-19	3.97E-21
CuO Porosity	ε		0.572	0.572	0.572	0.572
	Dcuo		20.02	2.267	1.00	0.20
	p		2.67E-02	2.67E-02	2.67E-02	2.67E-02

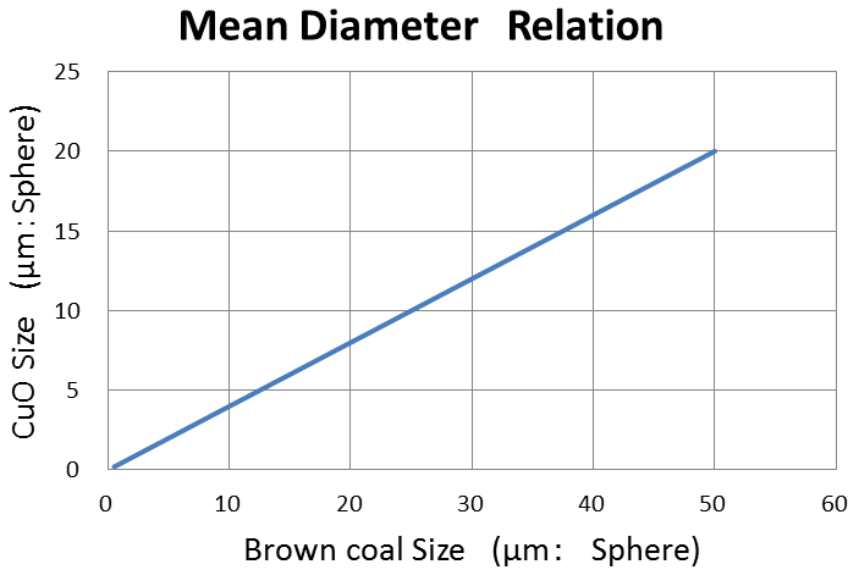

Fig. 5.9 Relation between CuO particle Size and brown coal size when using a coalesced particle formation model

5.3.3 Effect of Coal Size on CuO Particle Size

With the coalesced particle formation model, the size of the CuO produced correlates directly to the original brown coal size, as is shown in Fig.5.9. Note that the slower release of volatile matter and rate of reaction during low temperature combustion prevents the original brown coal particle from breaking into several fragments, remaining instead as a single particle. **Fig. 5.10** shows the particle distributions of the raw brown coal for different sieve ranges alongside the distributions of the CuO particles creating by burning this coal. This data indicates that a finer-sized raw brown coal produces finer CuO particle. SEM images of the Cu-loaded brown coals sieved to 25–45, 45–75 and 75–106μm size fractions are shown in **Fig.5.11**.

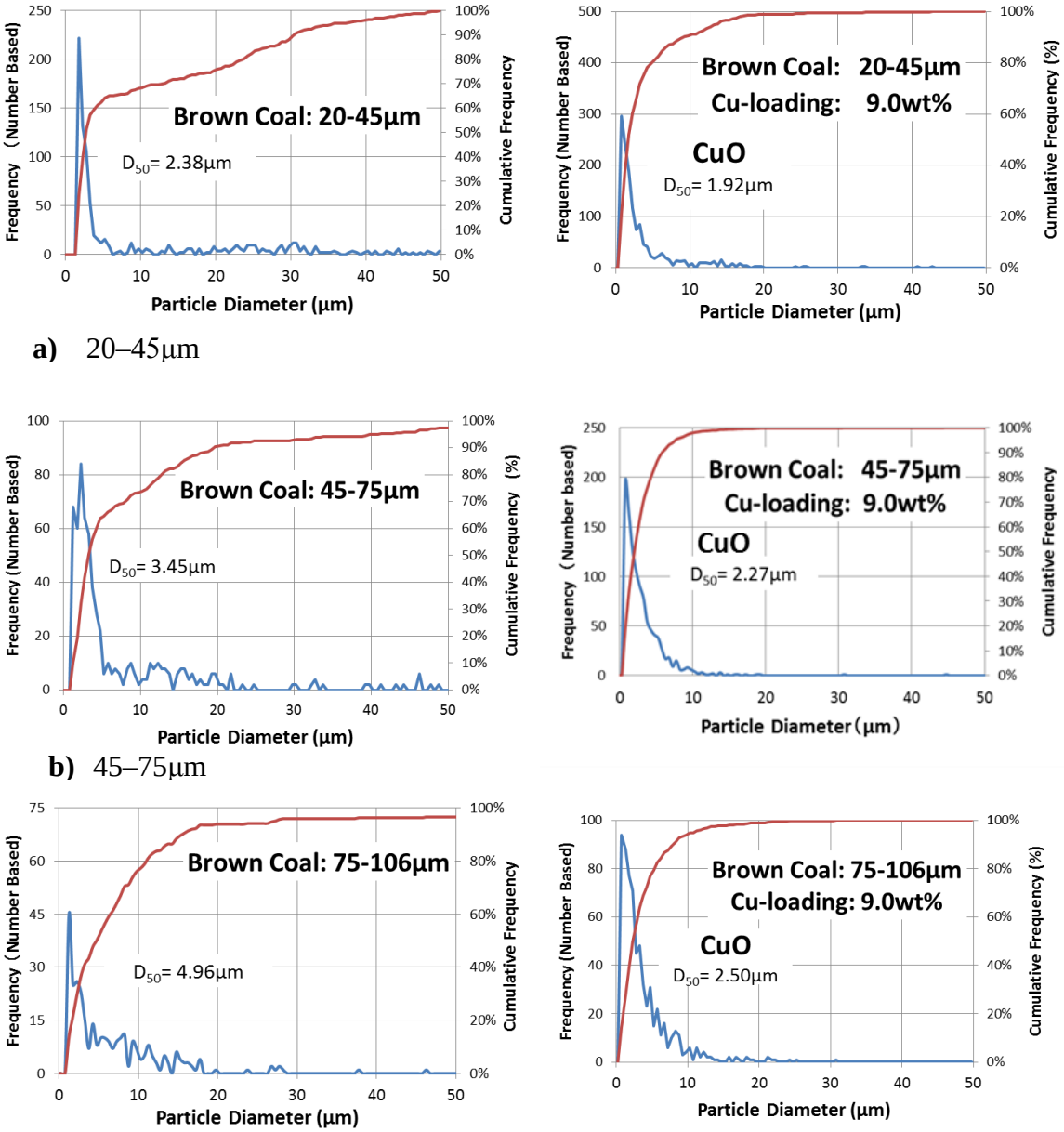

a) 20–45μm

b) 45–75μm

c) 75–106μm

Fig. 5.10 Particle distributions of different raw brown coal size fractions and the CuO produced by burning these coals; Brown coal: left, CuO: right (Cu-loading= 9.0wt%, Heating=10°C/min, 200°C)

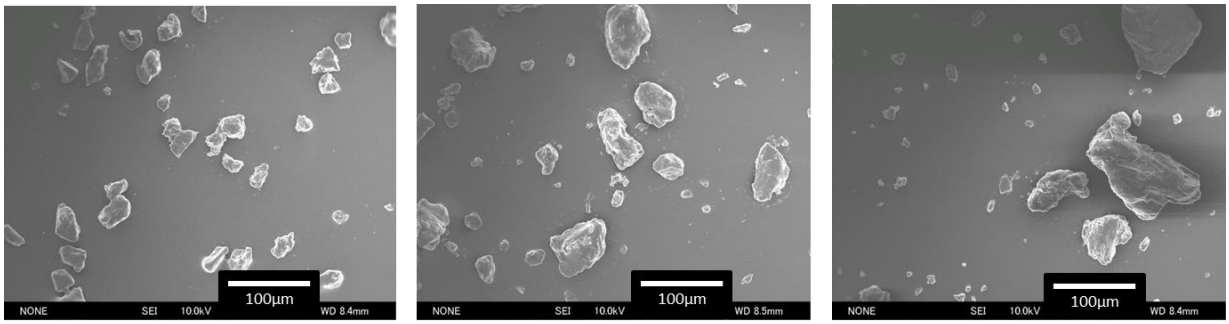

a)25-45μm b) 45-75μm c) 75-106μm

Fig. 5.11 SEM images of Cu-loaded brown coals sieved into size fractions of: a) 25–45, b) 45–75 and c) 75–106μm (Cu-loading= 9.0wt%)

SEM images of the CuO particles produced by burning the Cu-loaded brown coals are shown in **Fig.5.12.** In **Fig. 5.13**, we can see that the relation between the mean particle size of the raw brown coal and CuO is much the same for both the coalesced particle formation model and the experimental results. **Fig.5.14** provides the mode diameters for the brown coal and CuO particles, which is effectively the same at all sieve sizes. Since the particle size distributions were only measured after dispersion in methanol, fine particles attached to larger particles or present as coagulates should be correctly accounted for. The mode diameters of CuO are also similar at 0.56–0.66μm, with the relation between the mode diameters plotted in Fig.5.13 as square markers. This clearly shows that the mode size of CuO is determined by the mode size of the brown coal, and that this relation can be explained by the coalesced particle formation model.

The mode diameter of particles with a size of around 0.56-0.66μm seems to be the unit particle of the coalesced large particle seen in Fig.5.12. If it is assumed that there is a unit fragment surrounded by structural boundaries in the large brown coal particle, and that this is similar to the mode diameter of brown coal, then the unit Cu_2O particles that are later changed to CuO could be formed from the unit brown coal fragments. This means that coal macerals such as huminite could be the structural boundaries of the large brown coal. Moreover, as it seems likely that the mode diameter of the brown coal is generated during the pulverization of larger particles, the size is determined by structural boundaries. **Fig.5.15** shows an SEM image of attrinite, which is a maceral of the huminite group and consists of fine huminitic particles. Attrinite is a major component of soft brown coal, usually making up around 90% of the groundmass of brown coal,[4)] with its name being derived from the word attritus, meaning matter pulverized by attrition.[4)] Attrinite would therefore seem a likely candidate for providing the structural boundary in coal groundmass that regulates the growth of CuO to a polycrystalline size, and could also represent the mode diameter of brown coal produced by pulverizing. Given that attrinite grains are present in the original large brown coal particle, it is believed that primary CuO particles are formed by percolation inside attrinite grains, with secondary coalesced particles then forming inside the large brown coal particle.

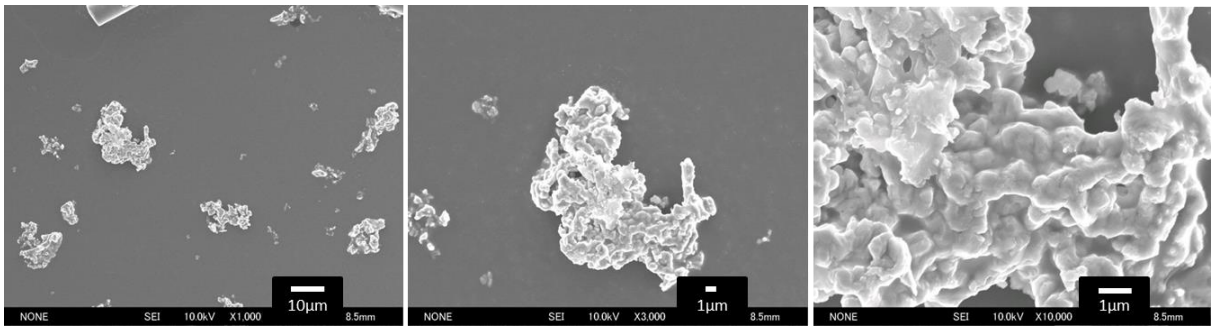

a) 25–45μm

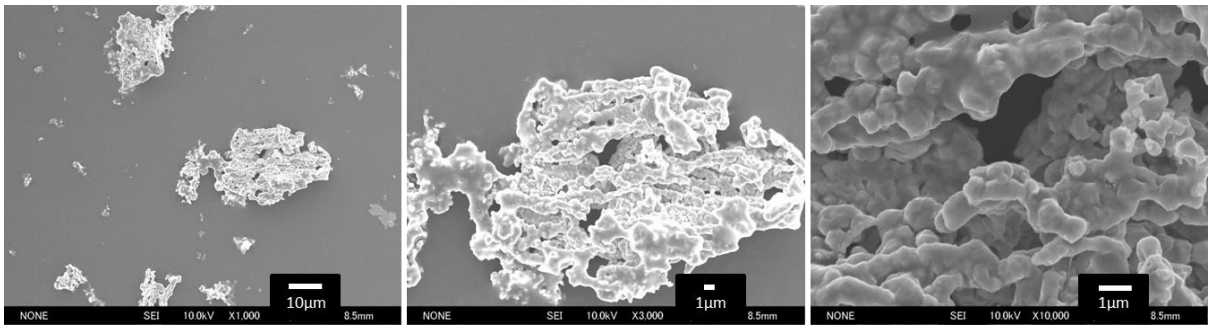

b) 45–75μm

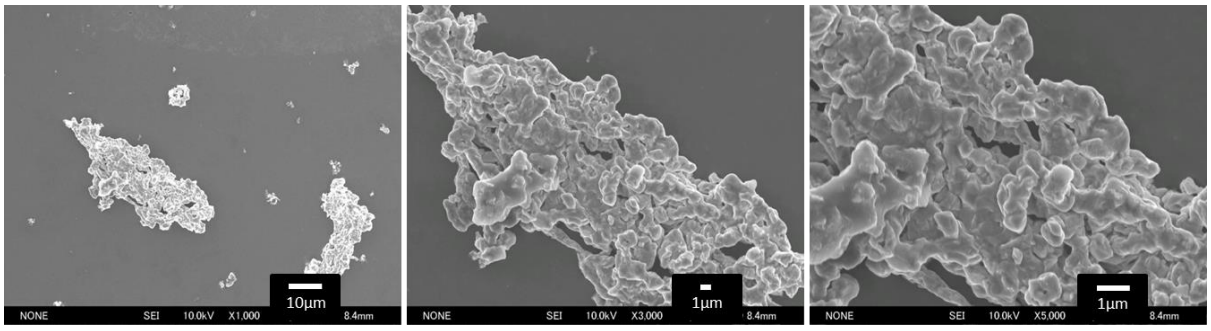

c) 75–106μm

Fig. 5.12 SEM images of CuO particles produced by burning Cu-loaded brown coal sieved to size fractions of: a) 25–45, b) 45–75 and c) 75–106μm (Cu-loading=9.0wt%, Heating=10°C/min, 200°C)

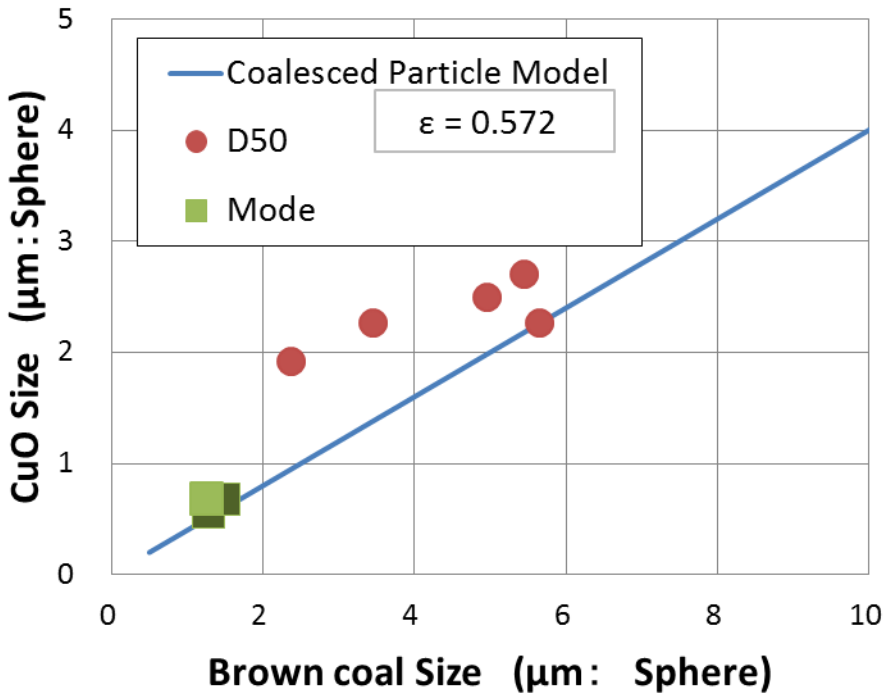

Fig. 5.13 Relation between the mean particle size of raw brown coal and CuO for the coalesced particle formation model and experimental results (number based) (Cu-loading=9.0wt%, Heating=10°C/min, 200°C)

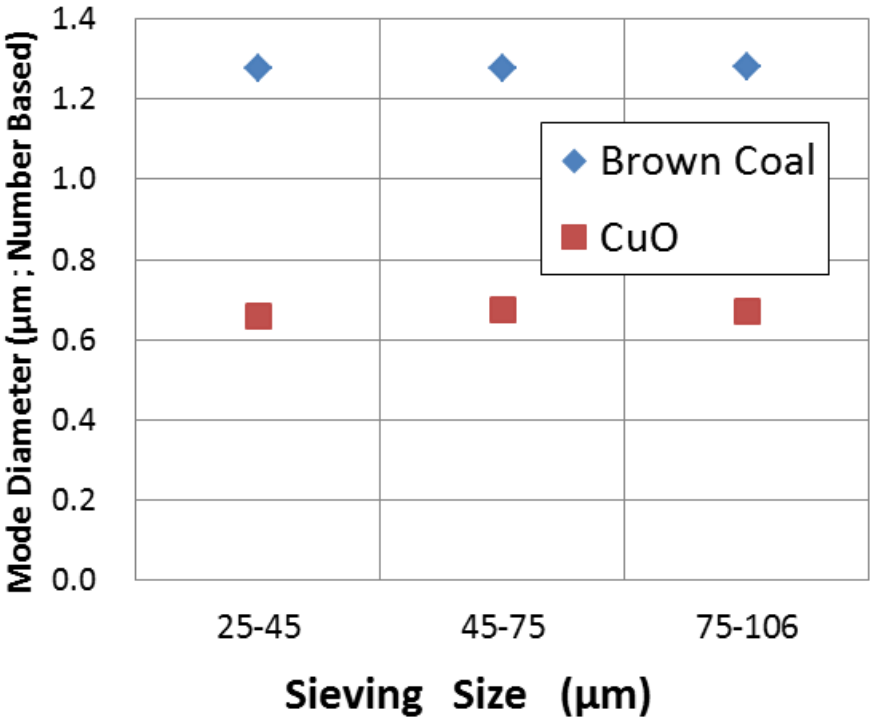

Fig. 5.14 Mode diameters of brown coal and CuO particles (Cu-loading=9.0wt%, Heating=10°C/min, 200°C)

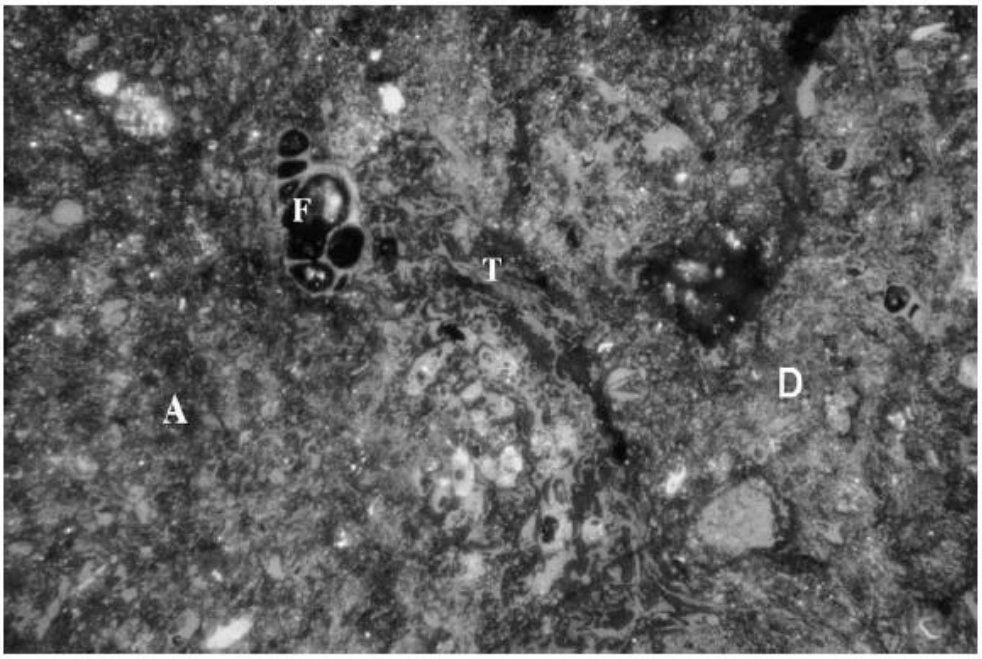

a) Attrinite (A), densinite (D), textinite (T), funginite (F). Field width:250μm

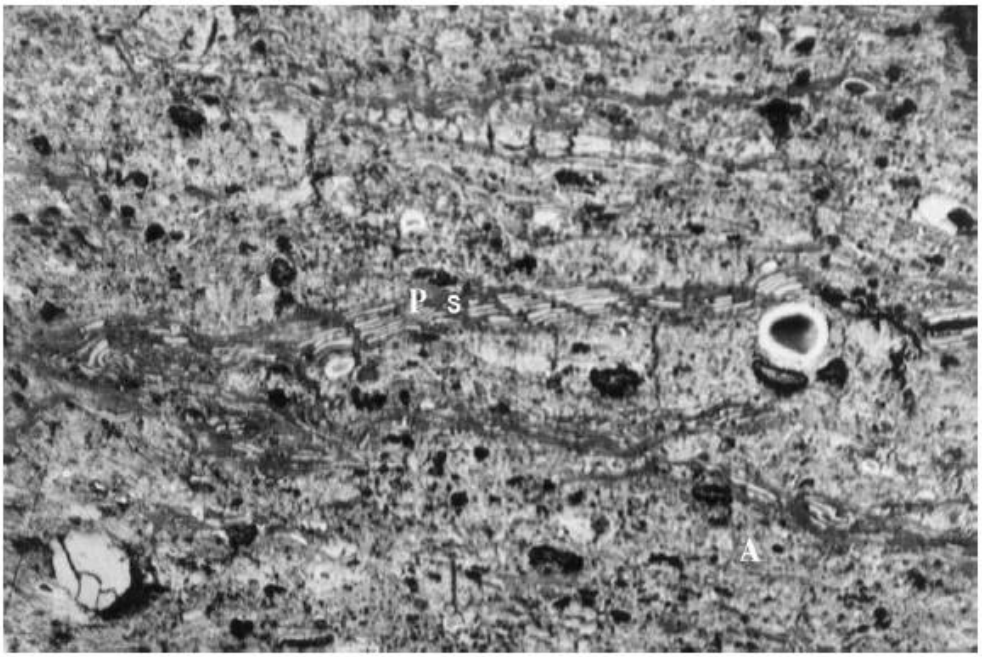

b) Attrinite (A), suberinite (S), phlobaphinite (P). Field width:240μm

Fig. 5.15 SEM images of Attrinite. Source: Sykorova et al. [4)]

5.3.4 Effect of Copper Loading on CuO Particle Size

The effect of Cu-loadings of 1.7, 4.8 and 9.0wt% on the CuO particle size produced by combustion is shown **Fig.5.16**, in which the D_{50} of the CuO clearly increases with Cu-loading. The conversions (x) at the percolation threshold were calculated in the same way as those presented in Table 5.1, with the results plotted in **Fig.5.17**.

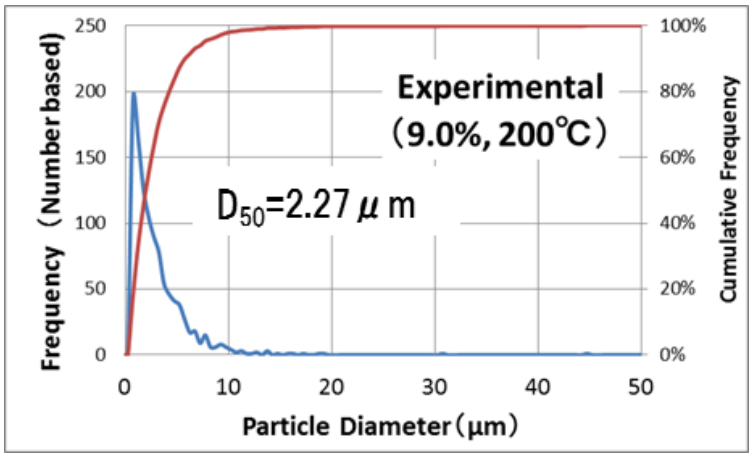

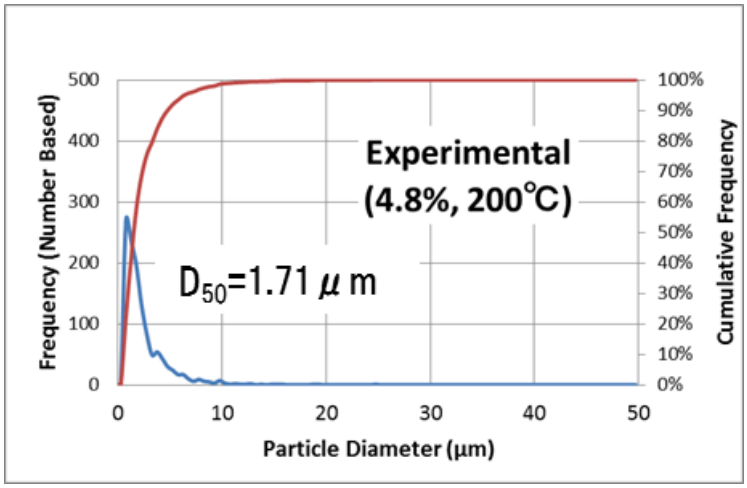

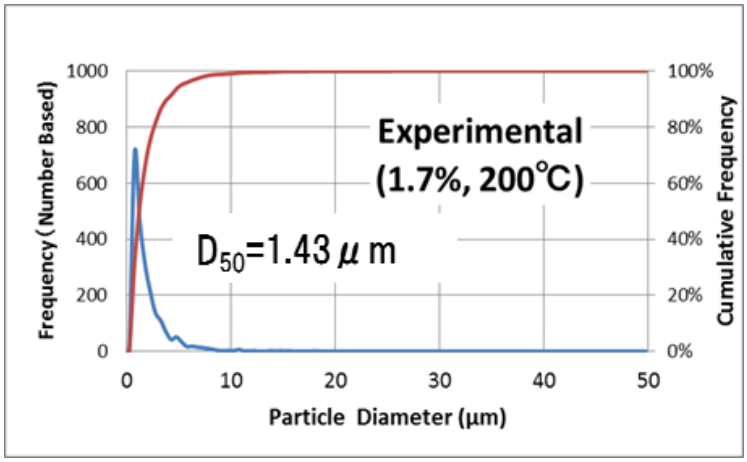

Fig. 5.16 a) CuO particle size distributions (number based) with brown coal copper loadings of 1.7, 4.8 and 9.0wt% (Heating=10°C/min, 200°C)

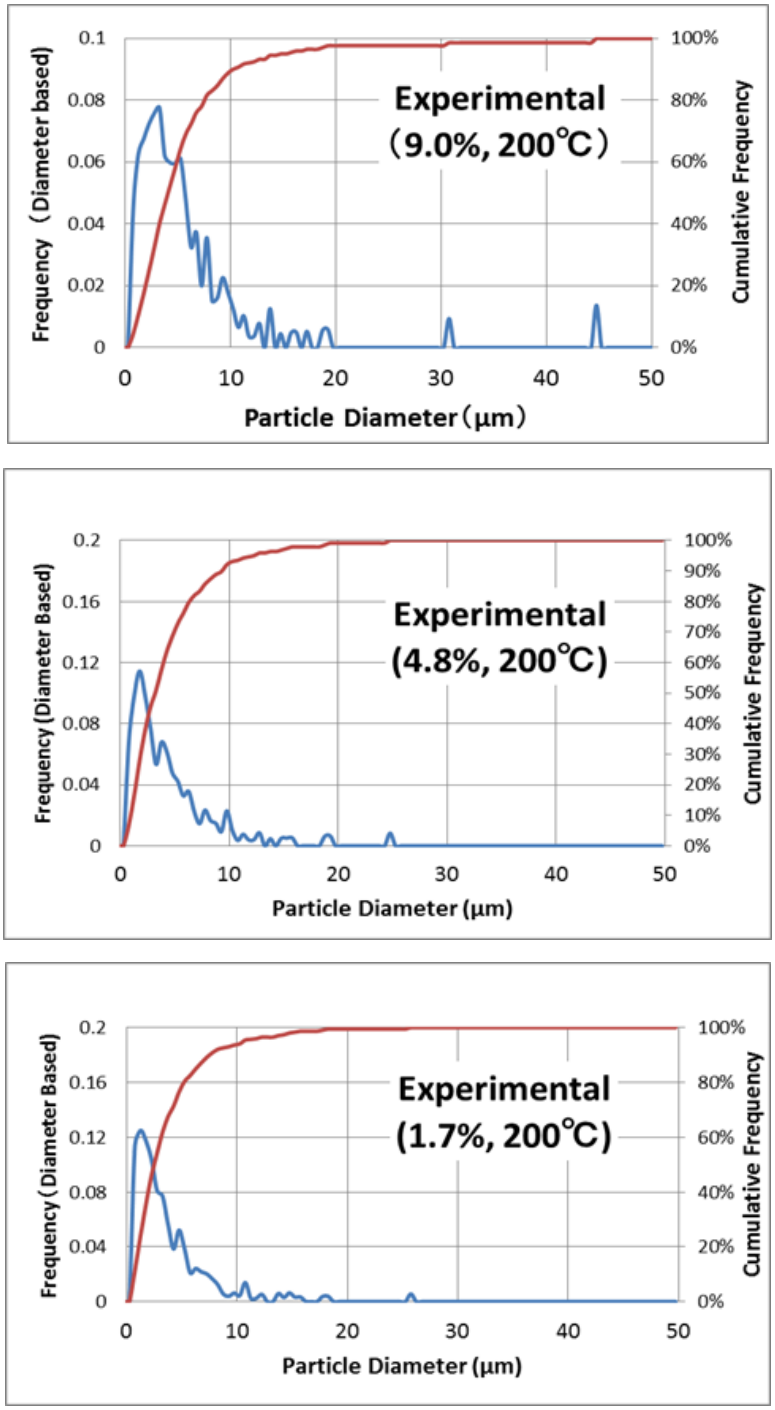

Fig. 5.16 b) CuO particle size distributions (diameter based) with brown coal copper loadings of 1.7, 4.8 and 9.0wt% (Heating=10°C/min, 200°C)

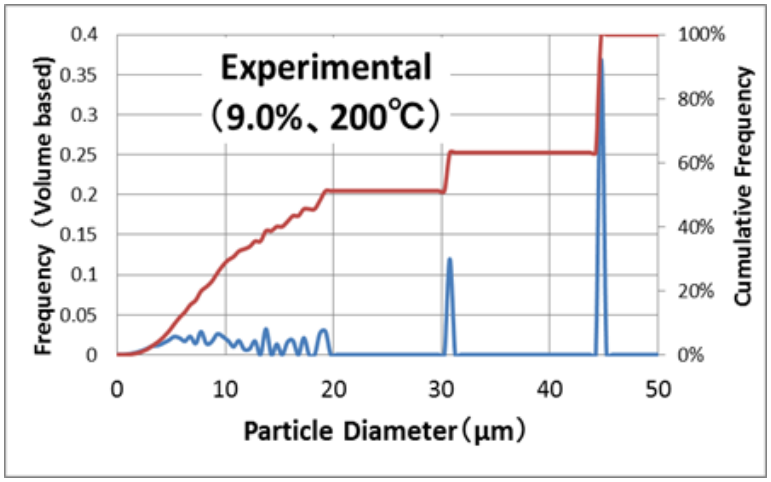

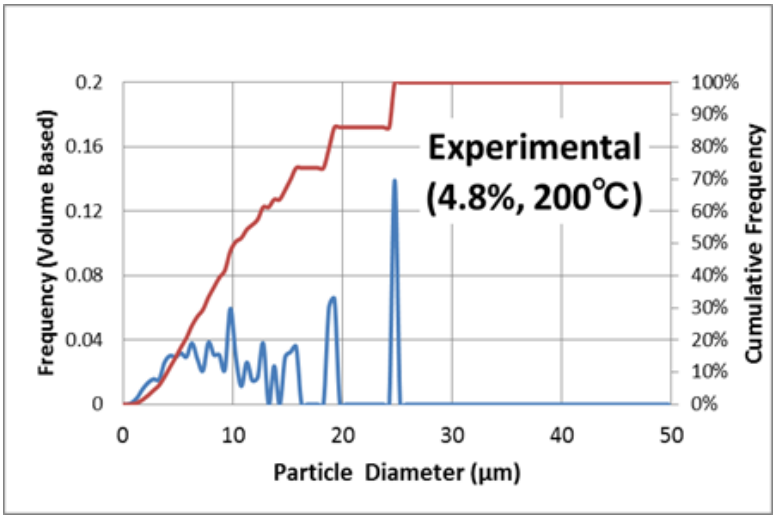

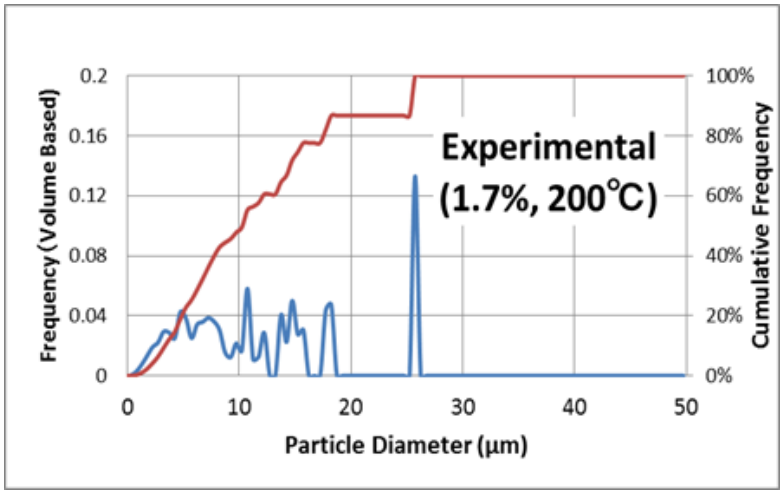

Fig. 5.16 c) CuO particle size distributions (volume based) with brown coal copper loadings of 1.7, 4.8 and 9.0wt% (Heating=10°C/min, 200°C)

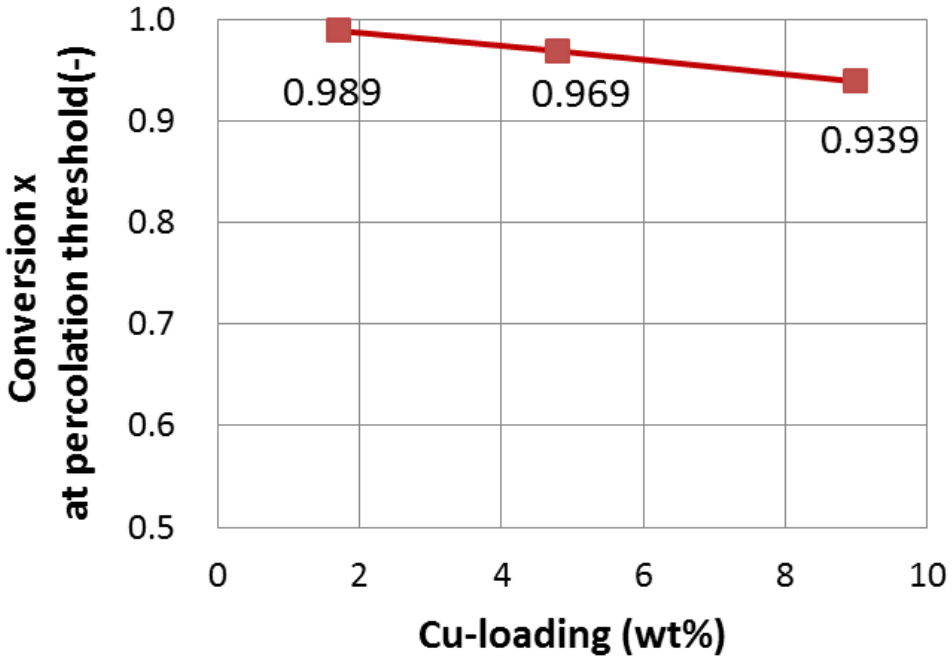

Fig. 5.17 Calculated conversion of coal by combustion at the percolation threshold

All three conversions were found to be close to complete combustion at the percolation threshold, and so it is expected that individual brown coal fragments change to a single CuO coalesced particle at this point. The CuO particle sizes with different initial Cu-loadings estimated by the coalesced particle formation model are compared with the experimental D_{50} values for CuO in **Fig.5.18**. This graph shows that the coalesced particle formation model and experimental results are in good agreement.

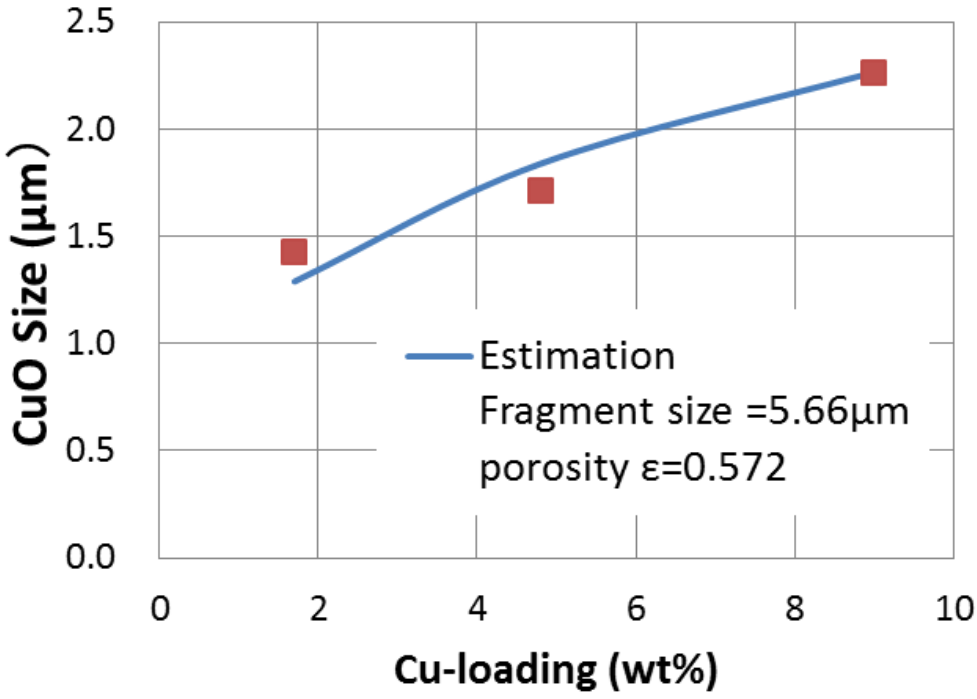

Fig. 5.18 Relation between CuO particle size and brown coal Cu-loading

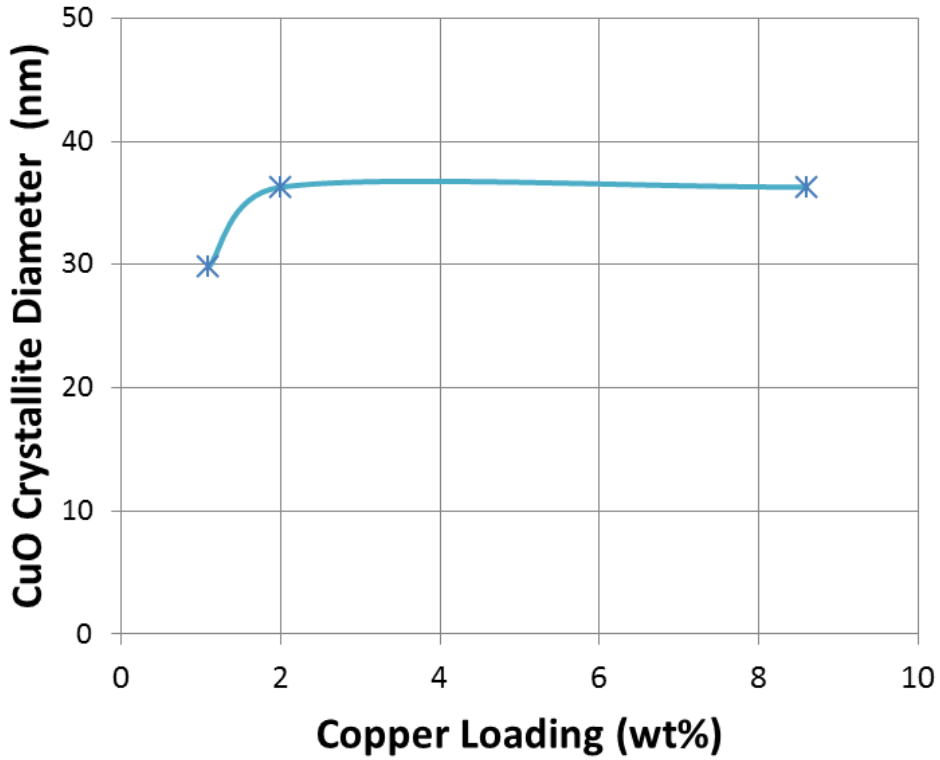

Fig. 5.19 Relation between CuO crystallite diameter and brown coal Cu-loading

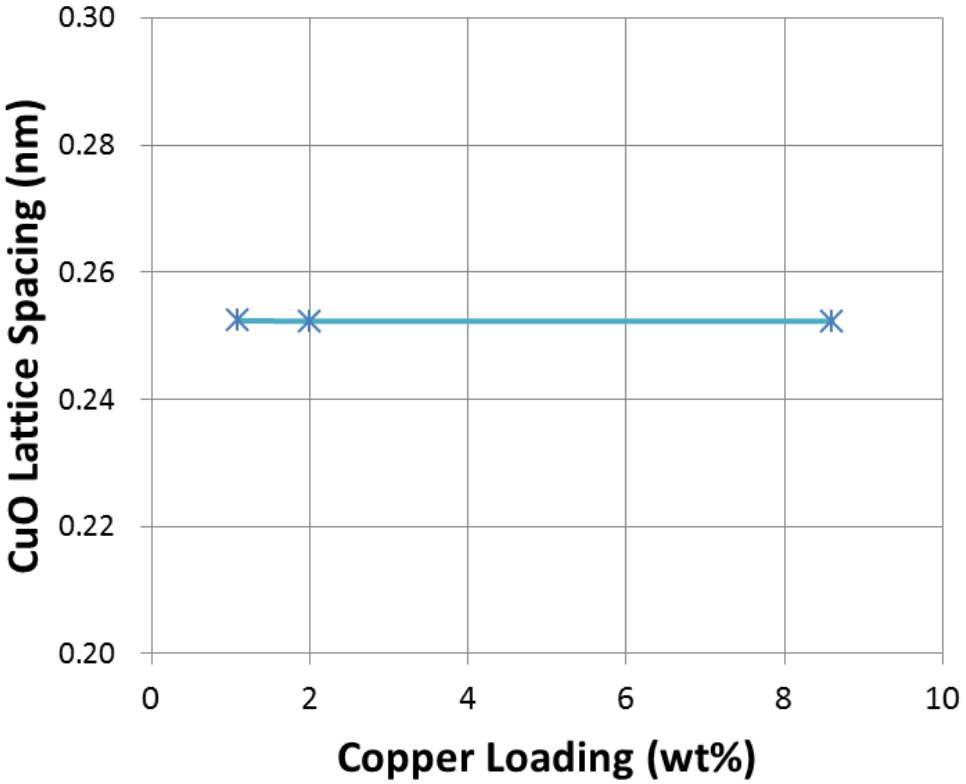

Fig. 5.20 Relation between CuO lattice spacing and brown coal Cu-loading

The crystalline diameter and lattice spacing are plotted in **Fig.5.19** and **Fig.5.20**. These clarify that the crystalline diameter is similar at different copper loadings, and that the CuO particle size decreases with decreasing copper loading. This can be explained by the fact that

high copper loadings (i.e., 8.6wt%) are achieved by ion exchange, whereas with loadings of less than 2wt% the copper is loaded by $Cu(OH)_2$ particle deposition and physical absorption. When copper is loaded as $Cu(OH)_2$, the initial particle size may be larger than ion exchange mechanism; however the CuO size at 1.1wt% Cu-loading is smaller than that of 8.6wt% Cu-loading despite the similarity in crystalline diameter. It is therefore believed that the $Cu(OH)_2$ is thermally decomposed and reduced to Cu^0 during the early stage of combustion.

5.4 Conclusion

In this chapter, the copper particle formation mechanism was studied and a modified percolation model was proposed along with a coalesced particle formation model.

1. At a point near complete combustion small particles of Cu compounds coalesce together, with this point being therefore defined as the percolation threshold.

2. There is a good relation between the D_{50} of brown coal and the D_{50} of CuO particles produced when it is burned, which can be explained by the coalesced particle formation model.

3. The mode diameter of CuO is determined by the mode diameter of the raw brown coal from which it is produced, and this relation is explained by the coalesced particle formation model.

In the low-temperature combustion of Cu-loaded brown coal, the CuO particle size is controlled by the original brown coal size. Thus, in order to produce fine primary CuO particles, it is necessary to control the mode diameter of the brown coal. This, in turn, is determined by structural boundaries such as macerals. It is also believed that the coalescence of secondary particles occurs near the end of combustion, and so incomplete combustion may be needed to avoid this in some circumstance.

5.5 References

1) Stauffer, D., Aharony, A., *"Introduction of percolation theory"*, Rev.2nd edition, Taylor and Francis
2) Suzuki, A., Yamamoto, T., Aoki, H., Miura, T., *Proceedings of the Combustion Institute*, 29, 459-466 (2002)
3) Miccio, F., Salatino, P., Tina, W., *Proceedings of the Combustion Institute*, 28, 2163-2170 (2000)
4) Sykorova, I., Pickel, W., Christanis, K., Wolf, M., Taylor, G.H., Flores, D., *Int. J. Coal Geol.*, 62, 85-106 (2005)

Chapter 6 Applications for Recovered Copper

6.1 Introduction

Copper compounds recovered from waste etching solution using brown coal were studied for use in several different applications. One viewpoint is to recycle the copper in or near the site of waste production to reduce the costs of processing and transportation cost, for which the recycling of copper compound solutions presents the simplest approach. The other viewpoint is to use the copper oxide particles recovered through combustion as a powder metallurgy material or copper catalyst, which adds value to the material.

6.2 Copper Compound Solution

6.2.1 Copper Chloride for Remaking Etching Solutions

Divalent copper chloride could be reproduced by re-ion exchange of the Cu-loaded brown coal with hydrochloric acid. Since heating is not required the brown coal could be reused as an ion exchange media, thereby presenting the most inexpensive process cost. In Chapter 3, it was found that copper-ammonium complex ions are captured in brown coal when ammonia is used as a pH adjusting agent.

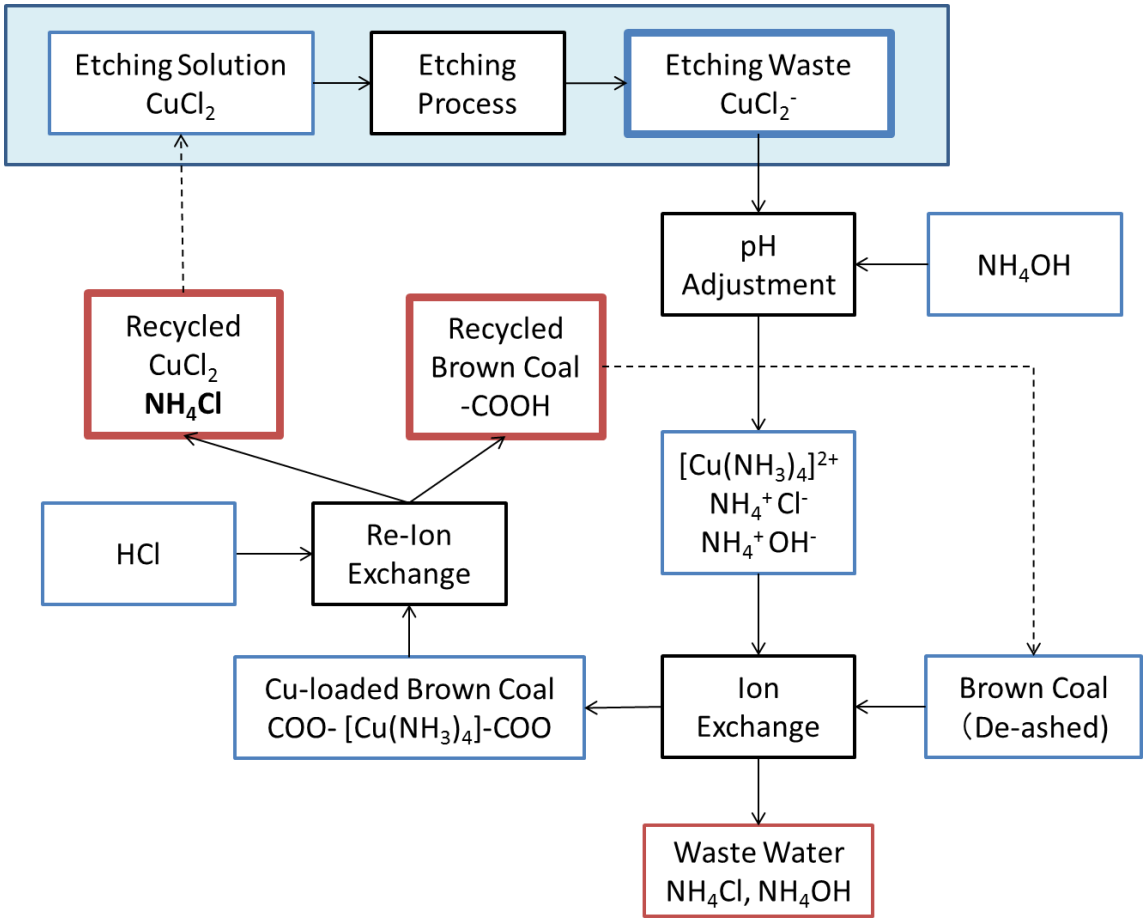

Fig. 6.1 Process for copper chloride recycling

Fig.6.1 shows the process by which copper chloride can be recycled. Note that if the

divalent copper chloride is recycled to etching solution, then ammonium chloride becomes concentrated in the recycle loop. Consequently, the separation of ammonium chloride from copper chloride is required in order to commercialize this process.

6.2.2 Copper Sulfate for use as a Plating Solution

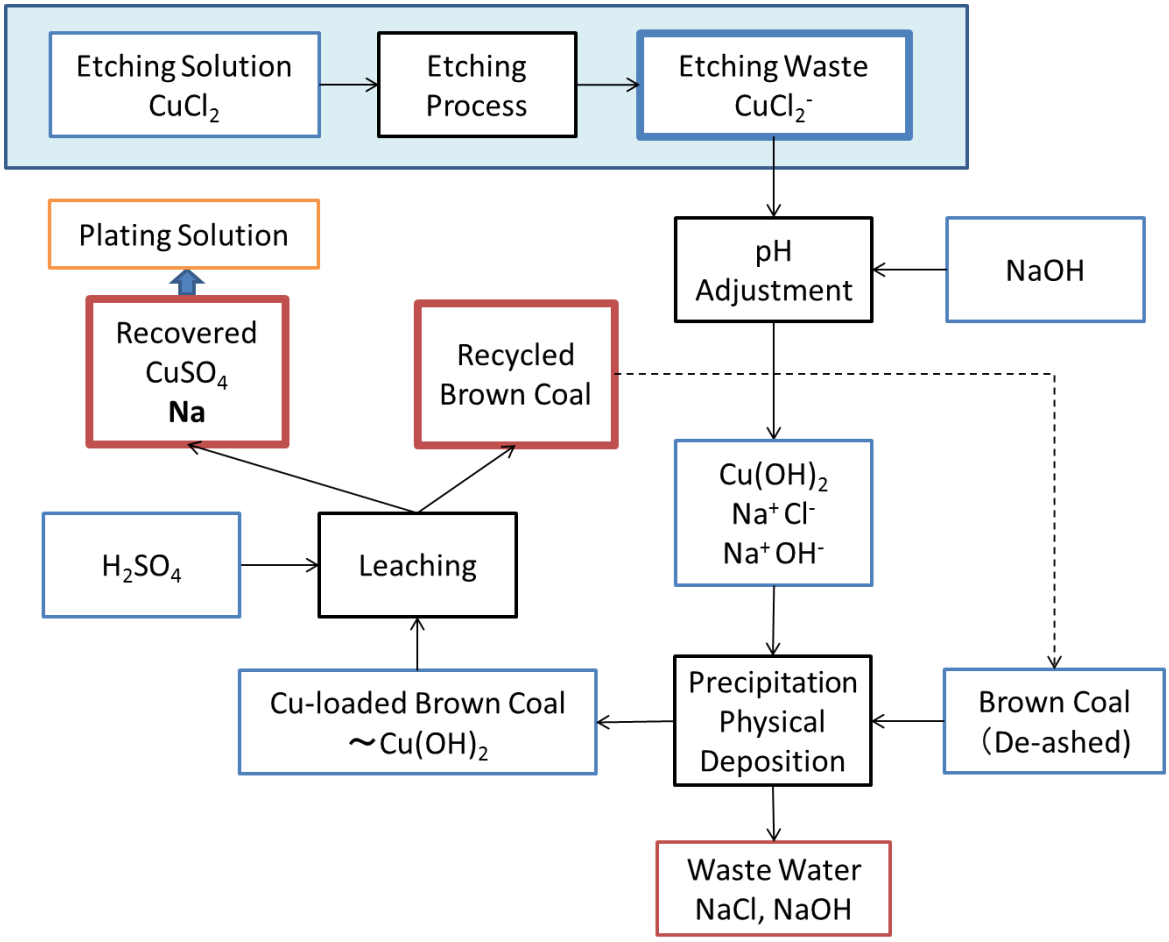

Fig. 6.2 Process for recycling copper sulfate

Copper sulfate can be used for making up copper plating solutions,[1)] but much like in Section 6.2.1, the use of ammonia as a pH adjusting agent contaminates the copper sulfate with ammonium chloride. Testing of copper sulfate electroless plating solutions produced from Cu-loaded brown coal with ammonia found that they have a NH_4^+ ion concentration of around 0.2–0.8wt%. The rate of copper deposition from these recovered plating solutions is in the order of 0.01–0.015μm/min, which is about one-third to half that of the original plating solution. Clearly, contamination by ammonium ions also cannot be allowed with plating solutions.

Fig.6.2 shows a process for recycling copper sulfate using sodium hydroxide as the pH adjusting agent, in which copper hydroxide particles precipitate on brown coal and are subsequently leached by sulfuric acid. Obviously in this case ammonium ions are not included in the plating solution, and so the deposition rate of around 0.28μm/min is not surprisingly

equivalent to the original plating solution. Although a small amount of sodium is included in the solution by using sodium hydroxide, these ions are considered harmless given that the plating solution is only used once; i.e., sodium ions have no opportunity to become concentrated in the solution. This means that a copper plating solution is a possible application for the recovered copper, though the costs of NaOH addition and waste water treatment will depend on the surrounding ancillary facilities of the etching plant. By rough estimate, however, it is believed that the end result should be a profit in most cases.

6.3 Copper Compound Particles

6.3.1 Copper oxide using for a powder metallurgical material

Copper metal is often added to powder metallurgy materials to improve their strength, high temperature lubricity, thermal conductivity and protection performance[2)]. The recovered copper oxide particles were therefore tested for their suitability for use in such applications, and the properties of the sintered metal produced were compared with original products.

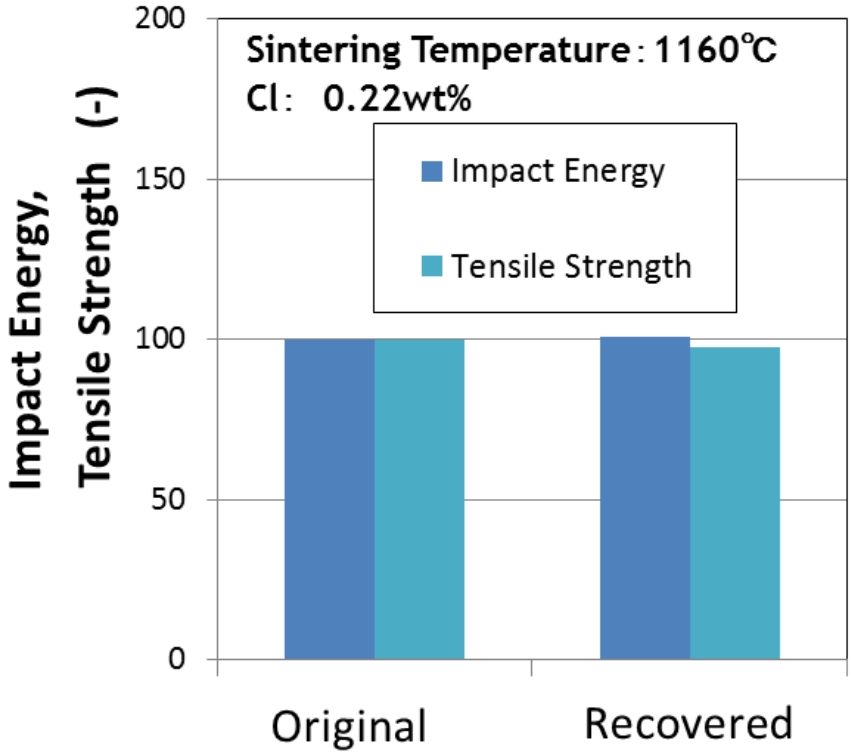

Fig. 6.3 Impact energy and tensile strength of sintered metal containing recovered copper

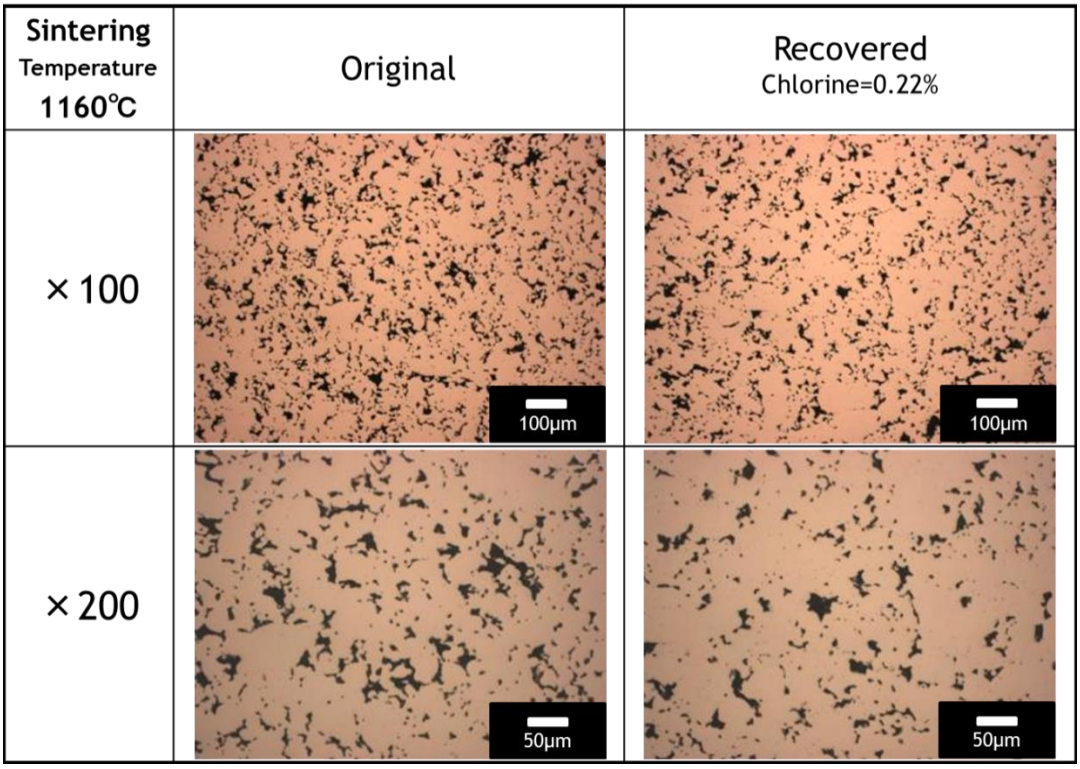

Fig. 6.4 Micrographs of pores in sintered metal with and without recovered copper

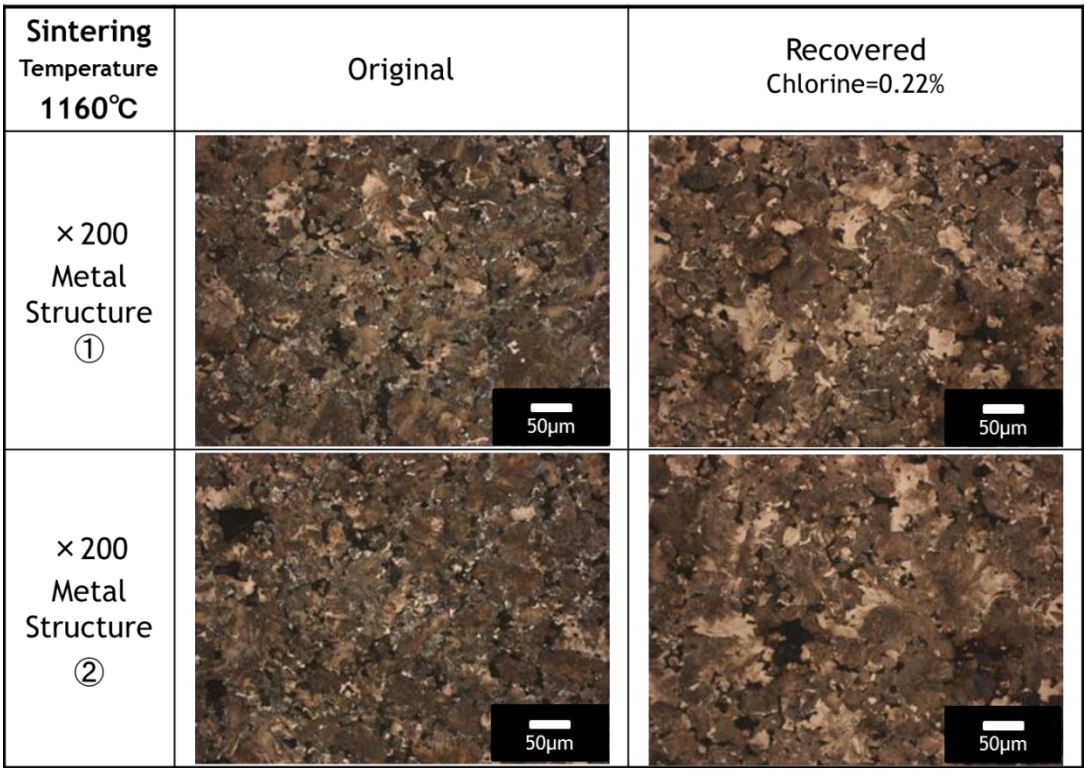

Fig. 6.5 Micrographs showing the structure of sintered metal with and without recovered copper

The test results of the sintered metal using recovered copper presented in **Fig.6.3** show that its impact energy and tensile strength were equivalent to the original structure. In the early stages of investigation it was found that when the residual chlorine is greater than 0.3wt% the tensile strength is lower than the target value, as residual chlorine directly affects

the sintering behavior. After improving the washing process the residual chlorine was lowered to 0.22wt%, and as a result the tensile strength was made equivalent when the sintering temperature was 1160°C. The micrographs in **Fig. 6.4** and **Fig. 6.5** show the pores in the resulting metal structure compared to the original, with very little difference evident between the two. This application would therefore also seem to be a possible candidate, but as a lower temperature is more attractive for reducing the energy consumption, reducing the residual chlorine is a challenge for the future. It should be noted though that 1160°C is an ordinary temperature for sintering, but if this can be lowered then the benefits of using recovered copper will only be increased. Furthermore, the use of recovered copper has the potential to provide good control over the particle without having to rely on material suppliers.

6.3.2 Prospects for Copper Catalyst Applications

Copper-loaded brown coal was in Chapter 4 to exhibit a catalytic ability for devolatilization and combustion, the possible applications of which are as follows:

1) Oxidation-Reduction

Copper-terminated Cu_2O could provide an activate catalyst for oxidation and reduction reactions, with inorganic catalysts containing copper having already been studied by many researchers for low-temperature gasification[3)-4)]. The effect of particle size has also been studied, through which it was found that nano-sized copper particles work very well in catalyzing the Ullmann reaction[5)]. In addition, NO reduction in automobile exhaust gas treatment has been studied using Cu_2O catalysts[6)]. In all these cases, it seems it is important to control the particle size and surface atoms of copper oxide.

2) Hydrogen generation catalyst for fuel cells

Copper compound catalysts have been studied by many researchers for the water gas shift reaction that occurs in fuel cells[7-8)]. Copper-metal oxide catalysts exhibit a particularly good activity for CO conversion, but it seems important to control the copper and metal oxide composition.

In all of these catalyst applications a high added value is obtained, but although Cu-loaded brown coal can function as a catalyst, it must be remembered that it is also combustible. The D_{50} of copper recovered through combustion is around 1.5–3μm (number based), and even the mode diameter is around 0.5–0.7μm. This means that even after complete combustion the particle size is still too large to exhibit the unique capabilities of nano-sized particles. Thus, in order to bring out the maximum activity in a copper catalyst, it is preferable to use the Cu-loaded brown coal as the copper compounds are still at a molecular size. However, if the Cu-loaded brown coal is used under oxidizing conditions, then it may combust along with the unburned target materials. Pyrolysis, gasification and reduction may be suitable for extending the life of Cu-loaded brown coal, though partial oxidation can also be used to create copper

terminated Cu_2O.

As this study was focused on the recovery of copper from waste etching solution, only copper loaded on brown coal was assessed. However, it may in fact be possible to load several metals onto brown coal, thereby creating a high degree of freedom in achieving the ideal metal composition for a specific application.

6.4 Conclusion

The potential applications for the copper recovered as either a copper compound solution or solid particle were studied and discussed in this chapter. In either case, it was found that the presence of impurities can affect the properties needed for these applications.

1. Residual ammonium ions produced by using ammonia as a pH adjusting agent affect the deposition rate of copper sulfate plating solutions. If, on the other hand, NaOH is used as the pH adjusting agent, then the deposition rate is equivalent to the original plating solution. Plating solutions are therefore a viable use for the recovered copper.

2. Residual chlorine in copper oxide particles affects the impact energy and tensile strength of sintered metal to which they are added, but with improvements in the washing process, both the impact energy and tensile strength become equivalent to the original metal. Thus, powder metallurgy presents a potential use for the recovered copper, with the added advantage that this allows very fine copper particles to be produced in-house.

3. The copper oxide particles produced by the complete combustion of Cu-loaded brown coal lack the unique properties of nano-scale catalysts, meaning that the Cu-loaded brown coal itself is the better candidate for catalyzing oxidation-reduction reactions. In order to extend the life of brown coal in such application, it is desirable to find a catalyst for gasification. There is also the possibility of loading multiple metals onto brown coal to create catalysts for other applications (e.g., the water gas shift reaction in fuel cells), though this was considered beyond the scope of this study.

6.5 References

1) http://www.hitachi-chem.co.jp/japanese/products/pm/008.html
2) Tsutsui, T., *Hitachi Chemical Technical Report*, 54, 13-21 (2011)
3) Stournas, S., Papachristos, M., Kyriakopoulos, G.B., *American Chemical Society National Meeting*, New Orleans, LA, USA (1987)
4) Domazetis, G., Liesegang, J., James, B.D., *Fuel Process. Technol.*, 86, 463-486 (2005)
5) Samim, M., Kausik, N.K., Maitra, A., *Bull. Mater. Sci*., 30, 5, 535-540 (2007)
6) Kasai, H., Padama, A.A.B., Nishihata, Y., Tanaka, H., Mitachi, C., *J. Jpn. Petrol.*

Inst., 56, 6, 357-365(2013)
7) Jeong, D.W., Jang, W.J., Shim, J.O, Han, W.B., Roh, H.S., Jung, U.H., Yoon, W.L., *Renewable Energy*, 65, 102-107 (2014)
8) Sagata, K., Imazu, N., Yahiro, H., *Catal. Today*, 201, 145– 150 (2013)

Chapter 7 Conclusion

7.1 Conclusion

The recovery of copper from printed circuit board manufacturing waste etching solutions using Loy Yang brown coal was studied, and the challenges identified were summarized in Chapter 2. The key points of the copper recovery process design are the highest copper loading condition, low-temperature combustion mechanism and copper oxide particle formation mechanisms. Since Cu-loaded brown coal combusts at low temperature, it is believed the copper provides a catalytic effect. These key factors, including the catalytic abilities, were investigated in detail in Chapter 3, 4 and 5.

In Chapter 3, the method of using Loy Yang brown coal as an ion exchange medium for copper recovery was studied, through which it was found that a copper ion loading of around 8.5wt% can be achieved at room temperature by adding ammonium hydroxide to adjust the pH to 9–11.5. Under these conditions, it is believed that copper and ammonium complex ions such as tetraamminecopper(II) $[Cu(NH_3)_4]^{2+}$ are produced and exchanged with protons of the carboxy groups in brown coal, with the result being that copper is highly dispersed in the brown coal. Further study of this loading mechanism by XPS analysis found that ion exchange is in fact not the only mechanism of the copper loading, as $Cu(OH)_2$ particle deposition and physical absorption are other possibilities. However, ion exchange tends to very effective because it works at room temperature, requires only a short time and has very low energy requirements.

Analysis of the reaction kinetics and low-temperature combustion mechanism of Cu-loaded brown coal by TG analysis in Chapter 4 found that Cu-loaded brown coal can burn at an extremely low temperature of 160–180°C, producing 0.5–1.0μm copper oxide particles as a residue. Since the XRD spectra at 165°C was consistent with Cu_2O, this phase is believed to play a role as a catalyst for gasification and/or oxidation. The activation energy of initial combustion is also affected by the amount of copper loading, with 8.6wt% copper reducing the activation energy to 56% that of raw coal. This is considered to be the result of an acceleration of the initial volatile matter gasification and/or combustion, as here copper is considered to be mainly in an ion exchanged state on the carboxy groups of brown coal (e.g., COO-$[Cu(NH_3)_4]$-OOC). This is subsequently reduced to Cu metal during the early stage of burning (X≈25wt%). A proposed reaction mechanism was also discussed, which is based on a Cu_2O-concentrated pore model of combustion and a Langmuir-Hinshelwood model of the surface of Cu_2O. This suggests that Cu-terminated Cu_2O could be an important factor in the catalytic reaction. Meanwhile, the relationship between ignition temperatures and activation energies analyzed by the Coats-Redfern method and Semenov theory suggests that copper loaded on brown coal plays a role in promoting heat transfer as well as functioning as a catalyst.

The reaction path of the Cu-ammonia complex to Cu metal was studied by Gaussian09,

which indicated that deammoniation should occur first. It is also found that $CO+CO_2$ emission from an 8.6wt%-Cu-loaded brown coal during the early stage of combustion is four-times larger than that of raw brown coal. The catalytic ability of decarboxylation is explained by the higher heat of reaction of Cu-loaded brown coal. It is concluded in Chapter 4 that low-energy recovery of copper is possible using the ion exchange capability of brown coal and the catalytic effect of Cu-loaded brown coal.

Chapter 5 studied the copper particle formation mechanism, through which a modified percolation model and coalesced particle formation model were proposed. Based on the similarity between the D_{50} of brown coal and D_{50} of CuO particles produced by its combustion, it is suggested that at a point near complete combustion (the percolation threshold) small copper compound particles coalesce together. Subsequent investigation of the effects of raw brown coal size and Cu-loading found that these effects can be explained by the coalesced particle formation model; i.e., the mode diameter of CuO is determined by the mode diameter of raw brown coal. Thus, producing fine CuO primary particles only requires controlling the mode diameter of the brown coal, which is determined by structural boundaries such as macerals. It was also estimated that the coalescence of secondary particles can occurred toward the end of combustion.

In Chapter 6, the potential applications for the recovered copper were studied and discussed. This found that residual ammonium ions can affect the deposition rate of copper sulfate plating solutions, but if NaOH is used as a pH adjusting agent instead of ammonia, the deposition rate is equivalent to original plating solution. Similarly, residual chlorine in copper oxide particles can negatively affect the impact energy and tensile strength of sintered metals in which they are used, but this difference can be eliminated by simply improving the washing process. The ability to produce fine copper particles in-house also presents a number of advantages in terms of allowing control over the particle size. The copper oxide particles produced by combustion were considered too large to be of use as a catalyst, but the Cu-loaded brown coal is a potential candidate for use as a catalyst in oxidation-reduction. However, in order to extend the life of brown coal under oxidizing conditions, a catalyst for gasification is needed. It may also be possible to load multiple metals onto brown coal, thereby creating unique catalysts.

It is concluded that copper can be recovered from waste etching solution with minimal energy consumption by using the ion exchange abilities of brown coal and the catalytic effect of Cu-loaded brown coal. Copper plating solutions, metallurgical additives and oxidation–reduction catalysts (e.g., for gasification) are all very strong potential uses for the recovered copper.

7.2 Prospects of this Study

1. Although percolation models for coal gasification and char combustion have been studied previously, the percolation model for the coalescence of a loaded metal presented

here represents a unique approach. Based on this, it is considered that the mode diameter of brown coal is determined by structural boundaries such as macerals, but this idea still needs to be verified by studying different kinds of coal made up of different types of macerals. If verified, then the metal loading on coal could provide a mold for the formation of metal oxide particles. Furthermore, as multiple metals can be loaded on brown coal, this could provide a mold for metal alloys and special ceramics suitable for use as catalysts or superconducting materials such as $La_{2-x}Ba_xCuO_4$.

2. Since Cu-loaded brown coal shows good activity as a catalyst for oxidation-reduction, it could be used for coal gasification or biomass gasification/combustion. This would offer the advantage of a better low temperature activity, allowing it to be used with low-temperature processes such as the in-situ removal of CO in fuel cells, or NO reduction in automobile exhaust gas when operating at low speed or under low fuel consumption conditions. In this way, it could provide a more desirable alternative to noble metals such as rhodium.

Acknowledgement

I would like to express my gratitude to my supervisors, Professor Takarada and Assistant Professors Sato and Kannari for providing useful discussion and guidance, as well as invaluable support throughout this research. I would also like to thank to Messrs. Hori and Yamato for helping with a number of experiments and providing discussion as collaborators.

I also wish to express my gratitude to the members of the supervisory committee, Professors Nakagawa, Katsura, Ozaki, Takarada and Dr. Takanohashi for their valuable advice regarding my interpretation of the results and verification methods, as well as their support and review of my thesis from its preliminary screening to public hearing.

Special thanks also go to all other members of Professor Takarada's laboratory and the university clerks. I particularly appreciate the assistance provided by Mss. Kojima, Sakamoto, Kakuage and Fjiu in dealing with the various paperwork matters while working as a student.

To my co-researchers at Hitachi Chemical, I would like to thank Messrs. Saikawa and Sekiguchi for studying potential applications of the plating solution and for their efforts in patent writing. Thanks must also go to Messrs. Tsutsui, Morita and Yamamichi for studying powder metallurgy applications, as well as to Messrs. Sumiya, Hirano and Hidaka for their advice and support with the instrumental analysis and computational chemistry.

Finally, I would like to thank from the bottom of my heart Messrs. Tsunoda and Kaneko for recommending my admission to the doctorial course and supporting this research.

September 2015
Atsushi Yoshino

List of Publications

1) **Yoshino, A.**, Hori, H., Sato, K., and Takarada, T., Cu Recovery from Industrial Wastewater via Low Temperature Combustion of Cu-loaded Brown Coal, *Journal of the Japan Institute of Energy*, 93, 542-547(2014)

2) **Yoshino, A.**, Yamato, R., Sato, K., Takarada, T., Cu Recovery from Industrial Wastewater using Brown Coal, *Fuel Processing Technology*, 136, 64-67 (2015)

List of Patents

1) 銅の回収方法及び酸化銅の製造方法

出願人　　：日立化成株式会社 、国立大学法人群馬大学
出願日　　：2013 年 7 月 2 日
出願番号 ：2013-139293
公開日　　：2015 年 1 月 19 日
公開番号 ：2015-010276
発明者　　：横島 廣幸 、長谷川 清 、**吉野 淳** 、才川 哲朗 、
関口 邦明 、廣山 幸久 、宝田 恭之 、佐藤 和好

List of Presentations

1) **Yoshino, A.**, Hori, H., Sato, K., Takarada, T., Cu Recovery from Etching Waste Solution via Low Temperature Combustion of Cu-loaded Brown Coal, *The 22nd annual meeting of Japan Institute of Energy*, Kogakuin University, Tokyo, Japan (Aug. 2013)

2) **Yoshino, A.**, Hori, H., Sato, K., Takarada, T., Cu Recovery from Industrial Wastewater via Low Temperature Combustion of Cu-loaded Brown Coal, *International Conference on Coal Science & Technology*, State College, PA, USA (Sep. 2013)

3) **Yoshino, A.**, Hori, H., Sato, K., Takarada, T., Cu Recovery from Industrial Wastewater using Brown Coal, *The 12th Japan-China Symposium on Coal and C1 Chemistry*, Kyushu University, Fukuoka, Japan (Oct. 2013)

4) **Yoshino, A.**, Yamato, R., Kannari, N., Takarada, T., Cu Recovery from the Waste etching solution using Brown Coal, *International Conference on Coal Science & Technology*, Melbourne, Australia (Sep. 2015, scheduled)

Appendix

A-1. Simulation of Langmuir-Hinshelwood（LH）model

＜Reaction Model：　Langmuir-Hinshelwood＞

$$CO + * \underset{k_{-1}}{\overset{k_1}{\Leftrightarrow}} CO_{ads} \quad (1)$$

$$O_2 + * \xrightarrow{k_2} 2O_{ads} \quad (2)$$

$$CO_{ads} + O_{ads} \xrightarrow{k_3} CO_{2ads} \xrightarrow{fast} CO_2 \quad (3)$$

$$O_{lattice} + * \underset{k_{-4}}{\overset{k_4}{\Leftrightarrow}} O_{ads} \quad (4)$$

$$v_m \cdot d\theta_{CO}/dt = k_1 \cdot Pco(1-\theta_{CO}-\theta_O-\theta_d) \cdot v_m - k_{-1} \cdot \theta_{CO} \cdot v_m - k_3 \cdot \theta_{CO}\theta_O \cdot v_m^2 \quad (i)$$

$$v_m \cdot d\theta_O/dt = 2k_2 \cdot Po_2 (1-\theta_{CO}-\theta_O-\theta_d) \cdot v_m + k_4 \cdot \theta_{Ol} (1-\theta_{CO}-\theta_O-\theta_d) \cdot v_m v_l - k_{-4} \cdot \theta_O (1-\theta_{Ol}) \cdot v_m v_l - k_3 \cdot \theta_{CO}\theta_O \cdot v_m^2 \quad (ii)$$

$$v_l \cdot d\theta_{Ol}/dt = -k_4 \cdot \theta_{Ol}(1-\theta_{CO}-\theta_O-\theta_d) \cdot v_m v_l + k_{-4} \cdot \theta_O(1-\theta_{Ol}) \cdot v_m v_l \quad (iii)$$

$$r = F \cdot [CO_2] = k_3 \cdot \theta_{CO}\theta_O \cdot v_m^2 \quad (iv)$$

項目	記号	単位	初期値
吸着ｻｲﾄ総数	v_m	mol/g-Cu	1.57E-02
格子酸素総数	v_l	mol/g-Cu	7.87E-03
CO吸着率	θ_{CO}	-	0
O吸着率	θ_O	-	0
無効吸着ｻｲﾄ率	θ_d	-	0.2
格子酸素存在率	θ_{Ol}	-	0.9
CO分圧	P_{CO}	-	0.00103
酸素分圧	P_{O2}	-	0.2
排ガス中CO_2濃度	$[CO_2]$	mol/Nl	0
排ガス流量	F	Nl/g-Cu･s	8.98E-01
CO吸着速度定数	k_1	1/s	3.00E-03
CO脱離速度定数	k_{-1}	1/s	2.70E-03
O_2吸着速度定数	k_2	1/s	3.00E-03
表面反応速度定数	k_3	g/mol･s	8.94E-02
格子酸素移動速度定数	k_4	g/mol･s	1.27E-01
格子酸素充填速度定数	k_{-4}	g/mol･s	1.14E-01

<Simulation Coad: Visual Basic for excel>

```
Private Sub CommandButton1_Click()
    ’ Initial parameters are assigned by Cells function to excel sheet table
vm = Cells(26, 5)
vl = Cells(27, 5)
thco = Cells(28, 5)
tho = Cells(29, 5)
thd = Cells(30, 5)
thol = Cells(31, 5)
Pco0 = Cells(32, 5)
PO2 = Cells(33, 5)
CO2 = Cells(34, 5)
F = Cells(35, 5)
k1 = Cells(36, 5)
k11 = Cells(37, 5)
k2 = Cells(38, 5)
k3 = Cells(39, 5)
k4 = Cells(40, 5)
k44 = Cells(41, 5)
k5 = Cells(61, 12)
w = Cells(52, 3) / 10000
V = Cells(55, 3)
    ’ Setting initial values
Pco = 0
t = 0: I = 0
dt = 1
tmax = 1 * 3600

10 'calc
  ‘ Experimental CO2 results are given as these paragraphs
If t / 60 >= 15 And t / 60 <= 25 Then Pco = Pco0 * (t / 60 - 15) / 10
If t / 60 > 25 And t / 60 <= 35 Then Pco = Pco0
If t / 60 > 35 And t / 60 <= 45 Then Pco = Pco0 - Pco0 * (t / 60 - 35) / 10
If t / 60 > 45 Then Pco = 0

  ‘ Kinetic equations
thco = thco + (k1 * Pco * (1 - thco - tho - thd) - k11 * thco - k3 * thco * tho * vm) * dt
tho = tho + (2 * k2 * PO2 * (1 - thco - tho - thd) + k4 * thol * (1 - thco - tho - thd) * vl - k44 * tho * (1 -
thol) * vl - k3 * thco * tho * vm) * dt
thol = thol + (-k4 * thol * (1 - thco - tho - thd) * vm + k44 * tho * (1 - thol) * vm) * dt
CO2 = k3 * thco * tho * vm ^ 2 / F * k5
```

```
Pco2 = CO2 * 22.4

    ‘    Error avoidances
If Pco2 <= 0 Then Pco2 = 0
If Pco <= 0 Then Pco = 0
If thco <= 0 Then thco = 0
If tho <= 0 Then tho = 0
If thol <= 0 Then thol = 0
If CO2 <= 0 Then CO2 = 0
If Pco2 >= 1 Then Pco2 = 1
If Pco >= 1 Then Pco = 1
If thco >= 1 Then thco = 1
If tho >= 1 Then tho = 1
If thol >= 1 Then thol = 1
If CO2 >= 1 Then CO2 = 1

I = Int((t - 1) / (tmax / 20))

    ‘ Writing calculated results into excel sheet
Cells(43, 4 + I) = t / 60
Cells(44, 4 + I) = thco
Cells(45, 4 + I) = tho
Cells(46, 4 + I) = thol
Cells(47, 4 + I) = Pco2
Cells(48, 4 + I) = Pco

t = t + dt
If t >= tmax Then End

GoTo 10

End Sub
```

A-2. 2D Simulation of Percolation model

<Simulation Code: Visual Basic for excell>

```
Sub ボタン 1_Click()
 ‘  Setting initial parameters
p = 0.0143   :’ Initial occupied ratio
I0 = 1
J0 = 1
R = 100
xc = 0.98   :’ Critical conversion
c0 = 0
p0 = 0

 ‘  Initial copper occupied cells are selected at random
For I = I0 To I0 + 100 - 1
   For J = J0 To J0 + 100 - 1
      If J > (R ^ 2 - I ^ 2) ^ 0.5 Then GoTo 20
      A = Rnd(1)
       If A <= p Then Cells(J, I).Interior.ColorIndex = 1: p0 = p0 + 1 Else Cells(J, I).Interior.ColorIndex =
          3: c0 = c0 + 1

20 '
   Next J
Next I

 ‘ Writing c0, p0 into excel sheet
Cells(110, 2) = c0   :’ Numbers of cells of unburnt carbon
Cells(111, 2) = p0   :’ Numbers of cells of copper
c = c0
Cells(112, 2) = ""

50 '

   x = 1 - c / c0          :’ Conversion
   pp = p0 / (c + p0)   :’ Occupied ratio
   If x >= xc Then GoTo 100

 A2 = Int(Rnd(1) * (R + 1))
 A3 = Int(Rnd(1) * (R + 1))
 A4 = Rnd(2)
```

```
    ‘ If selected cell which is selected at random is unburnt, it is burnt, and shrunk random direction.
      If selected cell is copper, nothing happen
        If Cells(I0 + A2, J0 + A3).Interior.ColorIndex = 3 And A4 >= 0.5 Then Cells(I0 + A2, J0 + A3).Delete Shift:=xlShiftToLeft: c = c - 1
        If Cells(I0 + A2, J0 + A3).Interior.ColorIndex = 3 And A4 < 0.5 Then Cells(I0 + A2, J0 + A3).Delete Shift:=xlShiftUp: c = c - 1

GoTo 50

100 '

    ‘ Writing the results into excel sheet
Cells(112, 2) = x
Cells(114, 2) = p0 / (c0 + p0)
Cells(115, 2) = p0 / (c + p0)

End Sub
```